SALT ACCUMULATION AND WATERLOGGING MONITORING SYSTEM (SAWMS) DEVELOPMENT

Van Niekerk A, Muller SJ, Pauw T, Stephenson G, Mashimbye E, Haarhoff D

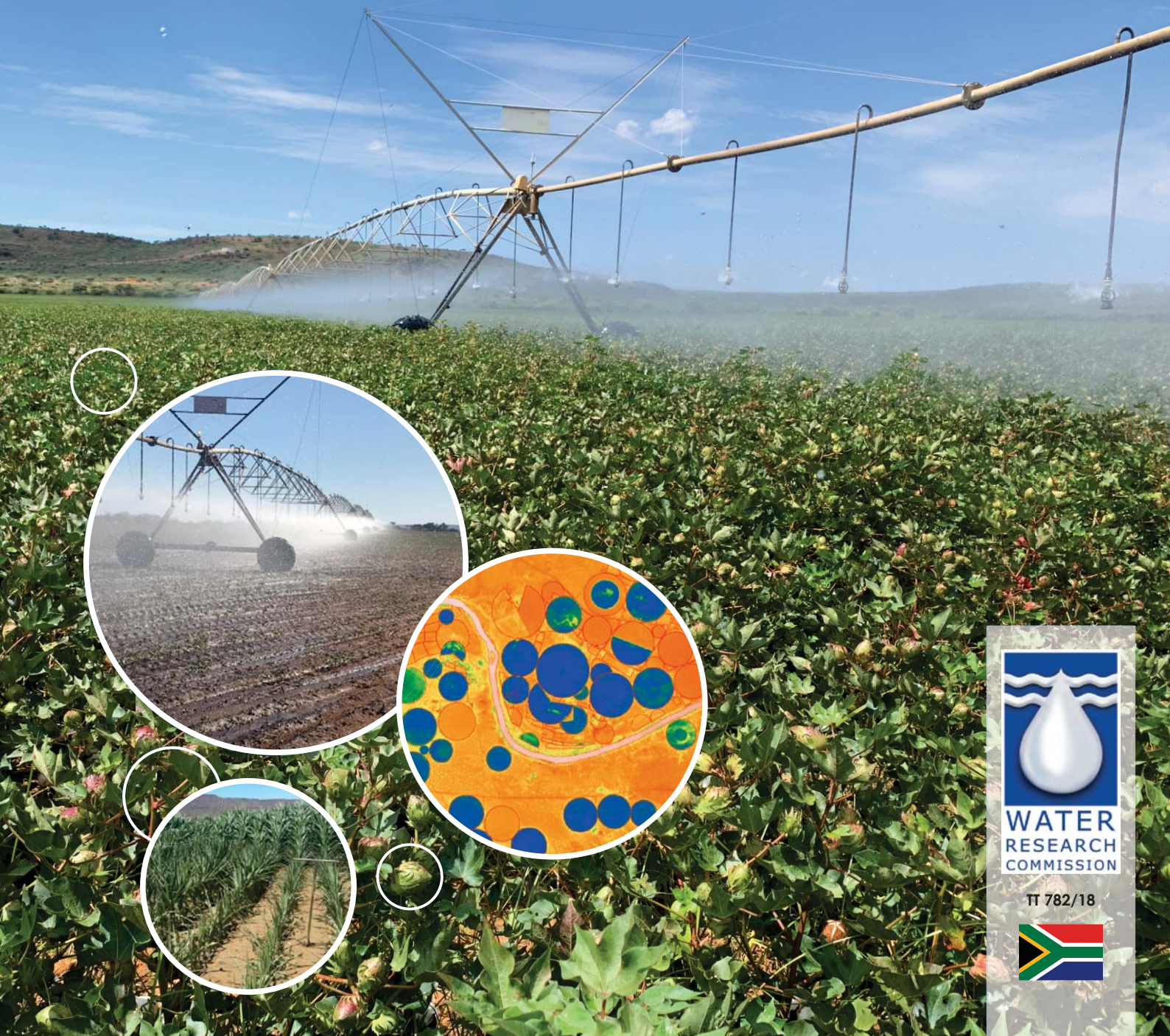

WATER RESEARCH COMMISSION

TT 782/18

SALT ACCUMULATION AND WATERLOGGING MONITORING SYSTEM (SAWMS) DEVELOPMENT

Report to the

WATER RESEARCH COMMISSION

Report by

Van Niekerk A[1], Muller SJ[1], Pauw T[1], Stephenson G[1], Mashimbye E[2], Haarhoff D[3]

[1] Centre for Geographical Analysis, Geography & Environmental Studies, Stellenbosch University
[2] Geography & Environmental Studies, Stellenbosch University
[3] GWK

Report No. TT 782/18

March 2019

UNIVERSITEIT·STELLENBOSCH·UNIVERSITY
jou kennisvennoot • your knowledge partner

GWK
innovate agriculture

CGA CENTRE FOR GEOGRAPHICAL ANALYSIS

Obtainable from

Water Research Commission
Private Bag X03
Gezina, 0031

orders@wrc.org.za or download from www.wrc.org.za

DISCLAIMER

This report has been reviewed by the Water Research Commission (WRC) and approved for publication. Approval does not signify that the contents necessarily reflect the views and policies of the WRC, nor does mention of trade names or commercial products constitute endorsement or recommendation for use.

ISBN 978-0-6392-0084-2

TABLE OF CONTENTS

TABLE OF CONTENTS I
EXECUTIVE SUMMARY III
ACKNOWLEDGEMENTS IX
LIST OF TABLES X
LIST OF FIGURES XI
LIST OF ACRONYMS XIV
1 INTRODUCTION AND OBJECTIVES 1
1.1 Introduction 1
1.2 Aims 3
1.3 Research and development activities and report structure 3
2 TECHNOLOGICAL OVERVIEW 4
2.1 Earth observation 4
2.2 High resolution optical satellite imagery 5
2.3 Image pre-processing and transformation 8
2.4 Detecting salt accumulation and waterlogging with satellite imagery 10
2.5 Multi-temporal image analysis 12
2.6 Object-based image analysis 13
3 WITHIN-FIELD ANOMALY DETECTION 14
3.1 Conceptual overview 14
3.2 Implementation and operationalisation 17
3.2.1 Image retrieval subsystem 17
3.2.2 Image orthorectification and radiometric correction 18
3.2.3 Image transformation 19
3.2.4 Image analysis workflow 19
3.2.4.1 Module 1: Set parameters 20
3.2.4.2 Module 2: Calculate mean field values 21
3.2.4.3 Module 3: Classify fields 22
3.2.4.4 Module 4: Calculate percentage difference and apply thresholds 22
3.2.4.5 Module 5: Anomaly frequency index (AFI) 23
3.2.5 Dealing with inaccurate field boundary data 25
4 WEB APPLICATION DEVELOPMENT 28
4.1 System design 28
4.2 System components 28
4.2.1 Storage platform 28
4.2.2 GIS server platform: exposing the data to the Internet 29
4.2.3 Programmatic ingestion of data 29
4.2.4 Platform selection 29
4.2.5 Graphical user interface (GUI) development 30
4.3 Overview of graphical user interface 30
5 DEMONSTRATION OF THE SAWMS IN SELECTED AREAS 38
5.1 Orange, Riet, Vaal and Harts (ORVH) Basin 38

5.2 Olifants River (Western Cape Province)....40
5.3 Breede River 42
5.4 Sundays River 44
5.5 Olifants River (Mpumalanga Province)....48
5.6 Great Fish River 50
5.7 Gamtoos River 53
6 DISCUSSION, CONCLUSIONS AND RECOMMENDATIONS....58
6.1 Main findings from applying the SAWMS in various irrigated areas....58
6.2 Proposals for future research 61
6.3 Operational recommendations 62
REFERENCES 64
APPENDIX I: USER FEEDBACK SESSIONS 70
APPENDIX II: CAPACITY BUILDING 72
APPENDIX III: PUBLICATIONS 74
APPENDIX IV: GUIDELINE TO USERS ABOUT THE IMPACT OF FIELD BOUNDARY QUALITY ON ANOMALY DETECTION 75
APPENDIX V: ACCESS TO DATA GENERATED THROUGH THIS PROJECT 78

EXECUTIVE SUMMARY

BACKGROUND

Crop production in irrigated areas is often negatively affected by salt accumulation and waterlogging. Excessive accumulation of salt in the plant root zone has a deteriorative effect on vegetative growth, resulting in reduced crop yield and barren soil and ultimately leading to a decrease in agricultural production. It has been estimated that 18% of South Africa's irrigated land is either moderately/severely salt-affected or waterlogged. Salt accumulation and waterlogging are closely linked as rising water tables prevent salts from being leached.

A recent study investigated salt accumulation and waterlogging in nine South African irrigation schemes and found that 6.3% of scheme surfaces were severely affected. Mitigative measures therefore need to be taken to prevent further loss of this limited resource. There is a critical need for active salinity monitoring so that rehabilitation and preventive measures can be implemented.

Conventional methods for monitoring salt accumulation within irrigation schemes involve regular field visits to collect soil samples, followed by laboratory analyses. Many field visits are required to monitor large irrigation schemes effectively. Salt-affected areas in South Africa are localised and relatively small in extent (often as narrow as 1–2 m in irrigated areas), which further limits the viability of relying on in situ methods. Remote sensing has been proposed as a less time-consuming and more cost-effective method for monitoring salt accumulation, as satellite images cover large areas on a regular, timely basis.

RATIONALE

In a completed WRC project, entitled *Methodology for monitoring waterlogging and salt accumulation on selected irrigation schemes in South Africa* (published as report TT 648/15), Stellenbosch University and the Agricultural Research Council evaluated a series of remote sensing and geospatial modelling techniques for identifying waterlogged and salt-affected areas within South African irrigation schemes. This work concluded that the most effective approach is to consider both direct and indirect salinity indicators, especially when salt-affected areas are relatively small. A new technique called within-field anomaly detection (WFAD) was found to consistently outperform the other techniques evaluated. Essentially, the technique identifies areas within cultivated fields that are consistently under stress (i.e. are anomalies) over several growing seasons, for example three years. The assumption is that if a particular area within a field is stressed over an extensive period, the cause is unlikely to be related to factors such as lack of water, nutrient deficiency or disease and more likely related to soil conditions. The principle of the WFAD is to analyse changes in multi-temporal vegetation indices (e.g. normalized difference vegetation index (NDVI)) and band ratios (e.g. image brightness) derived from high resolution satellite imagery in order to determine areas of consistently stressed crops.

It was evident from the comprehensive in situ validations, that the WFAD is very successful at identifying

salt-affected and waterlogged areas within irrigation schemes. However, the focus of this report was on finding an appropriate method for monitoring salt accumulation and waterlogging and not on operationalisation and technology exchange. Although the WFAD was tested within a selected number of areas within irrigation schemes, these applications were once-off implementations to validate the WFAD. More work was thus needed to streamline and automate the process so that it can be used for routine monitoring. A prerequisite for the establishment of WFAD as an operational tool in the proactive management of salt accumulation and waterlogging is that the detected anomalies must be made available to all stakeholders (e.g. farmers, extension officers and agribusinesses) in a timely and cost-effective manner. Ideally, the information should be delivered through a web-based service that is simple, intuitive and easy to use.

The aims of this project, which lead to the establishment of the Salt Accumulation and Waterlogging Monitoring System (SAWMS), were to:

1. Develop a system that automatically analyses multi-temporal (current and historical) satellite imagery in order to identify areas within cultivated fields that are likely affected by waterlogging or salt accumulation;
2. Disseminate information about waterlogged and salt-affected areas to end-users through the development and implementation of a web-based application;
3. Demonstrate, apply and evaluate the system in suitable irrigation schemes; and
4. Improve the system with the help of user feedback and make recommendations for national implementation.

METHODOLOGY

The project was carried out in four phases namely:

1. Image processing and anomaly detection;
2. Web application development;
3. System demonstration and evaluation; and
4. System application and recommendations for improvement.

An imagery requirement analysis was carried out during the first phase of the project, followed by an inventory of available satellite imagery. It was established that Sentinel-2 imagery is the most suitable source of data for use in the SAWMS, mainly because it has a relatively high (10 m) spatial resolution and five-day revisit time. Another very important consideration was that Sentinel-2 imagery is freely available from the European Space Agency (ESA) and the acquisition (downloading) of the imagery can be fully automated. Once the decision was made to make use of Sentinel-2 imagery, an automated image retrieval and transformation procedure was developed. This was followed by the implementation of the WFAD method. The SAWMS is a web-based application and Phase 2 involved designing and developing the various system components, including the storage platform, geographical information

system (GIS) server, ingestion system, web mapping platform and graphical user interface.

The prototype SAWMS was evaluated during Phase 3 of the project by implementing it in a test area. The chosen test site was the Orange-Riet-Vaal-Harts region in the Northern Cape, North West and Free State Province. GWK, the leading agribusiness in the area, was tasked to evaluate the anomalies detected by the system. This process included field visits and soil sample analyses. In Phase 4, the SAWMS was applied to several other irrigated areas, namely Olifants River, Breede River, Sundays River, Loskop, Great Fish River and Gamtoos River.

During the course of the project, it was established that the SAWMS will be most suitable for use by agricultural advisors such as agronomists, soil scientists and technical advisors rather than individual farmers/producers. Advisors at GWK and Humansdorp Koöperasie were consequently targeted to provide feedback on the validity, functionality and usability of the SAWMS. Two workshops were held in Kimberley and Humansdorp during which invaluable suggestions for improvement and recommendations for operationalisation were made.

MAIN FINDINGS

The general agreement among the SAWMS end-users (and reference group members) is that salt accumulation and waterlogging is of growing concern, especially with increasing uncertainties over water supply and quality. Although producers are improving water use efficiencies, there is a concern that this may lead to a gradual accumulation of salts due to the decrease in leaching. There is thus clearly a growing need for monitoring of salt accumulation.

Targeted end-users (mainly agronomists, soil scientists and agricultural advisors) commented that the WFAD approach is innovative and that the principle of identifying areas (management zones) in fields/orchards that are consistently underperforming is sound. It was agreed that multi-temporal image analysis is essential for monitoring salt accumulation and waterlogging, because the direct and indirect manifestations of salt accumulation and waterlogging vary, depending on the crop type and growth stage.

The main finding of implementing and applying the SAWMS in seven very diverse irrigated areas throughout South Africa is that the system provides invaluable information in support of soil conservation. The experience gained in the implementation process exposed several technical challenges, which were not anticipated prior to this project. Solutions to most of these problems were found during the course of the project, but some still require additional research and development. The SAWMS worked very well in the ORVH Basin, mainly because most of the crops planted are annuals such as maize, wheat and barley. These crops respond dramatically to salinity and waterlogging and affected areas could thus be easily differentiated from non-affected areas. The field sizes are also large, which meant that fewer errors were caused by inaccurate (generalised) field boundaries. Similar observations were made in the Olifants River (Mpumalanga) and Great Fish River. Applying the SAWMS in the Olifants River (Western Cape) was much more challenging as the fields are more

compact. Many errors in the existing field boundaries were noted and these had a detrimental effect on the WFAD method. Similar observations were made in Sundays and Gamtoos River areas – to such an extent that new field boundaries had to be manually delineated. Field boundaries that were automatically generated from multi-temporal Sentinel-2 imagery (the focus of the capacity building component of the project) were tested in the Gamtoos River area and showed potential for incorporation in future implementations of the SAWMS. However, more research is needed to improve the results and to operationalise such techniques.

Several improvements were made to the WFAD method since its conceptualisation. In particular, the use of Sentinel-2 imagery improved anomaly detection accuracies by allowing for the generation of anomaly layers at five-day intervals, instead of once a season. This high frequency approach enabled the development of monthly cloud-free anomaly layers, which were used to generate an anomaly frequency index (AFI) over a specified period (rolling window). Based on user feedback and visual inspections of the AFIs in several areas throughout South Africa, it seems that using Sentinel-2 imagery as input to the WFAD works very well in areas with medium (3 ha) to large (>10 ha) fields, but is less effective in areas with very small (<1 ha) fields, due to its 10 m spatial resolution. However, the high (five-day) temporal resolution of Sentinel-2 imagery is ideal for agricultural monitoring as 73 images (observations) are used to generate the AFI (if a rolling window of 12 months is used). This effectively removes the influence of short-term fluctuations and interference (e.g. clouds, cloud shadows, heatwaves, wind, irrigation events, harvesting), allowing emphasis to be placed on the long-term status of each pixel (zone) within each field.

It was agreed by the project team, users and reference group that the AFI should be used as a scoping mechanism to identify areas that must be prioritised for field visits. This functionality was seen by the end-users as the major contribution of the system. The AFI will also be helpful to identify areas where probes should be placed and where soil and leaf samples should be collected. Currently, this is done by walking through the fields and in large fields it can be easy to miss problematic areas. Based on the feedback from end-users, the maps are also invaluable for seasonal discussions by advisors with clients, as the SAWMS provides a historical record of areas in fields that are underperforming. Once the cause is determined (through site visits and, if needed, analyses of samples), agronomists can make recommendations on how production in such areas can be improved. It was agreed that the major value of the system is that a historical record is provided, which can be used for retrospective assessments such as investigating when a problem started. The system can also be used as a communication tool through which problems can be analysed and explained to producers.

RECOMMENDATIONS

South Africa has a limited availability of suitable land for irrigated crop production. With the added pressures of climate change, population growth, the decline in water availability and quality, the need for new technologies to monitor salt accumulation and waterlogging is critical. Frequently updated maps of the extent of affected areas will improve our understanding of the true effect of these phenomena on agricultural production and SA's limited arable land.

Several gaps in knowledge were identified during the course of this project. For instance, it became clear from interactions with potential users that little is known about the optimal observation period for capturing anomalies caused by salt accumulation and waterlogging. The general agreement was that 12 months should be adequate, but more research is needed to investigate whether shorter or longer periods may be more effective. Another aspect that requires investigation is the value of using different vegetation indices in the WFAD procedure and the incorporation of open source image segmentation algorithms to group pixels within fields into management zones. The use of machine learning to differentiate between different types of anomalies also warrants investigation.

The biggest limitation of the SAWMS is that it relies on pre-defined field boundaries. The current methodology for generating such a layer is to visually interpret very high resolution satellite imagery or aerial photography and manually delineate (digitise) individual fields. Mapping every field in South Africa in this manner requires substantial financial and human resources. Automated field boundary delineation was thus a major focus of the research component of the project. The range of automated field boundary delineation experiments carried out by the MSc students registered on this project suggests that the accuracy and completeness of the automated field boundary delineations can be improved by making use of more than one source of data. However, more research is needed to find a technique that can be operationalised and incorporated into the SAWMS.

From an operational point of view, it is recommended that the SAWMS is implemented as a cloud-based service. This will improve efficiencies as the large volumes of satellite imagery required by the system can be processed “in the cloud”, which will substantially reduce data (bandwidth) costs. It will also mitigate the unstable nature of power generation in South Africa. Currently, the SAWMS runs mostly on open source software, although some proprietary software is used for some of the processing steps. It is recommended that all functionality is implemented using open source software as this will reduce the operational costs as no licencing fees will be required.

The SAWMS processes are fully automated, but (as with most complex computer systems) a system administrator is required to monitor activities and ensure that the servers remain functional. Some of the software used (e.g. operating systems, database management systems and processing software) will require periodic updates, which will most likely require modifications to the system code. A system administrator familiar with the SAWMS procedures and code is consequently recommended.

Those who participated in the end-user feedback sessions (Appendix I) recommended that the operational costs of the SAWMS be funded by national government, in it was suggested that DAFF act as lead organisation, given their mandate to conserve agricultural soil and water. DWS should be a key partner, given the clear linkages between water use/quality and salt accumulation. Water user associations and agribusiness will play a critical role in the operationalisation of the SAWMS. Although producers will benefit from using the SAWMS, salt accumulation has a relatively small impact on yields compared to other factors such as cultivar selection, water availability, fertilisation and pest control. The users indicated that producers will only pay for something that has a direct and clear “value proposition”. The “FruitLook” model, where the Western Cape Provincial Government pays for the service to make

it freely available to producers, was proposed as the best solution for the SAWMS, at least until the "value proposition" becomes apparent.

This project demonstrated how Earth observation data and techniques can be operationalised to inform decisions made to support the conservation of agricultural land/soils. On-farm actions taken based on the information provided by SAWMS will likely lead to a reduction of input costs and increases in agricultural outputs. Given that SAWMS is capable of servicing a large (e.g. national) area, it can make a substantial contribution to economic development. The development of more Earth observation systems in support of agricultural decisions is recommended.

ACKNOWLEDGEMENTS

This report would not have been possible without the help of others. In particular, the project team would like to thank the following reference group members for their invaluable inputs and sage advice during the course of the project:

Dr GR Backeberg	Water Research Commission (WRC) (Chairman)
Mr HM du Plessis	Independent advisor
Mr D Haarhoff	GWK
Dr N Jovanovic	CSIR
Mr N Knoetze	South African Association for Water User Associations
Prof S Lorentz	University of Kwa-Zulu Natal (UKZN)
Dr M Lück-Vogel	CSIR
Prof LD van Rensburg	University of the Free State (UFS)
Dr T Volschenk	Agricultural Research Council (ARC)

In addition, the project team is grateful to the:

- WRC for funding this research
- European Space Agency (ESA) for supplying the Sentinel-2 data used in the SAWMS
- The Crop Estimates Consortium for supplying the national field crop boundaries database
- Western Cape Department of Agriculture (WCPDA), GWK and others for supplying field boundary and crop type data
- EE Publishers for providing exposure of the project
- Mr Adriaan Prins and Mr Barry Watkins, students at the Stellenbosch University who contributed to this research project
- GWK for supplying photographs for the report cover
- LinguaFix (www.linguafix.net) for providing editorial services on a very tight schedule

LIST OF TABLES

Table 2.1: Optical satellites available for Earth observations 6
Table 2.2: Sentinel-2 sensor characteristics 8
Table 3.1: Modifiable parameters of the image analysis workflow 20
Table 3.2: Suggested labels for the anomaly frequency index classification 25

LIST OF FIGURES

Figure 2.1: Electromagnetic spectrum and its relation to passive and active remote sensors 5
Figure 2.2: Reflectance characteristics of whole-rock samples of lithological units derived from an Analystical Spectral Devices (ASD) FieldSpec 3 in the United States, where: 1 – evaporate salt crust, 2 – Javelina Fm tan-weathering sandstone, 3 – Pen Fm tan-weathering shale, 4 – Aguja Fm tan-weathering sandstone, 5 – Chisos FM ash, 6 – Chisos Fm dark mafic unit, 7 – Chisos Fm tan-weathering basalt, 8 – Tertiary syenodiorite. 11
Figure 2.3: Spectral reflectance of water compared to green vegetation and dry bare soil 11
Figure 2.4: Typical reflectance spectrum of a healthy and stressed plant 12
Figure 3.1: Hierarchical within-field anomaly detection segmentation process 15
Figure 3.2: Process of anomaly detection in which the a) mean NDVI value of the parent object is used as reference against which the b) NDVI values of the child objects are compared, resulting in c) a set of identified anomalies (shaded in red) 16
Figure 3.3: Zonal statistics process where the Sentinel-2 imagery (A) is used together with the DAFF field boundaries (B) to generate mean field values for SAVI (C) and Br (D) 21
Figure 3.4: Classification of fields into vegetated and bare fields 22
Figure 3.5: The process of percentage difference calculation and threshold application for vegetated fields 23
Figure 3.6: Monthly anomaly creation by binary multiplication 24
Figure 3.7: Conceptualisation of the anomaly severity index for an arbitrary four-month period 24
Figure 3.8: False positive anomalies due to outdated field boundaries as compared to a recent a) true colour image, b) vegetation index and c) the resulting impact on the anomaly detection. 26
Figure 3.9: False positives due to multiple crops on a single field and the influence of clouds, as compared to a recent a) true colour image, b) vegetation index and c) the resulting impact on the anomaly detection. 26
Figure 3.10: Anomalies detected within a a) single month without the relative-area threshold rule applied compared to when b) the relative-area threshold rule was applied. 27
Figure 4.1: System design 28
Figure 4.2: The landing page for the SAWMS 30
Figure 4.3: Graphical user interface when web application is first loaded 31
Figure 4.4: When zooming in, field boundaries become visible 31
Figure 4.5: Changing the background layer to Sentinel-2 32
Figure 4.6: Field boundaries, anomalies and the background layer to Sentinel-2 NDVI background layer 32
Figure 4.7: Anomaly layer 33
Figure 4.8: Changing the date using the (top) dropdown list changes the (bottom) anomaly layers 34
Figure 4.9: The screen can be split in two for side-by-side viewing and comparison 35
Figure 4.10: Linking the dates of maps 35
Figure 4.11: Comparing anomalies of different months 35
Figure 4.12: Merging the split screen 36

Figure 4.13: Very high resolution aerial photograph background 36
Figure 4.14: NGI topographical maps 37
Figure 5.1: Geographical distribution of the irrigation schemes and agricultural areas where the SAWMS was applied 38
Figure 5.2: Example of the anomaly frequency index with overlaying diluted ECe values at three depths with a) at 5cm depth, b) at 20cm depth and c) at 40cm depth with vegetation index background. A relative increase in salinity levels, specifically at the 5 cm depth is visible. 39
Figure 5.3: Example of the anomaly frequency index with diluted ECe[9] values at a) 5cm, b) 20cm (with colour image in background) and c) 40cm depths (with a vegetation index in background). A relative increase in salinity levels within the detected anomalies is observed at all depths. 40
Figure 5.4: The AFI generated by SAWMS in the Olifants River irrigation scheme. 41
Figure 5.5: Examples of the anomaly frequency index generated by SAWMS in the Olifants River irrigation scheme for July 2018 at a (a) fine scale indicating field boundary inconsistencies, and at a (b) larger scale. 42
Figure 5.6: Example of the anomaly frequency index generated by SAWMS in a portion of the Breede River irrigation scheme selected for demonstration 43
Figure 5.7: Specific examples of the anomaly frequency index generated by SAWMS in the Breede River irrigation scheme for July 2018, where a) illustrates anomalies in pivot fields, b) shows false positive anomalies due to wind breaks, and c) shows the anomaly frequency index at a larger scale. 44
Figure 5.8: Example of the anomaly frequency index generated by SAWMS for part of the Sundays River irrigation scheme included in the evaluation using DAFF field boundaries 45
Figure 5.9: Example of the anomaly frequency index generated by SAWMS for part of the Sundays River irrigation scheme included in the evaluation, with manually re-digitised field boundaries 46
Figure 5.10: Examples of the anomaly frequency index generated by SAWMS in the Sundays River irrigation scheme for July 2018, where a) and b) give different examples where generalised field boundaries was the main cause of the anomalies identified 47
Figure 5.11: Examples of the anomaly frequency index generated by SAWMS applied in the Sundays River irrigation scheme for July 2018, where a) and b) represent the same area as Figure 5.10 with manually re-digitised field boundaries 48
Figure 5.12: Example of the anomaly frequency index generated by SAWMS for the Loskop Irrigation scheme 49
Figure 5.13: Specific examples of the anomaly frequency index generated by SAWMS in the Loskop River irrigation scheme for July 2018, where a) shows an anomaly identified with a corresponding NDVI image and b) and c) show anomalies with corresponding true colour images. 50
Figure 5.14: Example of the anomaly frequency index generated by SAWMS for the upper part of the Great Fish River irrigation scheme 51
Figure 5.15: Example of the anomaly frequency index generated by SAWMS for the lower part of the Great Fish River irrigation scheme 52

Figure 5.16: Examples of the anomaly frequency index generated by SAWMS in the Great Fish irrigation scheme, with a) anomalies at the centre of pivots, likely due to infrastructure, b) a field with severely affected areas, and c) anomalies with a corresponding NDVI image. 53
Figure 5.17: Example of the anomaly frequency index generated by SAWMS in the Gamtoos region with DAFF field boundaries 54
Figure 5.18: A close-up of the anomaly frequency index in the Gamtoos region with DAFF field boundaries 54
Figure 5.19: Example of the anomaly frequency index generated by SAWMS in the Gamtoos region with manually created field boundaries 55
Figure 5.20: A close-up of the anomaly frequency index in the Gamtoos region with manually created field boundaries 55
Figure 5.21: Various examples of the anomaly frequency index in the Gamtoos region where a) and b) show localized anomalies occurring with corresponding true colour images, and c) compares the result with a corresponding normalised difference vegetation index image. 56
Figure 5.22: Example of the anomaly frequency index generated using automatically derived field boundaries in the Patensie agricultural area in the Gamtoos irrigation scheme 57
Figure 5.23: Automatically delineated field vector boundaries (right) in the Patensie agricultural area showing relatively homogenous areas (few anomalies identified by the anomaly frequency index on the left) 57

LIST OF ACRONYMS

AFI	Anomaly frequency index
AWS	Amazon Web Services
CSS	Cascading style sheets
DAFF	Department of Agriculture, Forestry and Fisheries
DJ	Doolittle JA
EO	Earth observation
ESA	European Space Agency
GDP	Gross domestic product
GEOBIA	Geographical object-based image analysis
GIS	Geographical information system
GUI	Graphical user interface
IAW	Image analysis workflow
MeaD	Mean difference
MRS	Multiresolution segmentation
NDVI	Normalized difference vegetation index
ORVH	Orange, Riet, Vaal and Harts
PD	Percentage difference
SANSA	South African National Space Agency
SAVI	Soil adjusted vegetation index
SAWMS	Salt accumulation and waterlogging monitoring system
SNAP	Sentinel application platform
TOA	Top of atmosphere
TOC	Top of canopy
VHR	Very high resolution
WFAD	Within-field anomaly detection
WFS	Web feature service
WMS	Web mapping service
WRC	Water Research Commission

1 INTRODUCTION AND OBJECTIVES

1.1 Introduction

Crop production in irrigated areas is often negatively affected by salt accumulation and waterlogging. Excessive accumulation of salt in the plant root zone has a deteriorative effect on vegetative growth, resulting in reduced crop yield and barren soil, and ultimately leading to a decrease in agricultural production. It has been estimated that 18% of South Africa's irrigated land is either moderately/severely salt-affected or waterlogged (Backeberg et al., 1996). Salt accumulation and waterlogging are closely linked as rising water tables prevent salts from being leached. Nell et al. (2015) investigated salt accumulation and waterlogging in nine South African irrigation schemes and found that 6.3% of scheme surfaces were severely affected. Although these proportions are relatively small compared to the proportion of salt-affected areas in other countries (e.g. Argentina (34%), Egypt (33%), Iran (30%), Pakistan (26%) and the United States of America (23%) (Ghassemi et al., 1995), one should bear in mind that only 1.2% (about 1 464 000 ha) of South Africa's land area is suitable for irrigation (FAO, 1995), while about 1.1% (1 334 562 ha) is currently being actively irrigated (Van Niekerk et al., 2018). Mitigative measures therefore need to be taken to prevent further loss of this limited resource. There is a critical need for active salinity monitoring so that rehabilitation and preventive measures can be implemented.

Conventional methods for monitoring salt accumulation within irrigation schemes involve regular field visits to collect soil samples, followed by laboratory analyses. Many field visits are required to monitor large irrigation schemes effectively. According to Nell et al. (2015), salt-affected areas in South Africa are localised and relatively small in extent (often as narrow as 1–2 m in irrigated areas), which further limits the viability of relying on in situ methods. Remote sensing has been proposed as a less time-consuming and more cost-effective method for monitoring salt accumulation, as satellite images cover large areas on a regular, timely basis (Abbas et al., 2013).

A number of direct and indirect Earth observation approaches for detecting accumulated salts exists. The main direct indicators of salt accumulation and waterlogging include the detection of halophytic vegetation (García Rodríguez et al., 2007; Dutkiewicz et al., 2009), visible salt encrustations (Rao et al., 1995; Dwivedi et al., 1998; Metternicht & Zinck, 2003; Khan et al., 2005; Abood et al., 2011; Iqbal, 2011; Setia et al., 2013; Sidike et al., 2014) and surface ponding (Dwivedi et al., 1998), while the indirect approach focuses on monitoring physiological stress of vegetation (Wiegand et al., 1994; Lenney et al., 1996; Penuelas et al., 1997; Koshal, 2010; Abood et al., 2011).

In a completed WRC project, published as report TT 648/15 entitled *Methodology for monitoring waterlogging and salt accumulation on selected irrigation schemes in South Africa* (Nell et al., 2015), Stellenbosch University and the Agricultural Research Council evaluated a series of remote sensing and geospatial modelling techniques for identifying waterlogged and salt-affected areas within South African irrigation schemes (Nell et al., 2015; Muller & Van Niekerk, 2016b; a; Vermeulen & Van Niekerk, 2016; Muller, 2017; Vermeulen & Van Niekerk, 2017). This work concluded that the most effective

approach is to consider both direct and indirect salinity indicators, especially when salt-affected areas are relatively small. A new technique, called within-field anomaly detection (WFAD), was found to consistently outperform the other techniques evaluated. Essentially, the technique identifies areas within cultivated fields that are consistently under stress (i.e. are anomalies) over several growing seasons, for example three years. The assumption is that if a particular area within a field is stressed over an extensive period, the cause is unlikely to be related to factors such as lack of water, nutrient deficiency or disease and more likely related to soil conditions (Furby et al., 1995; Lenney et al., 1996). The principle of the WFAD is to analyse changes in multi-temporal vegetation indices (e.g. normalized difference vegetation index (NDVI)) and band ratios (e.g. image brightness) derived from high resolution satellite imagery in order to determine areas of consistently stressed crops.

The WFAD was validated in nine irrigation schemes throughout South Africa. It was found that the areas identified were related to salt accumulation or waterlogging in more than 75% of the cases, and in most irrigation schemes, the WFAD was able to identify salt-affected areas with an accuracy of more than 70%. The success of the technique is partly attributed to the use of geographical object-based image analysis (GEOBIA) for detecting and delineating the anomalies. This approach has the ability to group pixels with similar spectral properties into so-called image segments (or objects) in a hierarchical structure. This structure enables the interrogation of smaller child objects occurring within larger parent objects (fields) and specifically the comparison of the biomass or brightness of the parent field object to that of the child objects of that field to establish whether a particular child segment is an anomaly (or not).

It was evident from the comprehensive in situ validations (Nell et al., 2015), that the WFAD is very successful at identifying salt-affected and waterlogged areas within irrigation schemes. However, the focus of this report was on finding an appropriate method for monitoring salt accumulation and waterlogging and not on operationalisation and technology exchange. Although the WFAD was tested within a selected number of areas within irrigation schemes, these applications were once-off implementations to validate the WFAD. More work was thus needed to streamline and automate the process so that it can be used for routine monitoring. A prerequisite for the establishment of WFAD as an operational tool in the proactive management of salt accumulation and waterlogging is that the detected anomalies must be made available to all stakeholders (e.g. farmers, extension officers and agribusinesses) in a timely and cost-effective manner. Ideally, the information should be delivered through a simple, intuitive and easy to use web-based service.

1.2 Aims

The aims of this project, which lead to the establishment of the Salt Accumulation and Waterlogging Monitoring System (SAWMS), were to:

1. Develop a system that automatically analyses multi-temporal (current and historical) satellite imagery in order to identify areas within cultivated fields that are likely affected by waterlogging or salt accumulation;
2. Disseminate information about waterlogged and salt-affected areas to end-users through the development and implementation of a web-based application;
3. Demonstrate, apply and evaluate the system in suitable irrigation schemes; and
4. Improve the system with the help of user feedback and make recommendations for national implementation.

Although some research was carried out to find suitable solutions to technical problems (e.g. field boundary delineation), the focus of this project was on technology exchange, as most of the fundamental research was carried out and documented in WRC report TT 648/15 (Nell et al., 2015). An overview of the activities of this project is provided in the next section.

1.3 Research and development activities and report structure

The project was carried out in four phases namely:

1. Image processing and anomaly detection;
2. Web application development;
3. System demonstration and evaluation; and
4. System application and recommendations for improvement.

This report is loosely structured around these phases. The next chapter (Chapter 2) provides an overview of Earth observation, Sentinel-2 imagery and image analyses, while Chapter 3 includes a conceptual overview of the WFAD method and describes how it was implemented. These two chapters thus relate directly to Phase 1 (Image processing and anomaly detection). The activities relating to the web application development (Phase 2) is reported in Chapter 4, while Chapter 5 is devoted to demonstrating the SAWMS. The final chapter (Chapter 6) summarises the main findings of the research, makes recommendations for future research and highlights a number of operational considerations.

.

2 TECHNOLOGICAL OVERVIEW

An understanding of salt accumulation and waterlogging, its causes and effects, together with remote sensing and its capabilities, was vital for achieving the aims of this project. Consequently, this chapter (Chapter 2) summarises relevant Earth observation (EO) concepts and how it can be applied for detecting salt accumulation and waterlogging. The chapter gives a brief summary of EO, followed by an overview of high resolution optical imagery, the use of satellite imagery for detecting salt accumulation and waterlogging, multi-temporal image analysis and object-based image analysis. A conceptual overview of the WFAD method and the operationalisation thereof, resulting in the SAWMS, is then presented in Chapter 3.

2.1 Earth observation

Earth observation combines in situ data with remotely sensed data to derive information about the Earth's land and water surfaces. Remote sensing is the process of acquiring information from a distance (i.e. without being in contact with the observed target). The remotely sensed data, usually acquired from an overhead perspective, records electromagnetic (EM) radiation in one or more regions of the EM spectrum, reflected or emitted from the Earth's surface (Campbell, 2007). Passive sensors – the main source of data in this project – mainly operate in the visible and the infrared regions of the EM spectrum (Figure 2.1). The visible spectrum contains those wavelengths of radiation that can be perceived by human vision and ranges from violet to red light. Wavelengths longer than those of the visible spectrum (but shorter than those of microwave radiation) are termed infrared. The infrared region of the EM spectrum can be subdivided into near-, mid- and far-infrared. The primary source of near- and mid-infrared radiation is the sun and EM radiation in these wavelengths are reflected by the Earth's surface in the same manner as EM radiation in the visible wavelengths. Hence, the near- and mid-infrared wavebands, together with the visible bands, are often collectively known as the optical bands. Far-infrared radiation, however, is absorbed and then emitted by the Earth's surface in the form of heat, or thermal energy, and is sometimes known as thermal infrared radiation. Thermal infrared bands are generally less common in multispectral satellite imaging platforms than visible, near- and mid-infrared bands (Mather, 2004; Campbell, 2007).

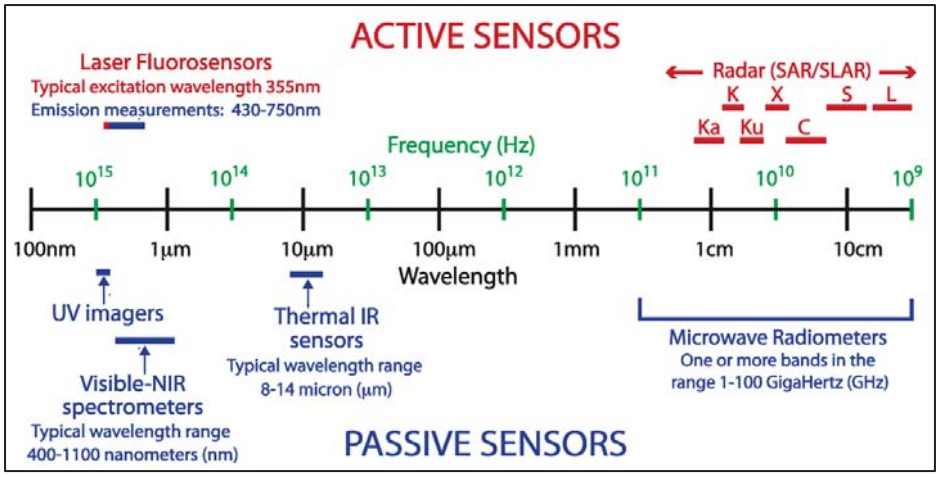

Source: SEOS (2016)

Figure 2.1: Electromagnetic spectrum and its relation to passive and active remote sensors

The longest wavelengths commonly used in remote sensing fall in the microwave spectrum, where solar irradiance is negligible. Although the Earth itself emits a small amount of microwave energy, this emitted energy is rarely measured in remote sensing as most microwave sensors are active. As opposed to passive sensors, which measure energy generated by an external source (usually the sun), active sensors emit their own energy to irradiate the ground and then measure the portion of that energy reflected back to them (Campbell & Wynne, 2011). Active microwave sensors are also termed RADAR (radio detection and ranging) sensors. An imaging radar system typically consists of a transmitter, receiver, antenna array and a recorder. The transmitter transmits repetitive microwave pulses at a specific frequency through the antenna array, which controls the propagation of the EM wave through devices known as waveguides. Usually, the same antenna then receives the echo of the signal. This is then accepted by the receiver, which filters and amplifies it as required and passes it on to the recorder (Campbell & Wynne, 2011).

A feasibility study carried out as part of a previous WRC project, published as report TT 648/15 (Nell et al., 2015), found that the use microwave remote sensing is not feasible for regional or national salt accumulation and waterlogging monitoring. It was therefore not employed in this study and the following subsection consequently focuses on high resolution optical remote sensing imagery, which was identified by Nell et al. (2015) to be most suitable for this application.

2.2 High resolution optical satellite imagery

There is a continual increase in the availability of satellite imagery suitable for EO. Table 2.1 provides an overview of available optical imagery available at the time of writing this report.

Table 2.1: Optical satellites available for Earth observations

		Satellite (commission period)	Sensors	Spectral bands	Spatial resolution	Revisit Time	Availability
Low resolution	**MODIS**	Terra (1999 -) Aqua (2002 -)	Moderate Resolution Imaging Spectro-radiometer (MODIS)	36	Red, NIR (250 m) Blue, Green, IR (500 m) Thermal (1 km)	2 times, daily	Freely available
	AVHRR	NOAA (1978 - 2009) multiple	Advanced Very High Resolution Radiometer (AVHRR)	6	VIS, NIR, Thermal, (1 km)	2 times, daily	Freely available
Medium resolution	**Landsat**	Landsat - 4 (1982 - 2001)	Multispectral Scanner (MSS); Thematic Mapper (TM)	4 7	VIS, NIR, Thermal (68 m by 83 m) VIR, NIR, Mid IR (30 m), Thermal (120 m)	18 days 16 days	Freely available Freely available
		Landsat - 5 (1985 – 2011 (TM) / 2013 (MSS))	MSS	4	VIS, NIR, Thermal (68 m by 83 m)	18 days	Freely available
			TM	7	VIR, NIR, Mid IR (30 m), Thermal (120 m)	16 days	Freely available
		Landsat - 7 (1999 -)	Enhanced Thematic Mapper Plus (ETM+)	8	Panchromatic (15 m), VIR, NIR, Mid-IR, SWIR (30 m) Thermal (60 m)	14 days	Freely available
		Landsat - 8 (2013 -)	Operational Land Imager (OLI) Thermal Infrared Sensor (TIRS)	9 2	Panchromatic (15 m), VIR, NIR, Mid-IR, SWIR (30 m) Thermal (100 m)	15 days 16 days	Freely available Freely available
	ASTER	Terra (1999 -)	Advance Space-borne Thermal Emission and Reflection Radiometer (ASTER)	14	VIS, NIR (15 m), SWIR (30 m), Thermal (90 m)	16 days	Commercially, Research
	CBERS	China-Brazil Earth Resources satellite CBERS-4 (2014 -)	Multispectral Camera (MUXCam); Panchromatic and Multispectral Camera (PanMUX); IRMSS-2 (Infrared Multispectral Scanner-2); WFI (Wide-Field Imager)	4, 4, 4, 4	VIS (20m); Panchromatic (5m), VIS, NIR (10 m); NIR, SWIR (40m), TIR (80m); VIS, NIR (64m)	26, 52, 26, 5 days	Freely available
	IRS	Indian Remote Sensing Satellite IRS-1A (1988 - 1996)	Linear Imaging Self Scanning Sensor (LISS) - I; LISS - II	4, 4	VIR, NIR, (72.5 m); VIR, NIR (36.25 m)	22 days	Commercially, Research
		IRS-1B (1991 - 2003)	LISS - I; LISS - II	4	VIR, NIR, (72.5 m); VIR, NIR (36.25 m)	22 days	Commercially, Research
		IRS-1C (1996 - 2007)	LISS - III	4	Panchromatic (5.8 m), VIR, NIR (23 m), SWIR (70 m)	24 days	Commercially, Research
		IRS-1D (1997 – 2010)	LISS - III	5	Panchromatic (5.8 m), VIR, NIR (23 m), SWIR (70 m)	24 days	Commercially, Research
High resolution	**IRS**	Resourcesat - 1 (2003 - 2013)	LISS - IV	4	Panchromatic, VIR, NIR (5.8 m)	5 days	Commercially, Research
		Resourcesat - 2/2A (2011 -)	LISS - IV	4	Panchromatic, VIR, NIR (5.8 m)	5 days	Commercially, Research
	Sentinel	Sentinel - 2 (A & B) (2015 & 2016 -)	Multispectral Instrument (MSI)	13	VIS, NIR (10 m), SWIR (20 m), other (60 m)	5 days	Freely available
	SPOT	SPOT-1 (1986 - 1990)	Visible High Resolution sensor (HRV)	4	Panchromatic (10 m), VIS, NIR (20 m)	26 days	Commercially, Research
		SPOT-2 (1990 - 2009)	Visible High Resolution sensor (HRV)	4	Panchromatic (10 m), VIS, NIR (20 m)	27 days	Commercially, Research
		SPOT-3 (1993 - 1997)	Visible High Resolution sensor (HRV)	4	Panchromatic (10 m), VIS, NIR (20 m)	28 days	Commercially, Research
		SPOT-4 (1998 - 2013)	Visible and Infrared High-Resolution sensor (HRVIR)	5	Mono-spectral (10 m), VIS, NIR, SWIR (20 m)	26 days	Commercially, Research
		SPOT-5 (2002 - 2015)	High Resolution Geometric sensor (HRG)	5	Panchromatic (2.5 m), VIS, NIR (10m), SWIR (20 m)	26 days	Commercially, Research
		SPOT 6 & 7 (2012 & 2014 -)	New AstroSat Optical Modular Instrument (NAOMI)		Panchromatic (1.5 m), VIS, NIR (6 m)	5 days	Commercially, Research
Very high resolution	**IKONOS**	IKONOS (2000 - 2015)	Optical Sensor Assembly (OSA)	5	Panchromatic (0.82 m), VIS, NIR (3.2 m)	Approx. 3 days	Commercially
	QuickBird	QuickBird (2001 - 2015)	Ball's Global Imaging System (BGIS 2000) sensor	5	Panchromatic (0.65 m), VIS,NIR (2.6 m)	3.5 days	Commercially
	RapidEye	RapidEye (2008 -) multiple	RapidEye Earth Imaging System (REIS)	5	VIS, NIR (5 m)	5.5 days	Commercially
	GeoEye -1	GeoEye-1 (2008 -)	GeoEye Imaging System (GIS)	5	Panchromatic (0.41-0.46 m), VIS, NIR (1.65-1.84 m)	8 to 10 days	Commercially
	WorldView	WorldView-1 (2007 -)	WorldView-60 camera	1	Panchromatic (0.5 m)	2 to 6 days	Commercially
		WorldView -2 (2009 -)	WorldView -110 camera	9	Panchromatic (0.5 m), VIS, NIR (2 m)	1 to 3 days	Commercially
		WorldView - 3 (2014 -)	WV-3 imager, CAVIS	17	Panchromatic (0.3 m), VIS, NIR (1.2 m), SWIR (3.7m)	1 to 5 days	Commercially

Adapted from Muller (2017)

The WFAD technique, as described in Nell et al. (2015), was originally developed based on pan-sharpened 2.5 m SPOT-5 imagery. The motivation for using SPOT-5 imagery was based on its relatively high spatial resolution (10 m; 2.5 m when pan-sharpened) and its availability for research purposes through a license agreement between the South African National Space Agency (SANSA) and Airbus Defence, the owner of the satellite. In addition, the SPOT-5 agreement has been in place since 2005, which meant that historical imagery was readily available. Although the SPOT-5 imagery was effective (Muller & Van Niekerk, 2016a), there are a number of factors that make the imagery less suitable for incorporation into the SAWMS. These include:

1. Suitable image scenes must be manually identified through the use of an online catalogue;
2. The agreement between SANSA and Airbus Defence stipulates that a limited number of scenes may be made available for research (or governmental) purposes, resulting in the unavailability of suitable imagery at a particular location and time (further accentuated by cloud cover);
3. Once identified, images need to be acquired through a written request to SANSA — a time-consuming process;
4. A process of extracting each image separately (by SANSA) then follows, which can take days (sometimes weeks); and
5. Due to the geometric (off-nadir) nature of the SPOT-5 sensor and the absence of offset values for automated radiometric corrections, it is near impossible to accurately translate the imagery's digital numbers to surface reflection values.

The primary consequence of these factors is that SPOT imagery cannot easily be incorporated into an automated EO processing workflow, which significantly decreases the cost-effectiveness of their use. Another factor to consider is that SPOT-5 is no longer in operation. Although two replacement satellites (SPOT6 and 7) are now available (with higher spatial resolutions, but fewer spectral bands), the factors listed above also apply to the new SPOT imagery. Consequently, it was decided to also consider other EO satellites. Focus was placed on services that provide imagery at no cost and that can be easily incorporated into an automated workflow.

Another requirement for the imagery to be used in the SAWMS is that it should have a suitably high spatial resolution. Muller & Van Niekerk (2016b) showed that very high resolution (VHR) satellite imagery (e.g. WorldView-2) is ideal for identifying salt-affected areas when using the indirect approach (i.e. vegetation monitoring), but concluded that "slightly lower spatial and spectral resolution imagery might produce comparable results." Specifically, RapidEye (5 m multispectral) and Sentinel-2 (10 m multispectral) data were suggested as notable candidates. RapidEye was not considered for the SAWMS given that it is a commercial (and expensive) product. Landsat-8 is freely available and arguably the most reliable source of EO imagery, but its relatively low spatial resolution (30 m multispectral) was judged to be too low for identifying salt-affected areas in South Africa.

Another alternative was Sentinel-2 satellite series. The Sentinel-2A satellite developed by the ESA and launched on 23 June 2015. This platform forms part of the European Union's comprehensive Copernicus EO programme aimed at performing terrestrial observations in support of services such as forest and agricultural monitoring, land cover change detection and natural disaster management. Sentinel-2A is the first of two identical, optical satellites. The second, Sentinel-2B, was launched on 7 March 2017. Both satellites acquire images at 10 m, 20 m and 60 m resolutions. Table 2.2 summarises the characteristics of the Sentinel-2 multispectral sensors.

Table 2.2: Sentinel-2 sensor characteristics

Sentinel-2 Bands	Central Wavelength (µm)	Resolution (m)
Band 1 - Coastal aerosol	0.443	60
Band 2 - Blue	0.490	10
Band 3 - Green	0.560	10
Band 4 - Red	0.665	10
Band 5 - Vegetation Red Edge	0.705	20
Band 6 - Vegetation Red Edge	0.740	20
Band 7 - Vegetation Red Edge	0.783	20
Band 8 - NIR	0.842	10
Band 8A - Vegetation Red Edge	0.865	20
Band 9 - Water vapour	0.945	60
Band 10 - SWIR - Cirrus	1.375	60
Band 11 - SWIR	1.610	20
Band 12 - SWIR	2.190	20

A number of factors influenced the use of Sentinel-2 imagery for the development of the SAWMS. First, the imagery is available from the ESA at no cost. Second, the downloading and processing procedures can be automated, which is a critical requirement for a near-real-time monitoring system such as the SAWMS. Third, the spatial resolution is the highest of any freely available imagery (other than the SPOT series), allowing NDVI (used in the WFAD method) to be generated from bands 4 and 8 at a 10 m spatial resolution. Although 10 m is slightly lower than the recommended 6 m by Muller & Van Niekerk (2016b), it is argued that the sensor's nadir viewing angle will compensate for the minor losses in spatial fidelity and (in contrast to SPOT-5) deliver geometrically and radiometrically consistent images. Finally, the Sentinel-2 constellation has a revisit time of five days, which mitigates image unavailability due to cloud cover. Taking all of these factors into consideration, Sentinel-2 imagery was chosen for use in the SAWMS. The next two sections provide an overview of how such imagery is typically processed and analysed.

2.3 Image pre-processing and transformation

Image pre-processing is a processing step often undertaken before analysis in order to improve image quality or ensure radiometric and geometric comparability between images (Campbell & Wynne, 2011). Radiometric variations in recorded EM energy can exist due to differences in sensor type and condition, Earth-sun distances and varying atmospheric conditions. Radiometric correction uses a variety of modelling techniques to convert the EM energy received by the sensor (recorded in unit-less digital numbers) to a physical entity (e.g. absolute radiance or percentage surface reflectance). Geometric inconsistencies can be caused by oblique distortions, relief displacement, Earth rotation and sensor

scan speed. Geometric correction corrects these effects using mathematical algorithms and reference imagery (Mather, 2004). Once remotely sensed imagery has been suitably pre-processed (radiometrically and geometrically), it can be used for comparison purposes and image transformations.

Image transformation is the process of generating a new image from one or more spectral bands with the use of arithmetic operators. The purpose of image transformation is the generation of a new image with properties more suitable to the specific analysis required than the original spectral bands from which it was derived. Various image transformations have been proposed through scientific research and each transformation serves a specific purpose (Campbell & Wynne, 2011).

Some of the well-known image transformations include vegetation indices (VIs), which are based on the principles of band ratioing and basic math operations to yield a single value that represents the degree of vegetation vigour in a single pixel (Campbell & Wynne, 2011). A wide range of VIs exist, with the most common being the NDVI (Equation 2.1). NDVI, like most other VIs, highlights the sharp contrast in the absorptive and reflective properties of vigorous vegetation occurring in the wavelengths between the red and NIR regions of the EM spectrum.

$$NDVI = (N - R)/(N + R)$$ Equation 2.1

where N is the reflectance in the NIR band; and

R is the reflectance in the red band.

Other image transformations used in the report are the soil adjusted vegetation index (SAVI) (Equation 2.2) and the brightness (Br) ratio (Equation 2.3).

$$SAVI = (1 + L)(N - R)/(N + R + L)$$ Equation 2.2

where N is the reflectance in the NIR band;

R is the reflectance in the red band; and

L is the soil adjustment factor (0.5 is a reasonable approximation of the factor when soil exposure is unknown).

$$Br = (B + G + R + N)/4$$ Equation 2.3

where B is the reflectance in the blue band;

G is the reflectance in the green band;

R is the reflectance in the red band; and

N is the reflectance in the NIR band.

2.4 Detecting salt accumulation and waterlogging with satellite imagery

Remote sensing has been proposed as a less time-consuming and more cost-effective method for monitoring salt accumulation and waterlogging, as satellite images cover large areas on a regular, timely basis (Abbas et al., 2013). Various techniques and applications of remote sensing for the identification of salt-affected and waterlogged areas have been published. Detection and monitoring can happen either directly or indirectly (Mougenot et al., 1993). The direct detection of the accumulation of salts involves identifying salt encrustation on the bare ground and for waterlogging it involves identifying surface ponding, while the indirect approach focuses mainly on vegetation responses to salt accumulation and waterlogging.

Several authors have successfully applied the direct approach for identifying salt accumulation (Rao et al., 1995; Dwivedi et al., 1999; Metternicht, 2003; Khan et al., 2005; Abood et al., 2011; Iqbal, 2011; Setia et al., 2013; Sidike et al., 2014). Most of these studies reported that salt crusts generally have high reflectance in the visible and near to mid-infrared regions of the EM spectrum, depending on the chemical composition of the salts (Metternicht & Zinck, 2003). The generally higher spectral reflectance of salt crusts are illustrated in Figure 2.2 where the reflectance of salt crust reaches nearly 80% surface reflectance and is significantly higher than the other lithological classes presented in the figure. Specific spectral ranges for direct salinity detection (identified by laboratory analyses) are in the visible region (550–770 nm), near-infrared region (900–1030 nm, 1270–1520 nm) and middle infrared region (1940–2150 nm, 2150–2310 nm, 2330–2400 nm) (Csillag et al., 1993). Metternicht (2003) observed that applying laboratory techniques to optical remote sensing data to detect salt accumulation is complicated by the variations in reflectance that cannot be attributed to a single soil property and salt type. Spectral variation in salt crusts can be attributed to the difference in the quantity of salts, the mineralogy of the salts (e.g. carbonates, sulphates or chlorides), soil water content, colour of the salt crust (white to dark) and surface roughness of the salt crust (smooth to rough), which all vary among chemical structures. The direct approach also fails to take into account salt accumulation that occurs in the sub-surface, since it is limited to monitoring surface conditions. Directly identifying surface ponding within fields, which generally has low reflectance values throughout the EM spectrum (water), can be directly related to waterlogging (Dwivedi et al., 1998). The spectral signature of water (surface ponding), compared to vegetation and bare soil, is illustrated in Figure 2.3 showing very low spectral reflectance.

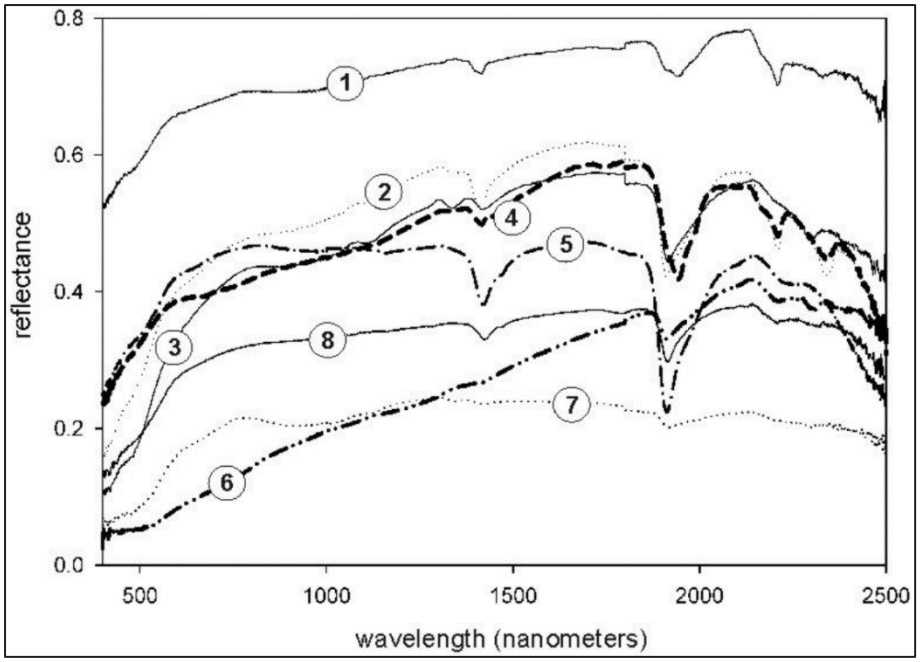

Leverington (2009)

Figure 2.2: Reflectance characteristics of whole-rock samples of lithological units derived from an Analystical Spectral Devices (ASD) FieldSpec 3 in the United States, where: 1 – evaporate salt crust, 2 – Javelina Fm tan-weathering sandstone, 3 – Pen Fm tan-weathering shale, 4 – Aguja Fm tan-weathering sandstone, 5 – Chisos FM ash, 6 – Chisos Fm dark mafic unit, 7 – Chisos Fm tan-weathering basalt, 8 – Tertiary syenodiorite.

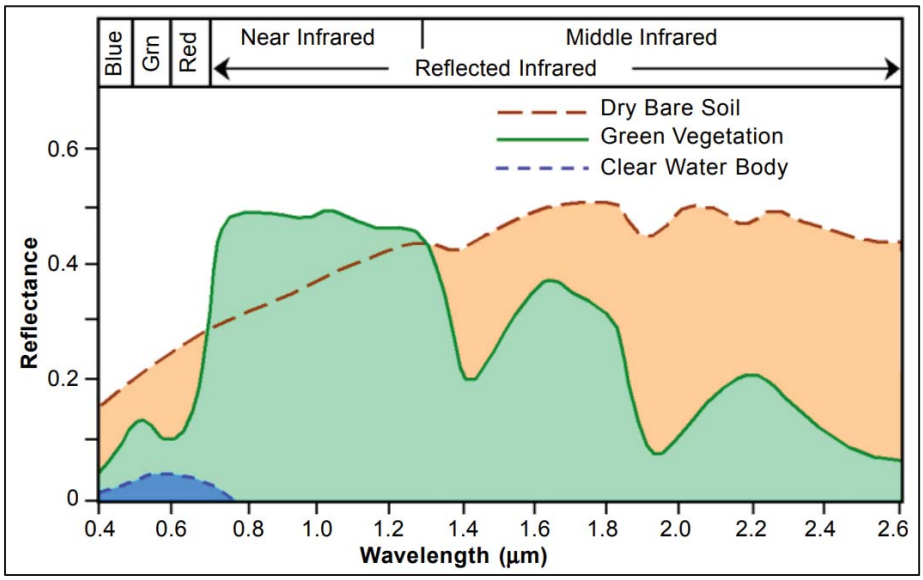

Smith (2012)

Figure 2.3: Spectral reflectance of water compared to green vegetation and dry bare soil

The indirect approach, which mainly focuses on vegetation monitoring, has also been successfully applied to remotely identify salt-affected areas. One approach is to identify halophytic vegetation types that commonly occur in salt-affected areas (Dehaan & Taylor, 2002; Dehaan & Taylor, 2003; García Rodríguez et al., 2007; Dutkiewicz et al., 2009). However, this method is less suitable for application in irrigated areas where natural vegetation is removed during field preparations. A more common approach in irrigated areas is to monitor vegetation (crop) vigour. For this purpose, vegetation indices (VIs) are primarily used to distinguish between healthy vegetation and stressed vegetation (Figure 2.4). Two of the most used VIs are the NDVI (Elnaggar & Noller, 2010; Aldakheel, 2011; Zhang et al., 2011;

Abbas et al., 2013; Platonov et al., 2013; Sidike et al., 2014) and the SAVI (Elnaggar & Noller, 2010; Koshal, 2010; Abood et al., 2011; Allbed et al., 2014). However, using vegetation response for identifying salinity conditions should be approached with caution because many factors besides soil salinity (e.g. farming practices) can contribute to loss of vegetation vigour (Metternicht, 2003). Different crops in different growing phases also have different tolerances to soil salinity, which further complicates the implementation of the indirect approach.

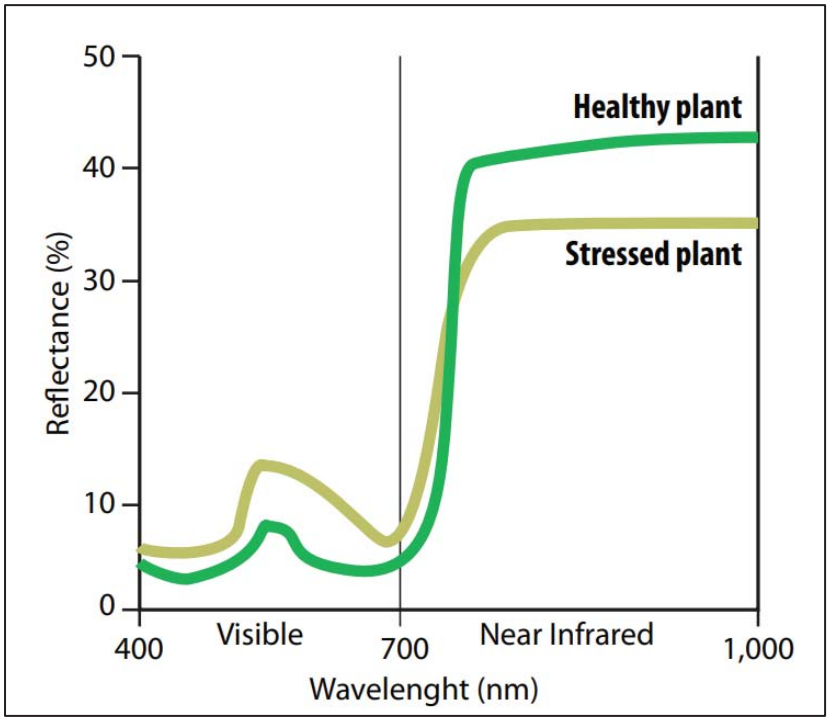

Verhulst & Govaerts (2010)

Figure 2.4: Typical reflectance spectrum of a healthy and stressed plant

2.5 Multi-temporal image analysis

Increased availability and easier access to remotely sensed data, as well as improvements in computer processing software and hardware, have made the analysis of multi-temporal imagery more viable (Pax-Lenney & Woodcock, 1997a; Brooks et al., 2012; Meddens et al., 2013; Jia et al., 2014). In the context of multi-temporal image analysis, it is important to differentiate between change detection (which employs more than one date of imagery to analyse the differences in phenomena over time) (Singh 1989) and multi-date image analysis (where multiple images are used to increase the accuracy of a classification).

The benefits of multi-date image analysis, especially in agriculture, have long been recognised. Steiner & Maurer (1969) illustrated how multi-date aerial photography and machine learning (ML) can be used for mapping crop types, while Badhwar (1982) applied a supervised classifier for crop discrimination using multi-temporal Landsat features. Pax-Lenney & Woodcock (1997b) suggest that, due to the potential for annual land cover fluctuation, single-date satellite images are insufficient for mapping agricultural land use and found a positive correlation between agricultural land use and land use change classification accuracy and the number of images used in the classification. In more recent examples,

Sanhouse-Garcia et al. (2017) conducted multi-temporal analysis of unsupervised Landsat imagery classification to detect agricultural change between 1990–2000 and 2000–2014 in the Culiacan river basin in Mexico, while Kyere et al. (2018) used machine learning to analyse multi-temporal Landsat 8 imagery for crop type mapping in North Hesse in Germany.

The monitoring of salt accumulation and waterlogging requires a multi-temporal approach. Platonov et al. (2013) illustrated the use of multi-temporal Landsat imagery for salinity mapping in the Syrdarya River Basin in Uzbekistan and concluded that multi-temporal analysis increased both the accuracy and cost-effectiveness of salinity mapping. A similar study was conducted by Azabdaftari & Sunar (2016), who concluded that higher spatial and temporal resolutions than those offered by Landsat would result in better correlations with salinity. Sentinel-2, which was used in this study, satisfies both of these requirements.

2.6 Object-based image analysis

The WFAD method was conceptualised within the object-based image analysis paradigm. While traditional methods of image analysis consider each pixel as an individual unit, the increased availability of high spatial resolution satellite imagery has exposed the limitations of per-pixel image analysis. The primary limitation in these analyses is spatial autocorrelation (features close to each other are more similar than features further away), which is inherently more likely to occur in high spatial resolution imagery (Blaschke et al., 2000; Lang, 2008). In addition to mitigating the “salt-and-pepper” effects caused when classifying high resolution imagery, GEOBIA offers the following advantages (Benz et al., 2004; Bock et al., 2005; Hay et al., 2005; Shiba & Itaya, 2006):

- meaningful statistical calculation of spectral and textural qualities;
- the availability of feature qualities such as shape and object topology;
- the intuitive spatial relations between real-world objects and image objects; and
- the ease of integration between GIS and remote sensing environments and flexibility among different software platforms.

At its most fundamental level, GEOBIA is comprised of image segmentation and classification (Castillejo-González et al., 2009; Blaschke, 2010; Peña-Barragán et al., 2011). Segmentation involves the delineation of areas of an image into individual objects. Although there are a variety of methods of segmentation, the bottom-up, region-growing method of multiresolution segmentation (MRS) has been shown to provide good results for a variety of applications and over an array of image types (Baatz & Schäpe, 1999). Repeated iterations of MRS at different scales can result in object layers of different dimensions, which are then analysed in a hierarchical object network. The result is a multi-scale hierarchy of building blocks defined through a process of repetitive testing that provides optimal information for the analysis and classification (Mitri & Gitas, 2002). The next chapter explains how this project made use of GEOBIA to identify areas with fields that are likely salt-affected or waterlogged.

3 WITHIN-FIELD ANOMALY DETECTION

3.1 Conceptual overview

The WFAD method analyses changes in multi-temporal vegetation indices (e.g. NDVI and image brightness) derived from high resolution satellite imagery (e.g. WorldView 2/3/4, SPOT-5/6/7, Sentinel-2) to accommodate both the direct and indirect indicators of salt accumulation and waterlogging (Section 2.3). Although the use of multi-temporal image analysis (Section 2.5) for detecting salt accumulation is not new (Metternicht, 2003), the main challenges of using such an approach are that:

- biomass varies as crops grow;
- the biomass characteristics of different crop types (e.g. citrus vs. grain) vary;
- the salinity tolerance of different crop types varies dramatically; and
- for many crop types, fields are not covered by vegetation throughout the season.

These variations make the identification of stressed areas very difficult, particularly if the multi-season satellite images are not acquired at exactly the same period in the growth cycle of a particular crop. The WFAD circumvents these complications by only considering relative biomass or soil brightness variations (as represented by the vegetation/brightness indices) within each individual field. If a particular area within a field has a relatively low biomass or high brightness compared to the rest of the field, it is flagged as an anomaly (different from the rest of the field). This process is repeated on historical imagery to identify areas that are consistently different (stressed).

The WFAD was compared to hundreds of in situ soil samples collected in nine irrigation schemes throughout South Africa as part of a published WRC project (report TT 648/15). The selected schemes represented varying climatic, environmental and agricultural conditions (e.g. crop types and farming practices) to effectively evaluate the WFAD's accuracy and robustness. Overall, salinity and/or waterlogging detection accuracies of 75% (0.6 kappa) were achieved. Most of the misclassifications were related to other soil conditions (e.g. compaction and rocks), which demonstrated the robustness and transferability of the approach as well as its value as a scoping mechanism to identify soil-related problems in irrigated fields.

The first step of the WFAD process is to perform image segmentation on the SPOT-5 image (Section 2.6) to produce objects that best represent the levels of homogeneity within a field. Hierarchical segmentation, one of the spatial features of GEOBIA, enables more than one level of segmentation and the sharing of inherent properties between object levels (Campbell & Wynne, 2011). A vector layer of previously delineated fields is used for the first (*parent*) segmentation level. Below the *parent* object level, MRS is used to populate the *parent* objects with smaller *child* level objects (Figure 3.1). Each *child* object inherits all the properties (e.g. mean NDVI) of its relative *parent* object.

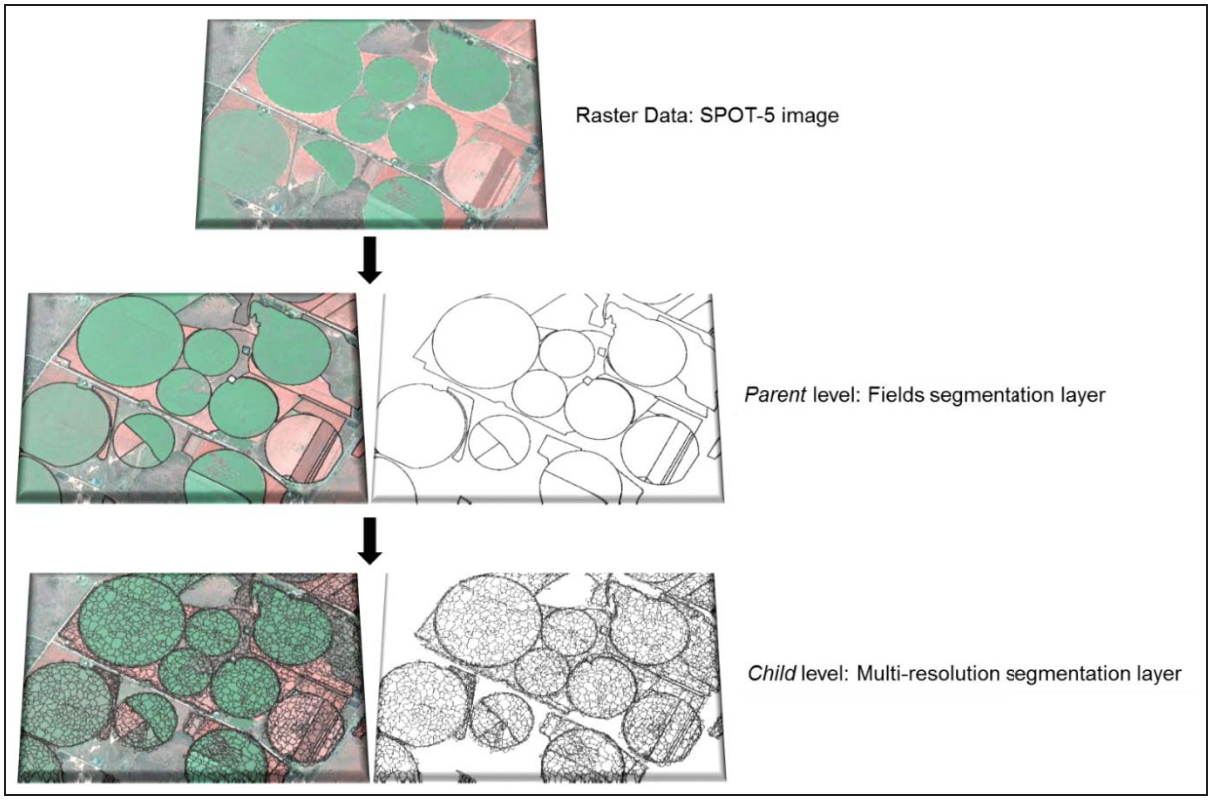

Figure 3.1: Hierarchical within-field anomaly detection segmentation process

The second step in the WFAD process is to classify the image objects. Although a wide range of classification approaches and procedures to assign classes to the objects is available, a rule-based (expert system) classification approach was preferred as it has the ability to accommodate observable differences and changes within the data. A ruleset approach also does not require training data and the rules can progressively be applied and refined while maintaining full control of the classification process (Lucas et al., 2007).

Fields of each irrigation scheme are firstly classified as *vegetated* or *bare* on the *parent* level using the NDVI. Secondly, for the identification of anomalies, the spectral response of each *child* object is compared to the average spectral response of its relative *parent* object. If a substantial difference occurs between a *child* object and the relative *parent* object, the *child* object is identified as an anomaly. This process is illustrated in Figure 3.2.

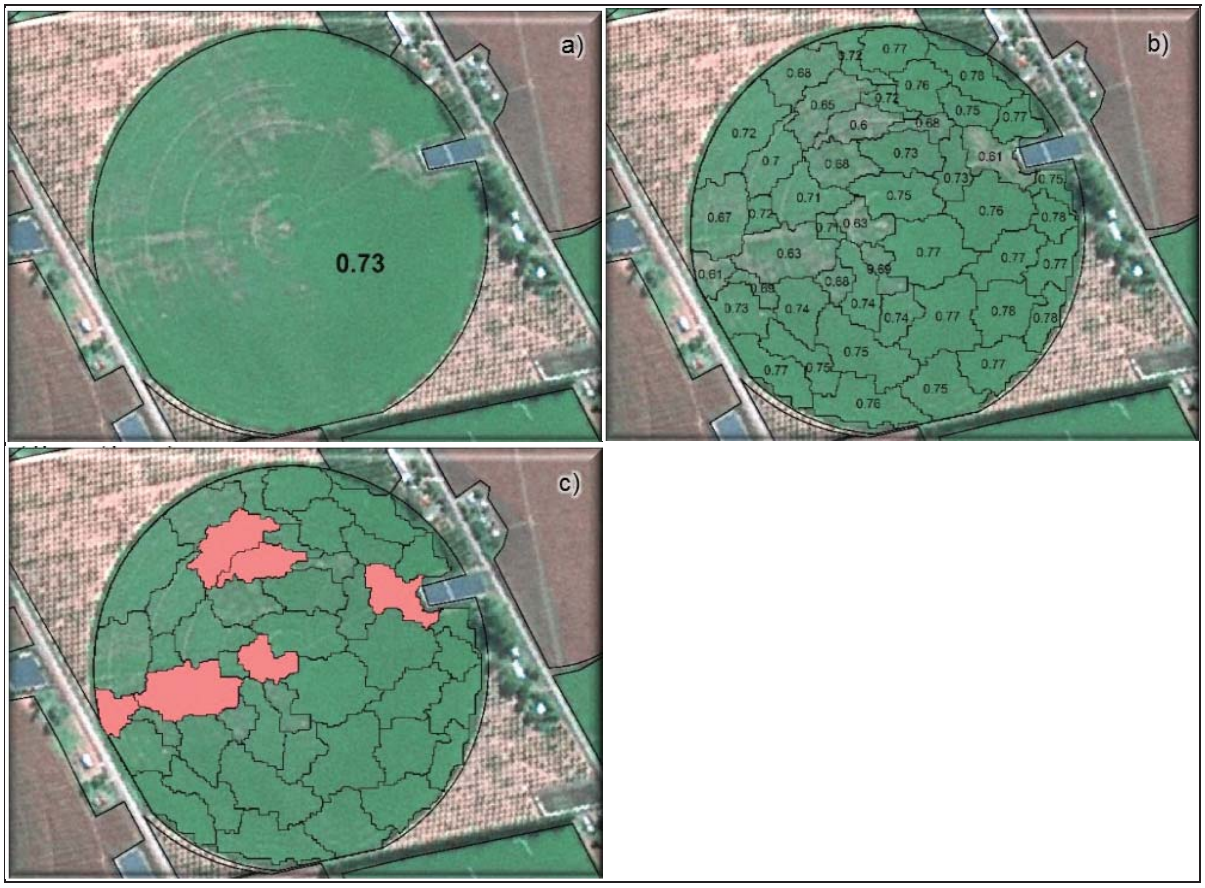

Figure 3.2: Process of anomaly detection in which the a) mean NDVI value of the parent object is used as reference against which the b) NDVI values of the child objects are compared, resulting in c) a set of identified anomalies (shaded in red)

An equation is used to calculate a threshold value that would highlight anomalies with a substantially different spectral response to the rest of the field. This threshold, called the mean difference (MeaD) threshold, is defined as:

$$MeaD = SR_{Child\ object} - SR_{Relative\ Parent\ object} \qquad \textbf{Equation 3.1}$$

where $SR_{Child\ object}$ is the mean spectral response of a child object; and

$SR_{Relative\ Parent\ object}$ is the mean spectral response of the relative parent object.

A positive MeaD threshold identifies a *child* object with a substantially higher spectral response compared to the relative *parent* object, while a negative MeaD threshold identifies a *child* object with a substantially lower spectral response compared to the relative *parent* object.

In order to accommodate the different indicators for soil salinity and waterlogging, different spectral responses are used for comparing the *child* and *parent* objects of vegetated (indirect indicators) versus that of fallow (direct indicators) fields.

The NDVI is used to identify anomalies in vegetated fields. Given that the main indicator of salt

accumulation and waterlogging in vegetated fields is physiological stress (Wiegand et al., 1994; Lenney et al., 1996; Penuelas et al., 1997; Fernandez-Buces, 2006; Koshal, 2010; Lobell et al., 2010; Abood et al., 2011; Zhang et al., 2011), only a negative MeaD threshold is used. Although halophytic vegetation can occur within vegetated fields, it was assumed that its growth vigour response would be less than that of a commercially grown crop.

For fallow fields, the NDVI and a brightness band ratio (*Br*) (Equation 2.3) are used. A positive MeaD threshold is implemented for the NDVI on bare fields to identify potential halophytic plants (Dehaan & Taylor, 2002; Dehaan & Taylor, 2003; García Rodríguez et al., 2007; Dutkiewicz et al., 2009; Elnaggar & Noller, 2010). To detect salt encrustations, which generally show high reflectance values in the visible and near-infrared regions, a positive MeaD threshold is used for the Br (Rao et al., 1995; Dwivedi & Sreenivas, 1998; Metternicht & Zinck, 2003; Khan et al., 2005; Elnaggar & Noller, 2010; Abood et al., 2011; Iqbal, 2011; Setia et al., 2013; Sidike et al., 2014). A negative MeaD threshold is used to accommodate the generally low reflectance values associated with waterlogging (ponding) (Dwivedi & Sreenivas, 1998). Anomaly detection is repeated for multiple images, and anomalies occurring in more than one image are considered as potential salt-affected or waterlogged areas. This multi-temporal approach is assumed to eliminate anomalies caused by factors unrelated to salt accumulation or waterlogging (Furby et al., 1995; Lenney et al., 1996; Lobell et al., 2010). The next section provides details of how the WFAD was modified for operational (automated and near real-time) monitoring of salt accumulation and waterlogging using Sentinel-2 imagery.

3.2 Implementation and operationalisation

3.2.1 Image retrieval subsystem

As explained in Section 2.2, while SPOT-5 imagery was used in the conceptualisation of WFAD, Sentinel-2 imagery was exclusively used for the operationalisation of the SAWMS. Sentinel-2 imagery is available for download from the Copernicus Programme's Scientific Data Hub[1]. Automated browsing and accessing requests can be sent to the application programming interface (API) Hub by making use of two dedicated API interfaces namely Open Data Protocol (OData) and Open Search (Solr). According to the API manual[2], "the OData interface is a data access protocol built on core protocols like HTTP and commonly accepted methodologies like REST that can be handled by a large set of client tools as simple as common web browsers, download-managers or computer programs such as cURL or Wget. OpenSearch is a set of technologies that allow publishing of search results in a standard and accessible format. OpenSearch is RESTful technology and complementary to the OData. In fact, OpenSearch can be used to serve as the query aspect of OData, which provides a way to access identified or located results and download them."

For the purposes of this project, a Python script that makes use of the Wget and Aria2 retrieval software was implemented. A script developed and distributed on GIThub[3] by Oliver Hagolle was modified for

[1] https://scihub.copernicus.eu/
[2] https://scihub.copernicus.eu/userguide/5APIsAndBatchScripting
[3] https://github.com/olivierhagolle/Sentinel-download

the purposes of the SAWMS. The Python script was set up to automatically download images according to the Sentinel-2 tile numbers (locations). A maximum cloud cover threshold of 20% was set to limit the number of download candidates to mostly cloud-free images.

For imagery to be comparable, it must first be prepared (pre-processed) for analysis by applying geometrical and radiometric corrections (Section 2.3). Once it is pre-processed, new information can be extracted through image transformation and classification. The following subsections discuss the pre-processing and transformation steps.

3.2.2 Image orthorectification and radiometric correction

According to ESA documentation[4], the level 1C Sentinel-2 images downloaded by the image retrieval subsystem are orthorectified (geometrically corrected Section 2.3) to sub-pixel accuracy (i.e. 10 m or better). Visual inspections of the downloaded images confirmed this. There was thus no need to implement an additional geometrical correction procedure into the SAWMS workflow.

In terms of radiometric corrections, Sentinel-2 imagery is provided in top of atmosphere (TOA) reflectance. The raw digital numbers captured by the Sentinel-2 sensor are thus corrected for the effects of differences in illumination geometry by using solar angle measurements, Earth-sun distances and sensor specific calibration information. Most quantitative remote sensing implementations require TOA reflectance to be converted to top of canopy (TOC) reflectance (also known as surface reflectance). This involves an additional step to remove the effects of the atmosphere and terrain. Most atmospheric correction methods require information about the atmospheric conditions at the time of image acquisition. Such data are often not available, which means that many methods require settings that qualitatively describe the expected conditions for a particular region (e.g. “clear”, “dry”) or a procedure to quantify the visibility level. Deciding on the appropriate settings requires interactive (pre- and post-correction), manual inspection of spectral responses of different land covers per individual image. Inappropriate settings can lead to “over corrections”, which can have a deteriorating effect on the imagery. Due to the uncertainties involved in setting appropriate parameters and the need for manual inputs, TOA is used by many automated classification systems (Baraldi et al., 2010).

Given the uncertainties involved in setting appropriate parameters and the need for manual inputs, it was decided to utilise TOA reflectance, as provided by the level 1C product, for the SAWMS implementation. Another justification for not attempting to transform TOA to TOC reflectance is that the WFAD method uses unitless band ratios and indices (e.g. NDVI and brightness) as input, which are less affected by atmospheric influences (especially indices that use longer wavelengths, such as in the red and near-infrared region of the electromagnetic spectrum). In addition, terrain effects on the radiometric quality of the TOA imagery will likely be very limited given that most agricultural fields are relatively flat (Act 9238 of 1984 prohibits the ploughing of slopes exceeding 20%). Errors and interference originating from terrain and atmospheric effects will also be reduced due to the use of a

[4] https://earth.esa.int/web/sentinel/user-guides/sentinel-2-msi/product-types/level-1c

multi-temporal approach (i.e. interference is reduced by making repeated observations).

For the sake of future improvements of the system, it is suggested that more research should be done in finding an operational solution for automated atmospheric corrections. This would be of particular value should the functionality of the SAWMS be extended to include quantitative analyses such as the studying of spectral profiles of salt-affected soils to distinguish between salt types. A likely solution would be to incorporate the open source Sentinel Application Platform (SNAP) into the workflow, but more research is needed to assess the outputs of this model.

3.2.3 Image transformation

Software was developed to automatically calculate a variety of vegetation indices and band ratios and to perform principal component analyses on the input imagery. The vegetation indices and band ratios used in the SAWMS are the NDVI (Equation 2.1), the SAVI (Equation 2.2) and an image brightness ratio (Br) (Equation 2.3).

These indices are based on the research carried out as part of WRC project 1880/15 Nell (Nell et al., 2015), but other indices can easily be incorporated in the workflow. All the original spectral bands from the Sentinel-2 imagery are retained by the system, which means that new indices or band ratios can easily be implemented should it be required.

3.2.4 Image analysis workflow

As explained in Section 3.1, the WFAD method was originally developed for VHR (2.5 m) SPOT-5 imagery. The use of such high resolution imagery allowed for the detection of small affected areas, but such imagery is also susceptible to within-class variabilities (i.e. variations within affected areas), which necessitated the use of a GEOBIA approach (Section 2.6). By defining objects of similar but not identical spectral response, the MRS algorithm implemented in eCognition software was particularly useful in eliminating such variations (Muller 2017).

As discussed in Section 2.2, the Sentinel-2 imagery that was selected for use in the SAWMS has a spatial resolution of 10 m. Using a GEOBIA approach on such imagery would provide little benefit over a per-pixel approach, as the objects of interest (salt-affected and waterlogged areas) are often less than 10 m in width. Additionally, Gilbertson et al. (2017) showed that GEOBIA provided almost no advantage over per-pixel methods for crop type classification using pan-sharpened (15 m) Landsat 8 imagery and found that the risk of selecting “inappropriate” segmentation parameters can have a substantial deteriorating effect on accuracy. This is particularly true for fully automated procedures, as the selection of segmentation parameters is considered an ill-structured problem requiring manual experimentation for each scene and application. In addition, implementing a GEOBIA approach as part of the SAWMS workflow would require the segmentation of each downloaded image, which would substantially increase processing requirements and running costs. It was therefore decided that a per-pixel approach would be sufficient for the SAWMS’s image analysis workflow. The WFAD method was consequently modified accordingly. This involved the implementation of a per-pixel, parent-child comparison

procedure (which is inherent in GEOBIA) using an agricultural field boundary layer as the parent layer and the individual pixels as the child layer instead of groupings of pixels (i.e. objects).

The SAWMS image analysis workflow (IAW) was designed to automatically generate a monthly set of anomalies per Sentinel-2 tile. The IAW was developed using the Python scripting language together with the ArcGIS Python application programming interface (arcpy). The IAW consists of five modules as described in the following subsections.

3.2.4.1 Module 1: Set parameters

The IAW was developed to automatically detect and delineate anomalies based on the modifiable parameters listed in Table 3.1. The first parameter (A) determines the storage location of the images that were downloaded and prepared for analysis. Parameter B specifies which field boundary vector dataset to use in the SAWMS. This allows for updating the field boundary vector data when more up-to-date data becomes available. Parameter C specifies the Sentinel-2 tile number to consider in the analysis (i.e. it determines the geographical extent of the SAWMS). The period within which imagery should be considered is determined by parameter D. Parameter E specifies a list of input image features to use, as well as a list of thresholds for each. All of these parameters can either be set manually or updated programmatically.

Table 3.1: Modifiable parameters of the image analysis workflow

#	Name	Description
A	Database paths	A database path is necessary to link the downloaded and transformed images to the IAW
B	Vector field boundaries	The specific field boundary vector data used in the SAWMS needs to be specified
C	Sentinel-2 tile number	Limits or extends the processing extent of the IAW according to the tile numbers specified (e.g. 34JDP, 34JEP)
D	Date query	Limits or extends the processing extent of the IAW according to the specified start and end date
E	Feature and threshold list	The specified image features (e.g. SAVI, Br) with their accompanying threshold values to detect anomalies

For parameter E at least two image features and their relative threshold values must be specified to accommodate bare (direct indicators of salt accumulation or waterlogging) and vegetated fields (indirect indicators of salt accumulation or waterlogging) respectively. Threshold values are based on a percentage difference (PD) unit defined by Equation 3.2 and applied on a pixel level.

$$PD = \left(\frac{Pixel}{Field} * 100\right) - 100 \qquad \text{Equation 3.2}$$

where $Pixel$ is the pixel value; and

$Field$ is the mean response of the field containing the pixel.

A negative PD value implies that the pixel has a lower value than the mean value of its bounding field, while the opposite is implied by a positive value. The PD threshold is applied using the same theory as stipulated in the conceptual overview (application of the *MeaD* threshold in Section 3.1).

SAVI and Br can be replaced by other indices (e.g. NDVI and brightness that excludes NIR) by simply modifying parameter E. This allows for easy experimentation with different indices and thresholds.

3.2.4.2 Module 2: Calculate mean field values

The second IAW module calculates the means of observations (pixels) per field for each of the specified image features (e.g. SAVI, Br). This is achieved using the field boundary vector data (Figure 3.3 B) as input to ArcMap's Zonal Statistics function. In essence, this procedure calculates the sum of all SAVI and Br values (pixels) within each field, which is divided by the number of pixels to generate mean SAVI and Br values.

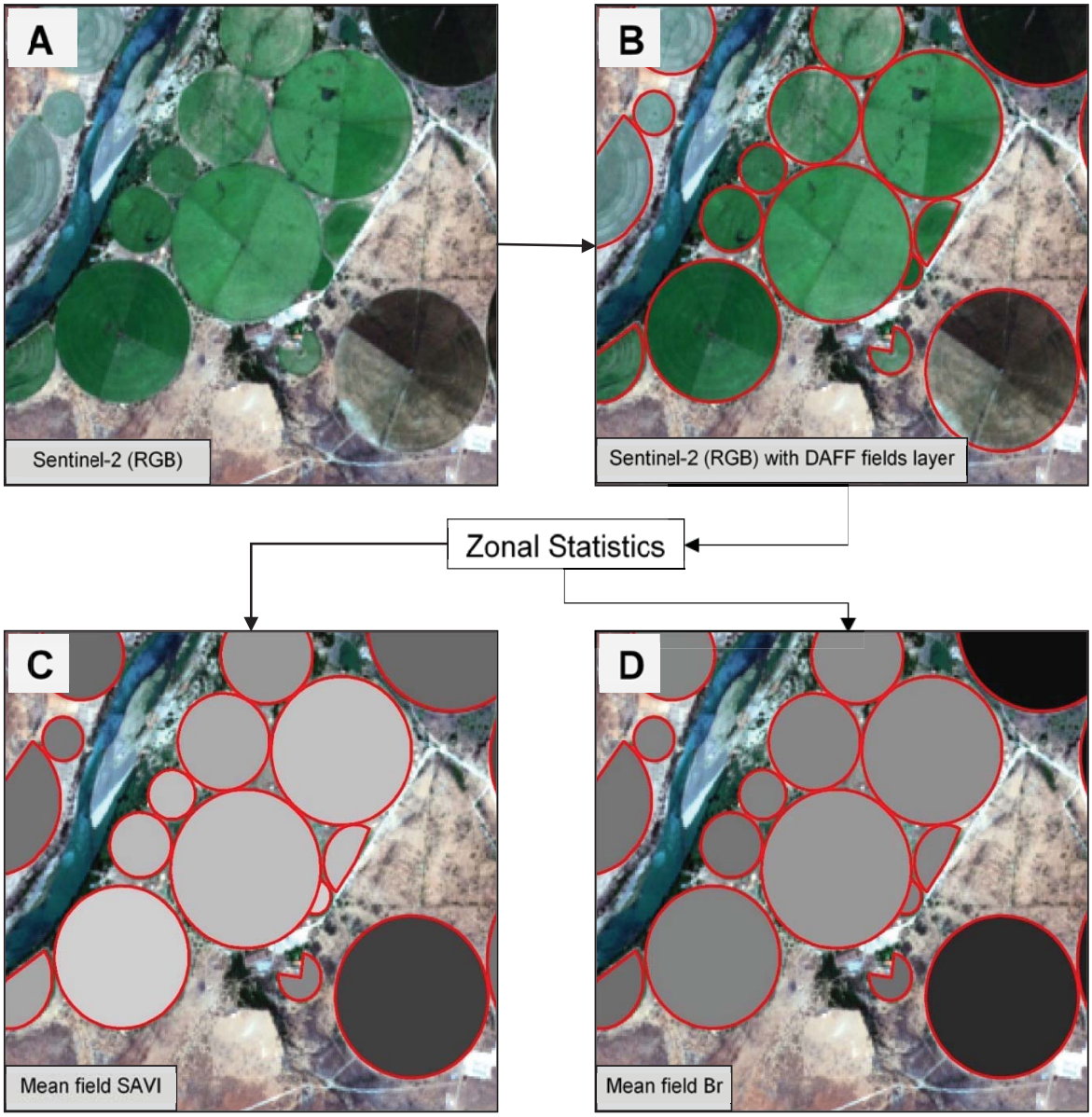

Figure 3.3: Zonal statistics process where the Sentinel-2 imagery (A) is used together with the DAFF field boundaries (B) to generate mean field values for SAVI (C) and Br (D)

3.2.4.3 Module 3: Classify fields

An expert system approach is used to group fields into “vegetated” or “bare” classes. A simple threshold of 0.3 is applied to the mean SAVI values generated in Module 2 for this purpose (Figure 3.4) (SAVI > 0.3 vegetated; SAVI < 0.3 bare). This grouping enables the application of both direct and indirect salt accumulation and waterlogging approaches (as overviewed in Nell et al. (2015)).

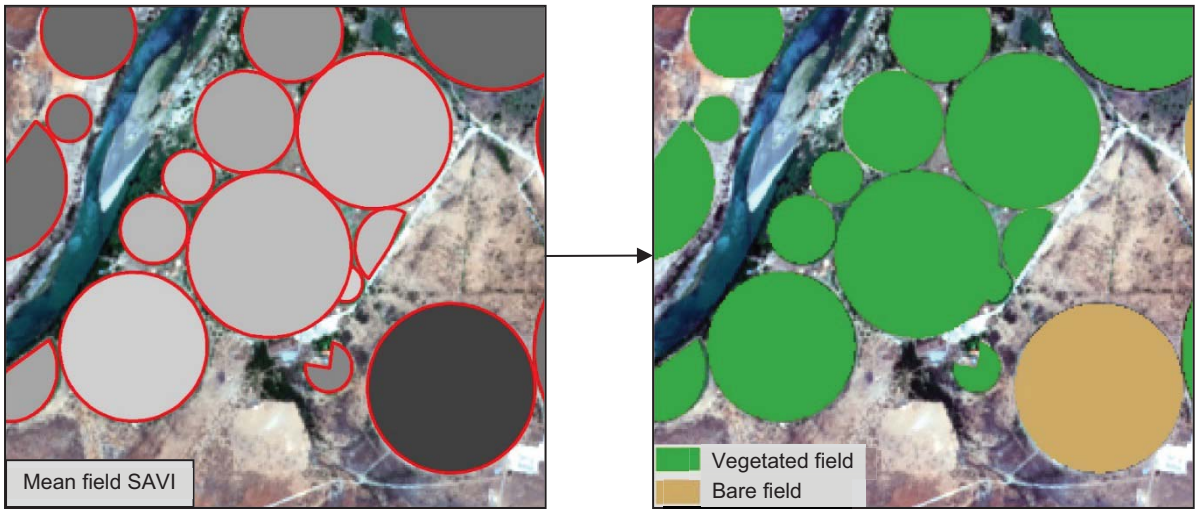

Figure 3.4: Classification of fields into vegetated and bare fields

3.2.4.4 Module 4: Calculate percentage difference and apply thresholds

In Module 4, raster layers representing the PDs specified in Equation 3.2 are calculated using pixel and mean field values. Once the PD layers are available, their associated PD thresholds are applied depending on whether they are vegetated or bare. This results in an anomaly layer as illustrated for vegetated fields in Figure 3.5. A similar approach is used to identify anomalies in bare fields. The final step in the module is to combine the anomalies detected for vegetated and bare fields into a single anomaly layer.

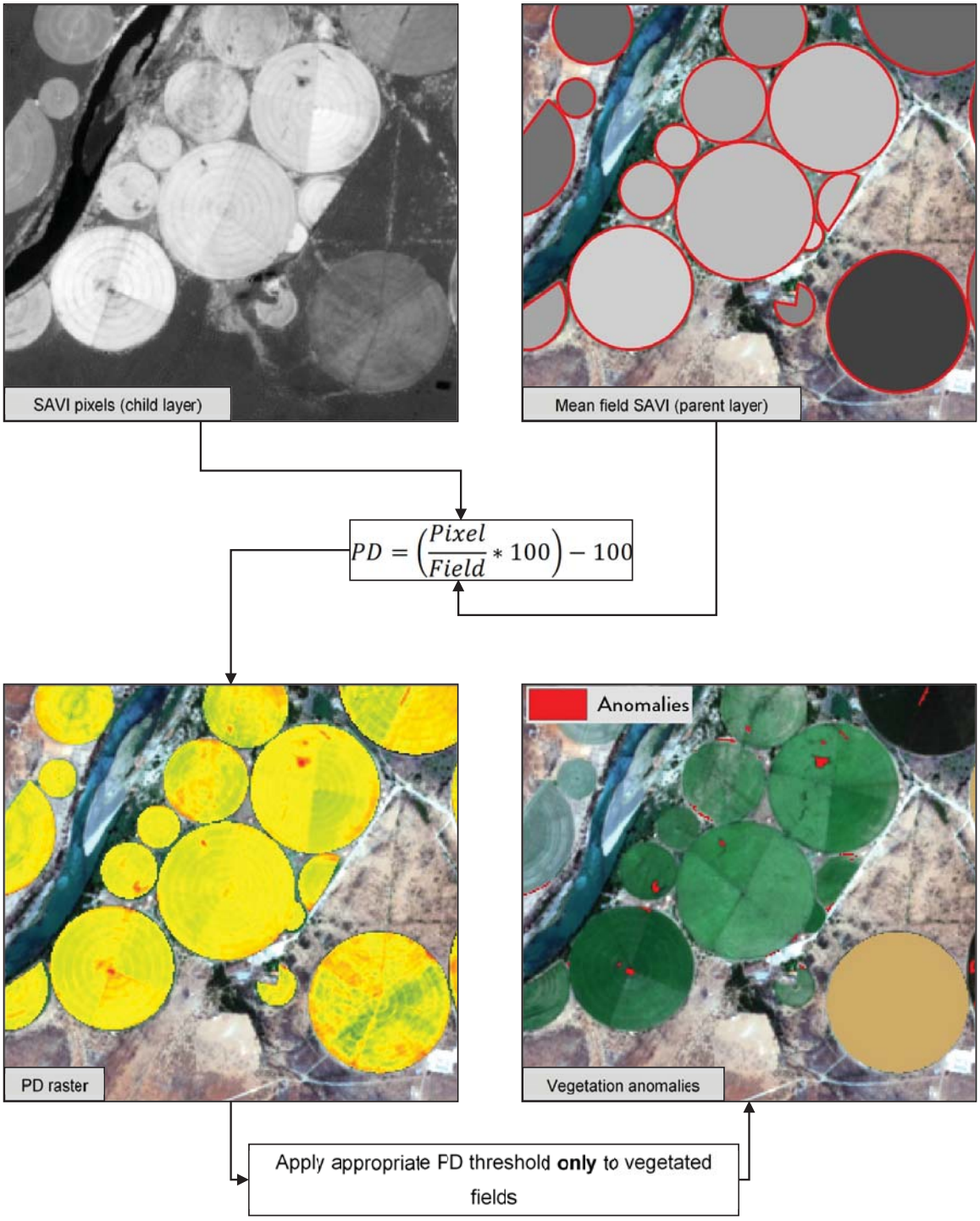

Figure 3.5: The process of percentage difference calculation and threshold application for vegetated fields

3.2.4.5 Module 5: Anomaly frequency index (AFI)

An important feature of the SAWMS is its utilisation of Sentinel-2 imagery, which allows for the generation of within-field anomalies at a five-day interval. Anomalies are mapped for each acquisition date (scene) over a period – up to six per month – which are then combined through binary multiplication to represent anomalies on a monthly interval (Figure 3.6).

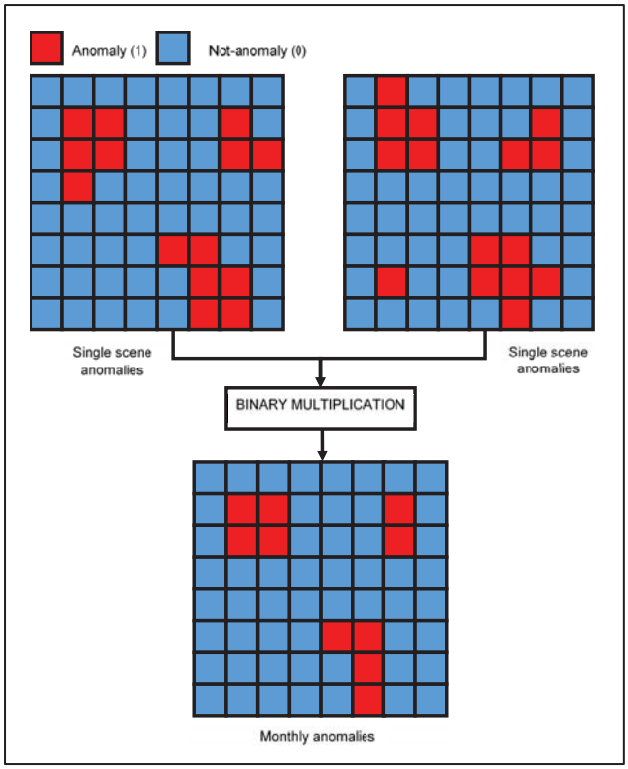

Figure 3.6: Monthly anomaly creation by binary multiplication

The next step is to produce an anomaly frequency index (AFI) by summing the anomaly layers for a specified number of months, as illustrated in Figure 3.7.

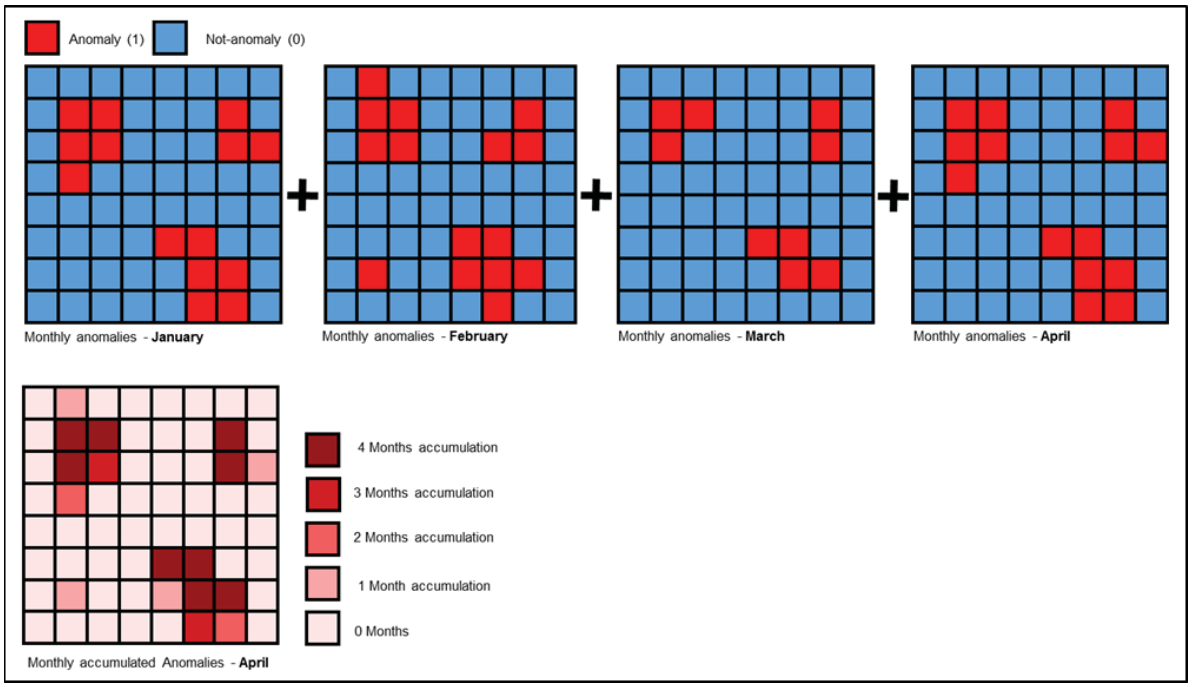

Figure 3.7: Conceptualisation of the anomaly severity index for an arbitrary four-month period

The SAWMS is currently configured to consider a rolling six-month period for generating the monthly AFI. Each AFI layer therefore ranks anomalies according to severity (consistency) from 0 to 6. Table 3.2 explains how this ranking can be interpreted.

Table 3.2: Suggested labels for the anomaly frequency index classification

Number of accumulated months/severity factor	Recommended action [5]
0	Area is very likely unaffected (ignore)
1	Low risk of salt accumulation (ignore)
2	Potential emerging problem and closer inspection is warranted (e.g. compare to previous month for context)
3	Potential problem, field visit is recommended
4	Likely to be an affected area
5	Salinity/waterlogging (or other) problem very likely
6	Definitely a problem area, needs urgent attention

Further refinements to the AFI layer can include the weighting of months, where earlier months receive a lower weighting (importance) compared to more recent months when calculating the anomaly severity factor.

3.2.5 Dealing with inaccurate field boundary data

The SAWMS relies on existing field boundary data to act as the parent objects (see Section 3.1). Currently, the only national field boundary dataset is one collated and distributed by the DAFF as part of the Crop Estimates Consortium (Crop Estimates Consortium 2017). This dataset is updated on a regular basis and the latest version (2017) of the agricultural field boundaries comprises the majority of agricultural field boundaries of SA, digitised from a 1.5 m SPOT 6/7 true colour mosaic. This data is ideal for its intended use (crop estimations at regional scales), but for the purposes of the SAWMS it has a number of drawbacks, namely:

- The digitising was carried out at a relatively small (1:10 000) mapping scale and as such, the boundaries are in some instances too generalised to be used for the WFAD method;
- The boundaries were digitised from a mixture of 2013, 2014 and 2015 imagery, resulting in some of the boundaries being outdated; and
- The dataset does not include sugarcane fields.

Spatial and temporal errors within the existing field boundary databases cause false positive anomalies within the SAWMS. For instance, false positive anomalies are created when fields on the ground have changed since the creation of the field boundary database, which result in a heterogeneous spectral

[5] Note: recommended actions are not verified, and require refinement through further research

signature within the (incorrectly delineated) field. The impact of this is illustrated in Figure 3.8. Another example is when single field polygons contain more than one crop type. In such cases, anomalies can be generated because of the different spectral responses of the different crop types (Figure 3.9).

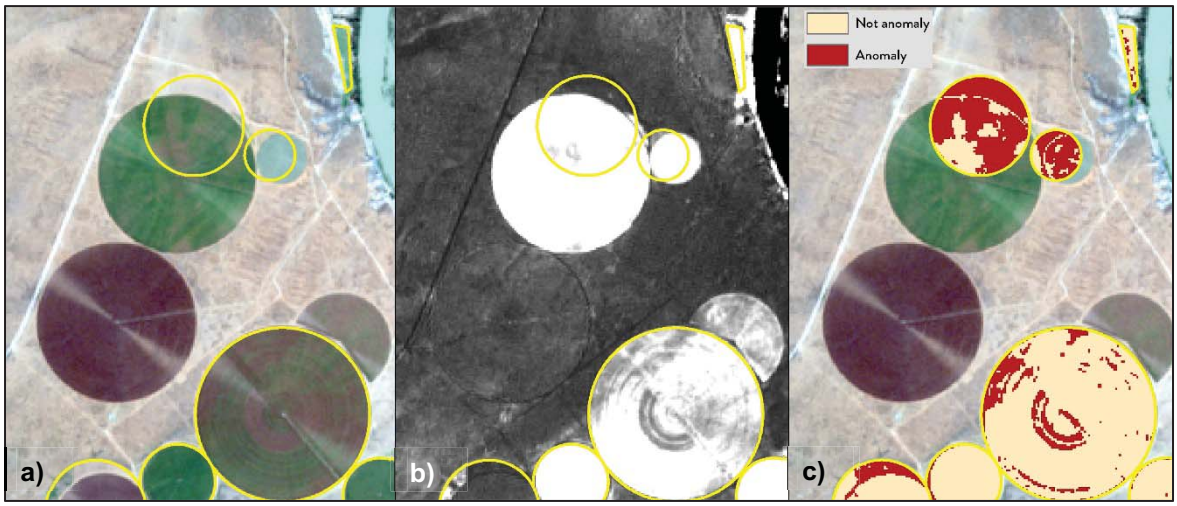

Figure 3.8: False positive anomalies due to outdated field boundaries as compared to a recent a) true colour image, b) vegetation index and c) the resulting impact on the anomaly detection.

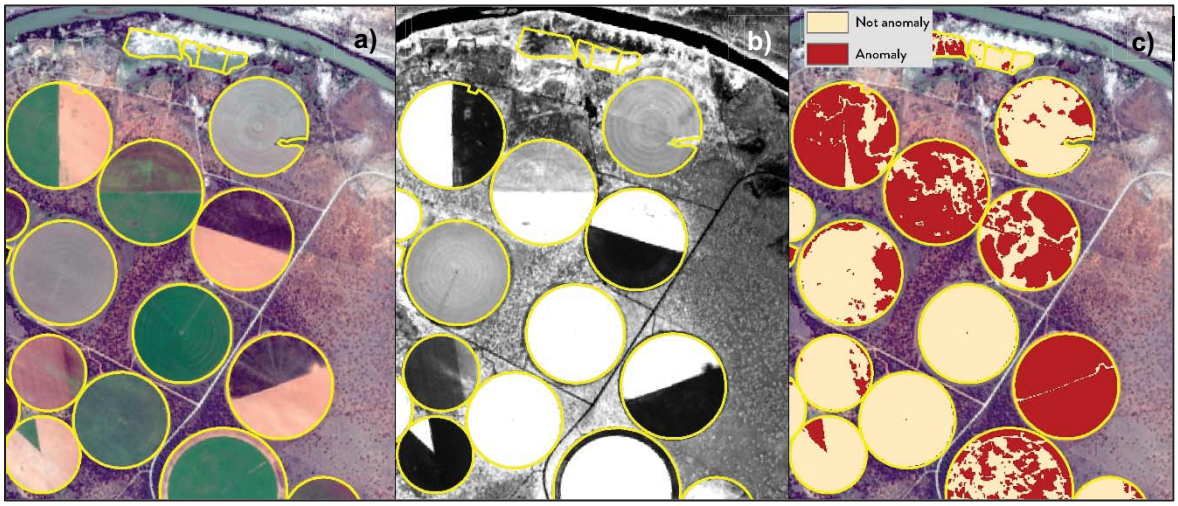

Figure 3.9: False positives due to multiple crops on a single field and the influence of clouds, as compared to a recent a) true colour image, b) vegetation index and c) the resulting impact on the anomaly detection.

These errors are unavoidable as there will always be a mismatch between digitised field boundaries and the imagery, mainly because of the time difference between images used for digitising and those used by the system. However, given that the focus of the SAWMS is to identify smaller areas within fields that are salt-affected and not to identify entire fields that have been abandoned due to salinity, some assumptions can be made to improve the resulting anomaly maps. It was assumed that if the total area of a within-field anomaly is bigger than a certain percentage of the total size of its bounding field, it is likely that the anomaly is a false positive (i.e. not an affected area). Currently, an area threshold of 80% is applied in the SAWMS. This rule thus removes any anomaly with an area that is bigger than

80% of its bounding field (Figure 3.10). A disadvantage of this relative-area rule is that the threshold might remove large anomalies that are legitimately caused by salt accumulation or waterlogging, which could negatively impact the quantifications. However, it is conceivable that the end-user (farmer) would most likely be aware of fields that are affected by more than 80% and would therefore not need to use the SAWMS to identify such fields.

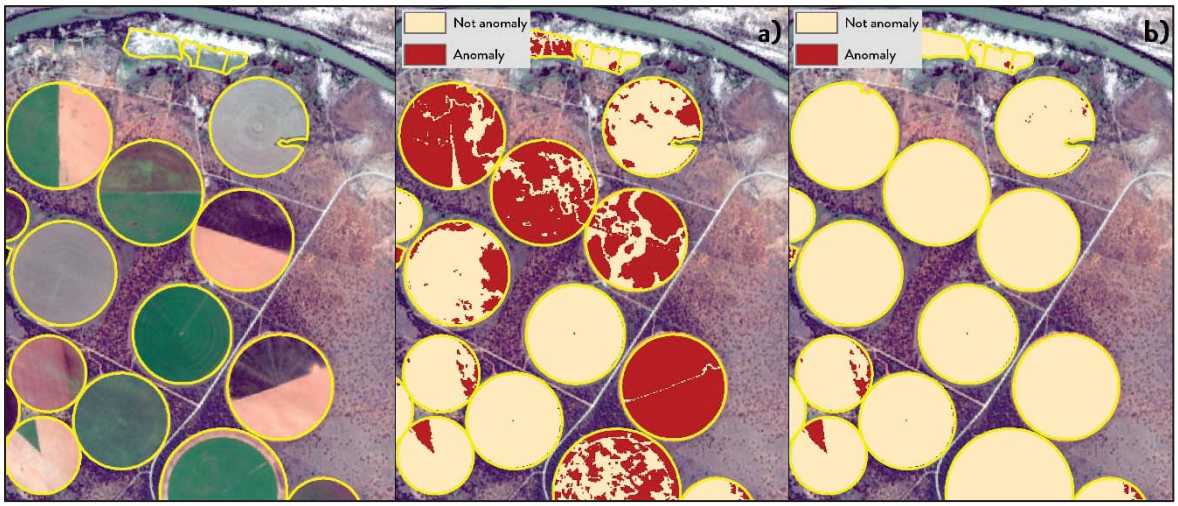

Figure 3.10: Anomalies detected within a a) single month without the relative-area threshold rule applied compared to when b) the relative-area threshold rule was applied.

It should be stressed that false positive anomalies are exceptions and that the vast majority of anomalies are "true positives" or actual anomalies caused by spectral variations within fields. The reader is referred to Appendix III, which is a guideline about the impact of field boundary quality on AFI.

The following chapter provides an overview of the web-based application development.

4 WEB APPLICATION DEVELOPMENT

The SAWMS has been designed to leverage the unique capabilities of the Web as a platform for spatial decision support systems. Web applications offer several advantages for such applications when compared to traditional desktop GIS platforms. More users can be reached, and if a relatively simple and focused design is used, these users do not necessarily need expert knowledge to use the system. Updates to the application or its data can also be done instantaneously. However, web platforms do not typically offer all the processing or visualisation functionality that desktop platforms do, so it is critical that the system is designed in such a way that the needs of the end-users are met.

4.1 System design

The SAWMS was designed to be as simple and easy to use as possible while providing all the functions required by the end-user. The main considerations were to allow the users to leverage the temporality of the data and to provide sufficient context for them to identify their location of interest. The colours chosen for the anomalies and other layers should allow the users to clearly understand the dynamic maps.

The structure of the web application is illustrated in Figure 4.1. More detail of the individual components is provided in the next section.

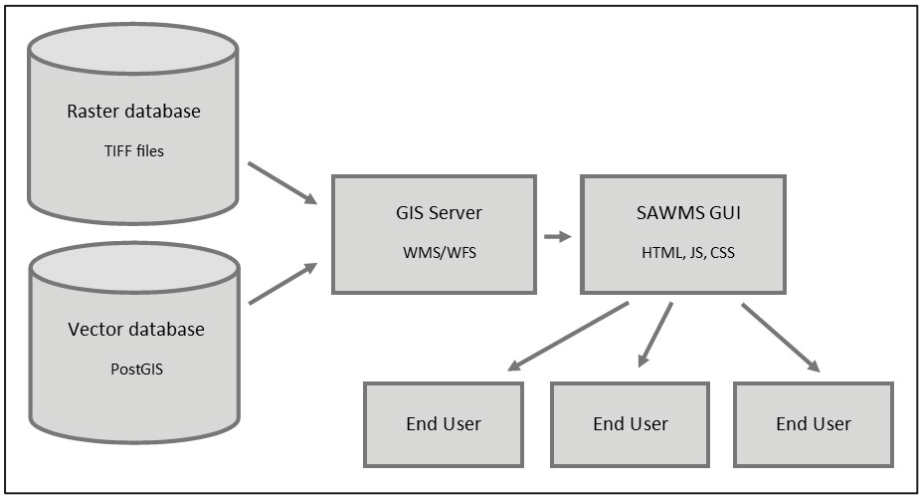

Figure 4.1: System design

4.2 System components

4.2.1 Storage platform

The SAWMS uses one vector layer (the fields boundary layer) and four raster layers (the AFI, the severe anomalies layer, the true colour Sentinel-2 imagery and the derived NDVI). The vector layer is stored in a PostGIS database and the rasters as GeoTIFF files (with Geoserver's ImageMosaic extension providing temporality). The reasoning behind this approach was that these platforms meet the following requirements:

1. accessibility by multiple concurrent web and other users;
2. relatively fast access to the data;
3. allowing for a temporal dimension to the data;
4. allowing for programmatic updates to the data; and
5. being compatible with the chosen GIS server platform as well as common GIS application programs such as ArcGIS or QGIS.

4.2.2 GIS server platform: exposing the data to the Internet

The GIS server exposes the GIS data (vector or raster) stored in the database to the Internet through web services. These services can allow for viewing and/or editing of the data. The GIS server platforms considered for the SAWMS were ArcGIS Enterprise (formerly known as ArcGIS Server), ArcGIS Online, Geoserver and Mapserver.

Geoserver was selected as platform for the SAWMS as it is free, performs well compared to other proprietary platforms and provides the required functionality. The various layers are exposed by Geoserver in open source formats that can be used by a wide variety of web-based clients and GIS software. This effectively means that the layers generated by the SAWMS can be seamlessly incorporated into an existing GIS or be accessed by the many feely available online viewers. The vector datasets (the field boundaries) are served as a web feature service (WFS), which is an open source standard that allows for both feature viewing and editing[6]. The raster datasets are exposed as web mapping service (WMS) layers, which is a similar open source standard that allows for viewing, but not editing, of vector and raster layers (including optional tiling of rasters[7]).

4.2.3 Programmatic ingestion of data

The web application organises the data by month of satellite image acquisition. This allows for cloud-free image composites for most areas, while still providing a high temporal resolution for anomaly monitoring (change analyses). Currently, the interface provides dropdown selectors for month and year (as illustrated in Section 4.3). When the end-user changes the date, both the anomalies and the background Sentinel-2 imagery are updated to match the selected date.

Software has been implemented to update these monthly datasets in an automated manner. The system creates monthly cloud-free composites of the Sentinel-2 imagery and NDVI and converts them to 8-bit rasters in Web Mercator projection. Whenever new monthly anomaly rasters are created, the Geoserver is updated so that they are reflected in the SAWMS.

4.2.4 Platform selection

Various application programming interfaces (API's) that provide GIS functionality to web applications running HTML and Javascript are available. OpenLayers was selected for the SAWMS as it is a fully

6 http://www.opengeospatial.org/standards/wfs
7 http://www.opengeospatial.org/standards/wms

featured and mature open source solution. Other options considered were Leaflet, as well as the ArcGIS API for Javascript and the pre-built, customisable Javascript web applications offered in ArcGIS Online and Portal for ArcGIS.

4.2.5 Graphical user interface (GUI) development

The web application has the primary function of displaying anomalies identified during the WFAD analyses. To contextualise the anomalies, the end-user is able to compare them to monthly cloud-free composites of Sentinel-2 imagery (true colour and derived NDVI). A temporal component is also available through which the end-user can view the anomalies and satellite imagery for previous months and years.

The GUI was developed using the combination of HyperText Markup Language (HTML), Javascript and Cascading Style Sheets (CSS). Geographic functionality is provided by OpenLayers 4.3.3. It features a simple, clear interface with three dropdown boxes to select the year, month and background layer. A demonstration on the use of the GUI is provided in the next section.

4.3 Overview of graphical user interface

When accessing the SAWMS through the web application, the user is presented with a landing page (Figure 4.2), allowing the desired irrigation scheme or agricultural region to be selected.

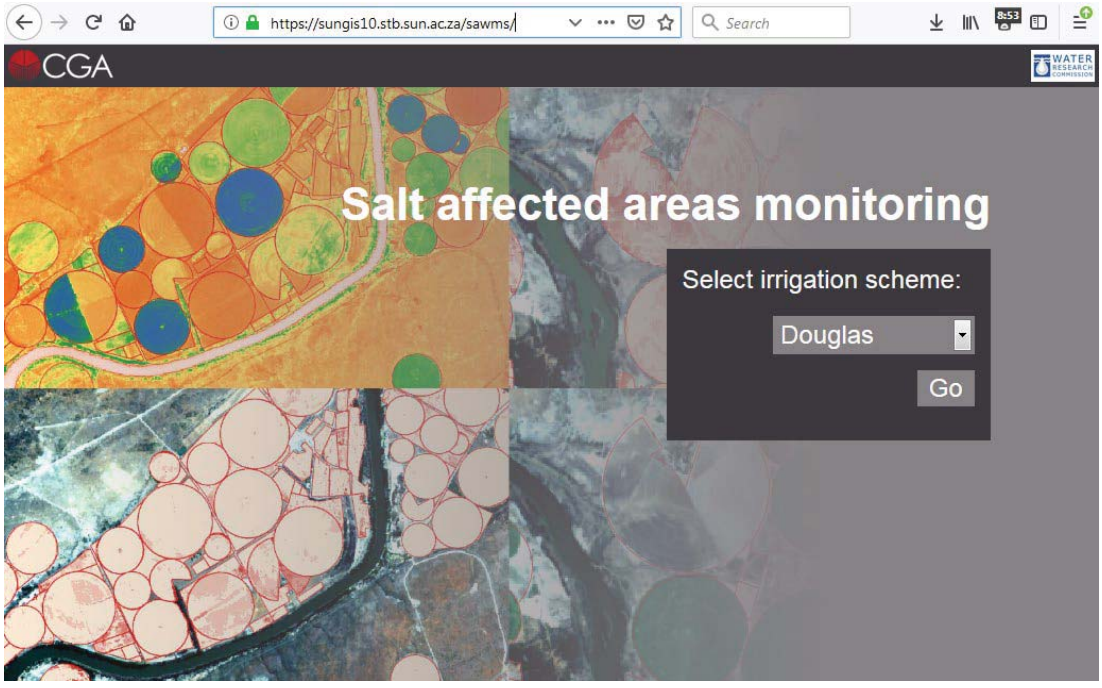

Figure 4.2: The landing page for the SAWMS

The SAWMS web application has a simple GUI with three dropdown boxes. One box controls the available background layers (NGI[8] aerial imagery, Topographical maps, OpenStreetMap, monthly Sentinel-2 true colour and NDVI). The other two boxes (year and month) control the date of the

8 Short for Department of Rural Development and Land Reform: Chief Directorate: National Geospatial Information

anomalies and the Sentinel-2 background layers (Figure 4.3). When loading, the GUI shows the extent of the selected irrigation scheme with OpenStreetMap in the background. OpenStreetMap is considered an ideal backdrop for orientating the user as it provides a good overview of towns, roads and rivers.

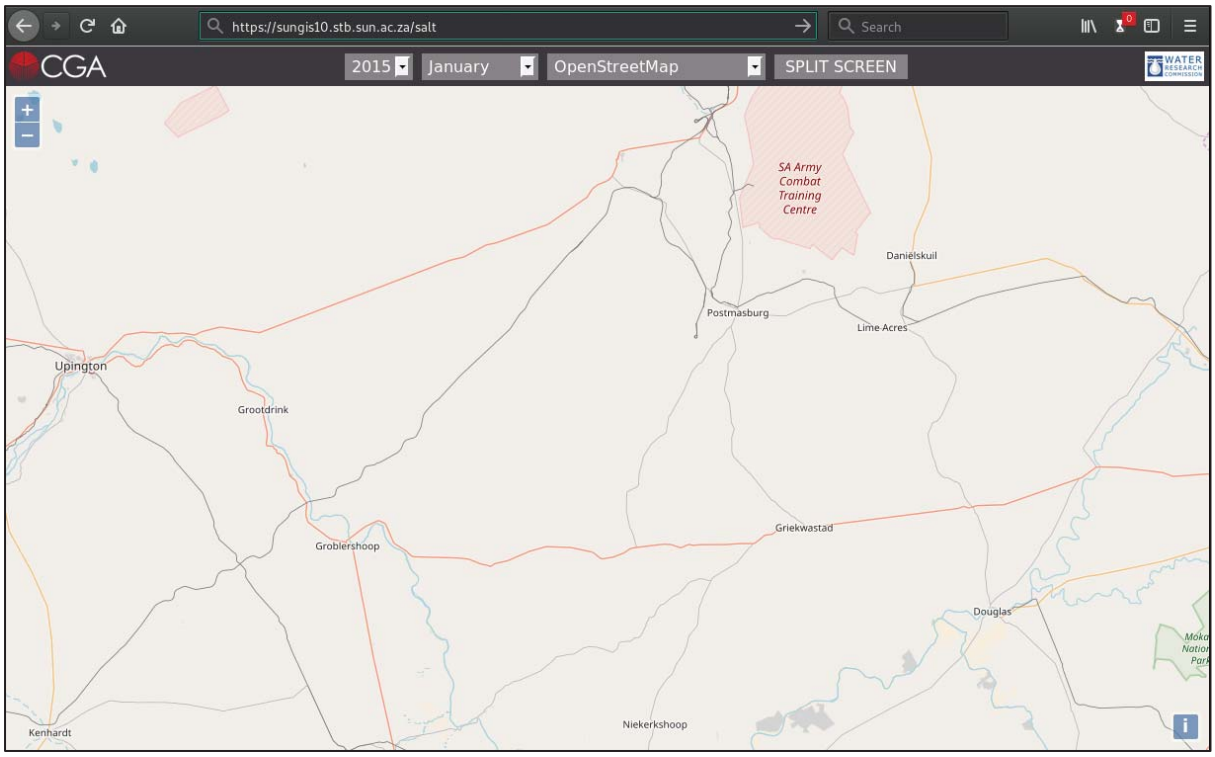

Figure 4.3: Graphical user interface when web application is first loaded

To reduce the loading times of the field boundaries file, fields are only displayed on-screen when the user zooms in to an area of interest (Figure 4.4).

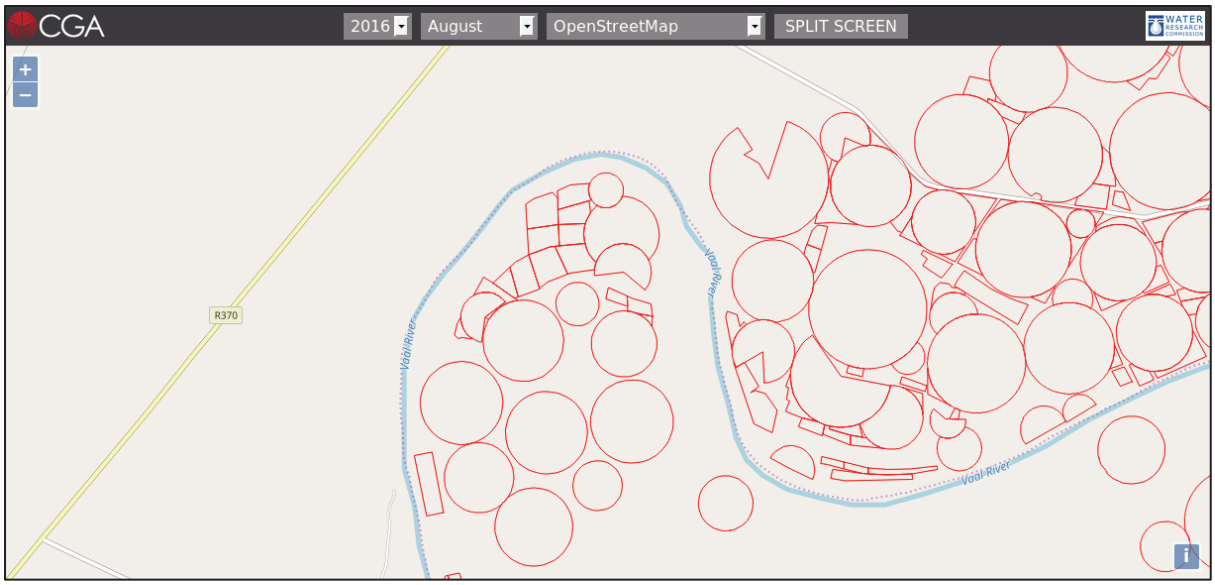

Figure 4.4: When zooming in, field boundaries become visible

The user is then able to change the background to the composite Sentinel-2 image for the selected month. Figure 4.5 shows the web application interface with the Sentinel-2 true colour layer in the

background (the dropdown box showing the background layer is highlighted in yellow).

Figure 4.5: Changing the background layer to Sentinel-2

Figure 4.6 shows the page should the end-user select monthly NDVI composite images (generated from Sentinel-2 imagery) in the dropdown box, while Figure 4.7 shows the page should the end-user choose to view the anomalies for a specified month. A legend has been provided to assist the user in interpreting the AFI.

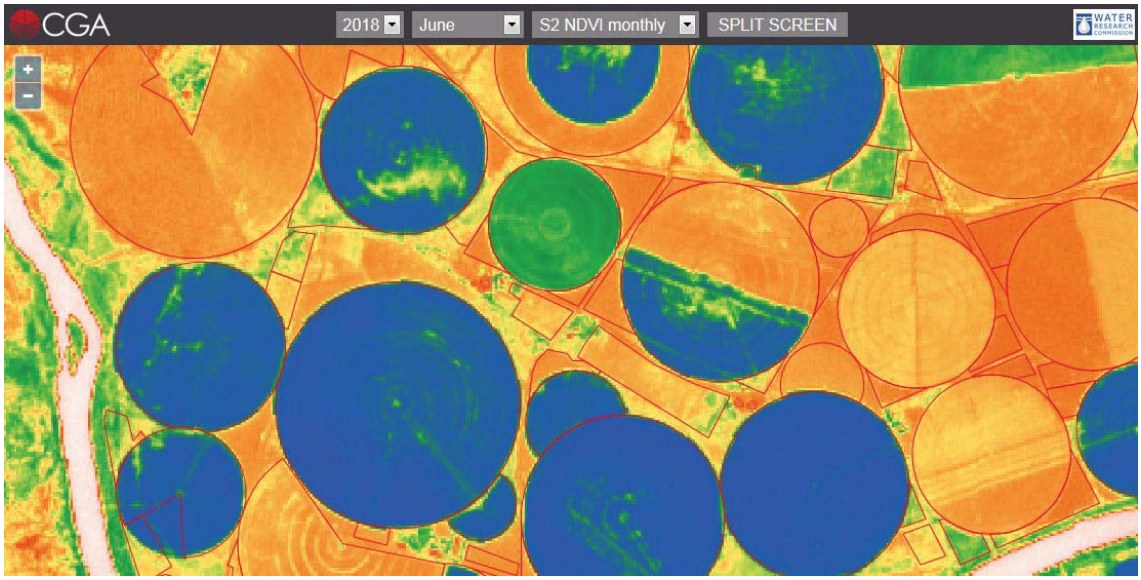

Figure 4.6: Field boundaries, anomalies and the background layer to Sentinel-2 NDVI background layer

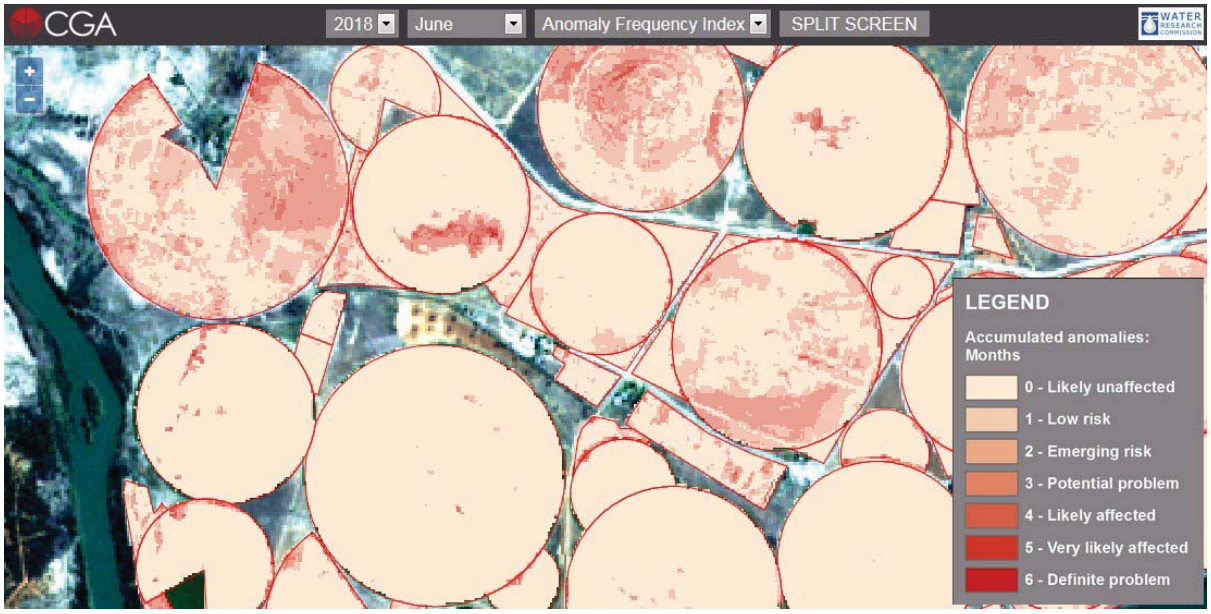

Figure 4.7: Anomaly layer

Figure 4.8 illustrates how to select and view different months. In order to allow direct comparison, a split screen function is provided so that the anomalies can be compared between months or against the Sentinel-2 colour or NDVI imagery (Figure 4.9). This mode is selected by clicking the SPLIT SCREEN button, which opens a new set of dropdown boxes for the second map. Should the user wish to change both maps concurrently, the dates can be linked by clicking “Link Dates” (Figure 4.10). Alternatively, one can compare anomalies (or other layers) from different months (Figure 4.11). The MERGE SCREEN button can be used to return to a single map (Figure 4.12).

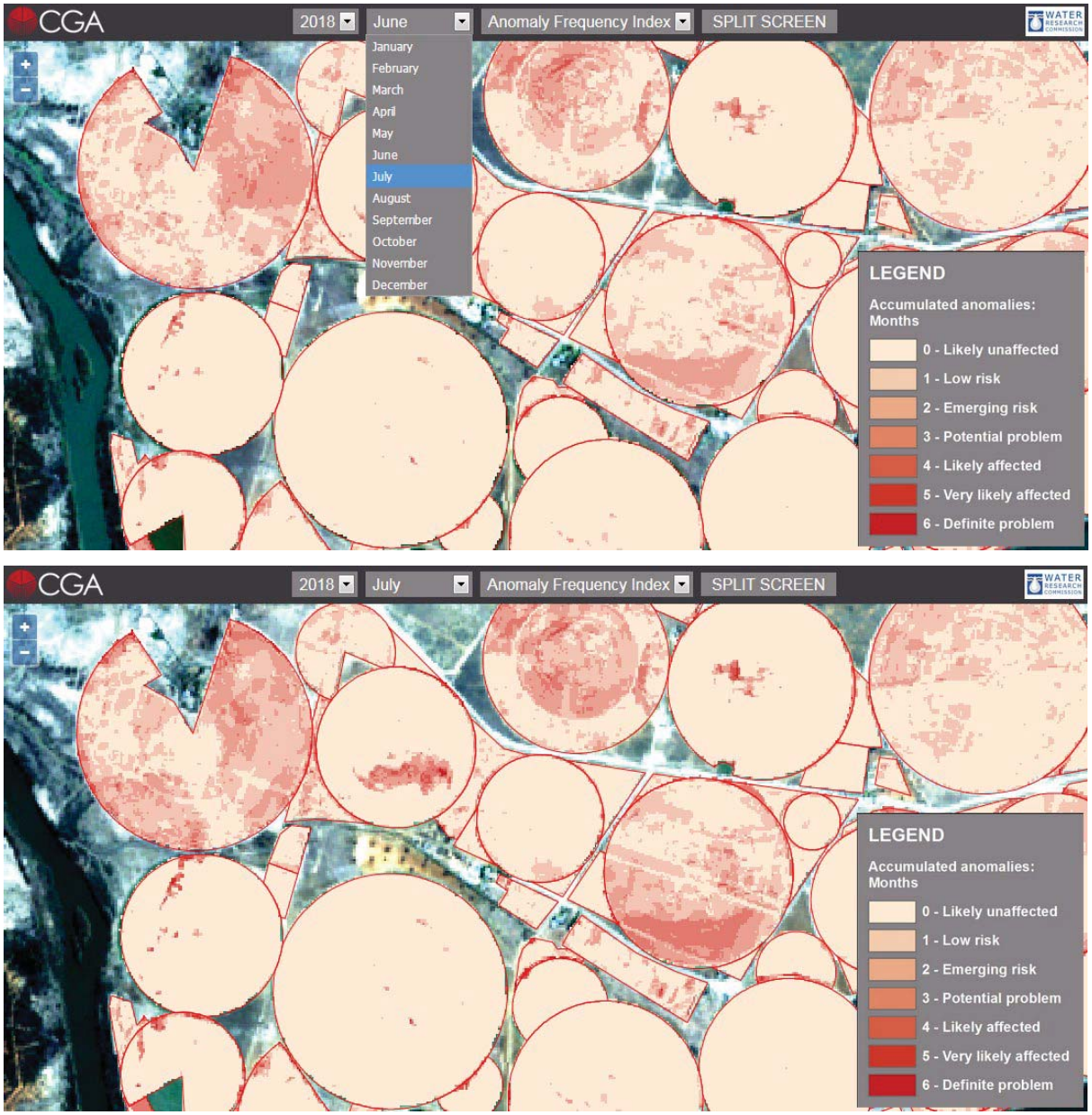

Figure 4.8: Changing the date using the (top) dropdown list changes the (bottom) anomaly layers

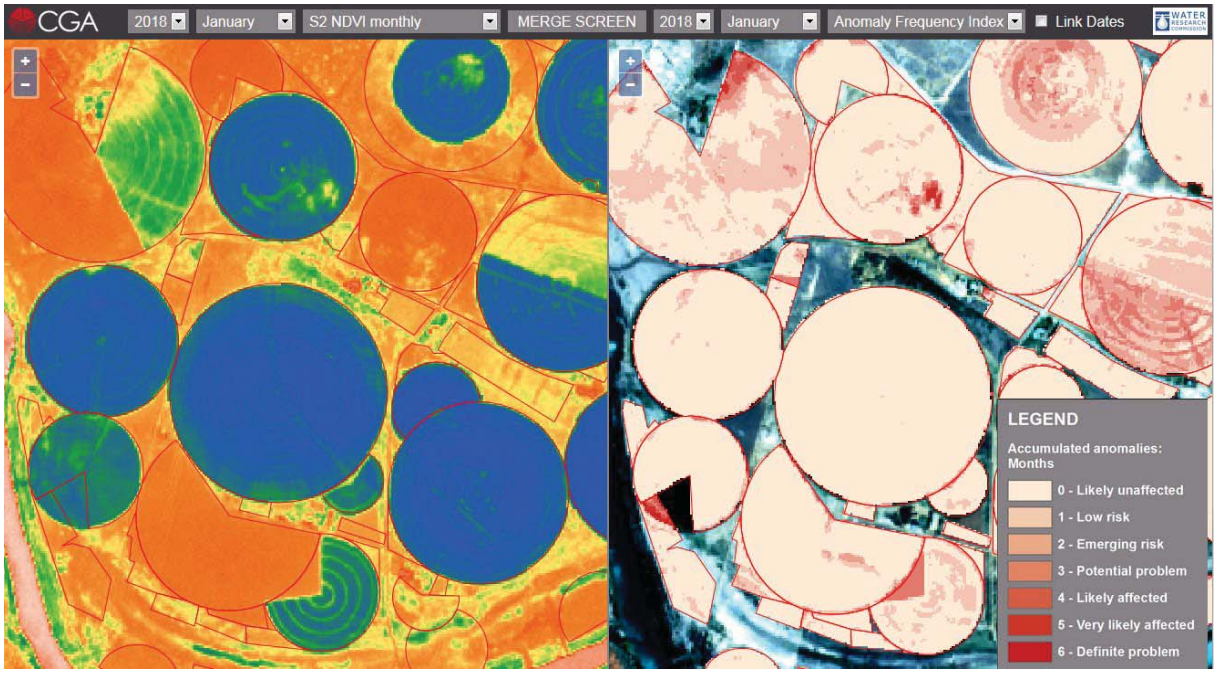

Figure 4.9: The screen can be split in two for side-by-side viewing and comparison

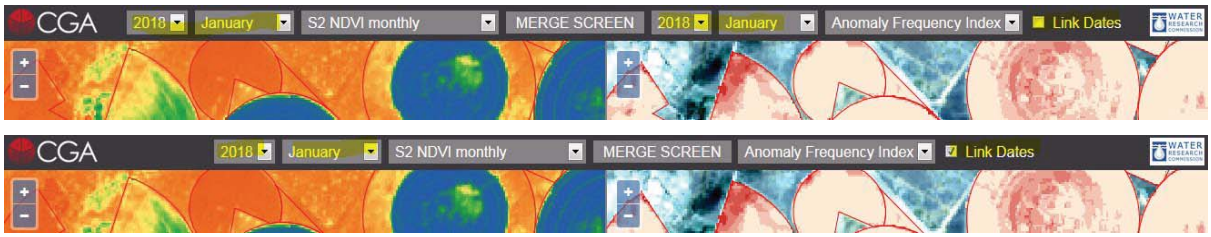

Figure 4.10: Linking the dates of maps

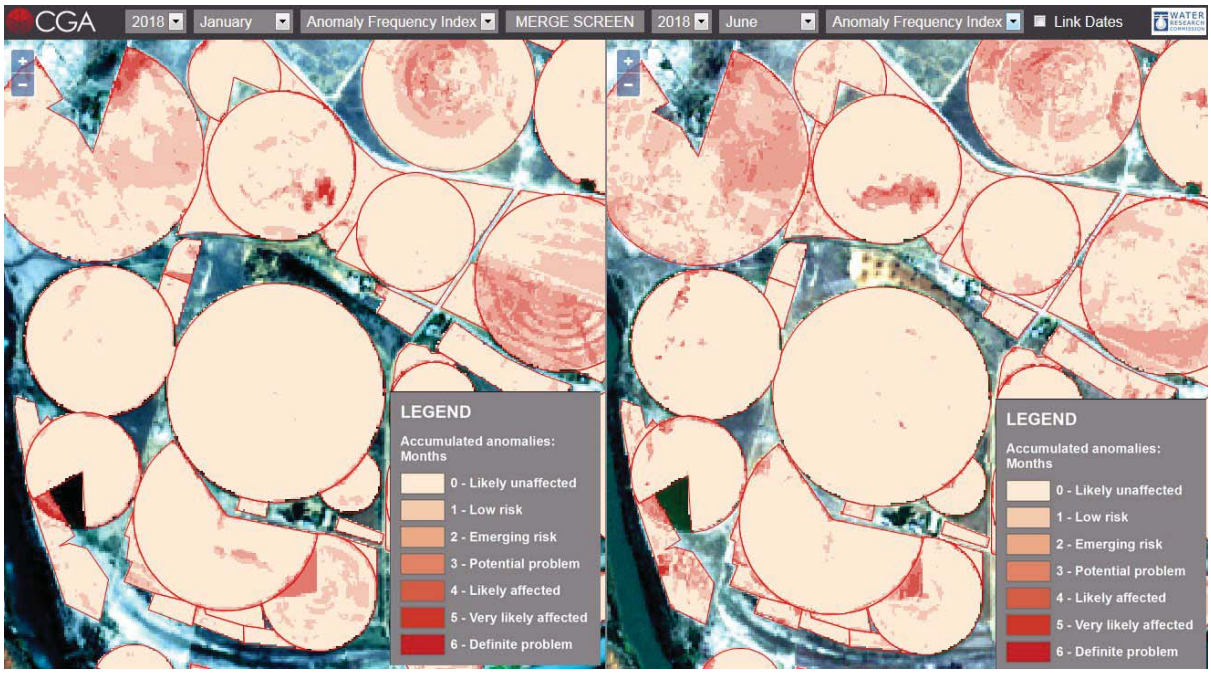

Figure 4.11: Comparing anomalies of different months

Figure 4.12: Merging the split screen

The NGI aerials (aerial photographs) layer provides the highest resolution backdrop imagery in the SAWMS. However, the user is advised to note that these aerials are usually several years older than the more contemporary Sentinel-2 images (Figure 4.13).

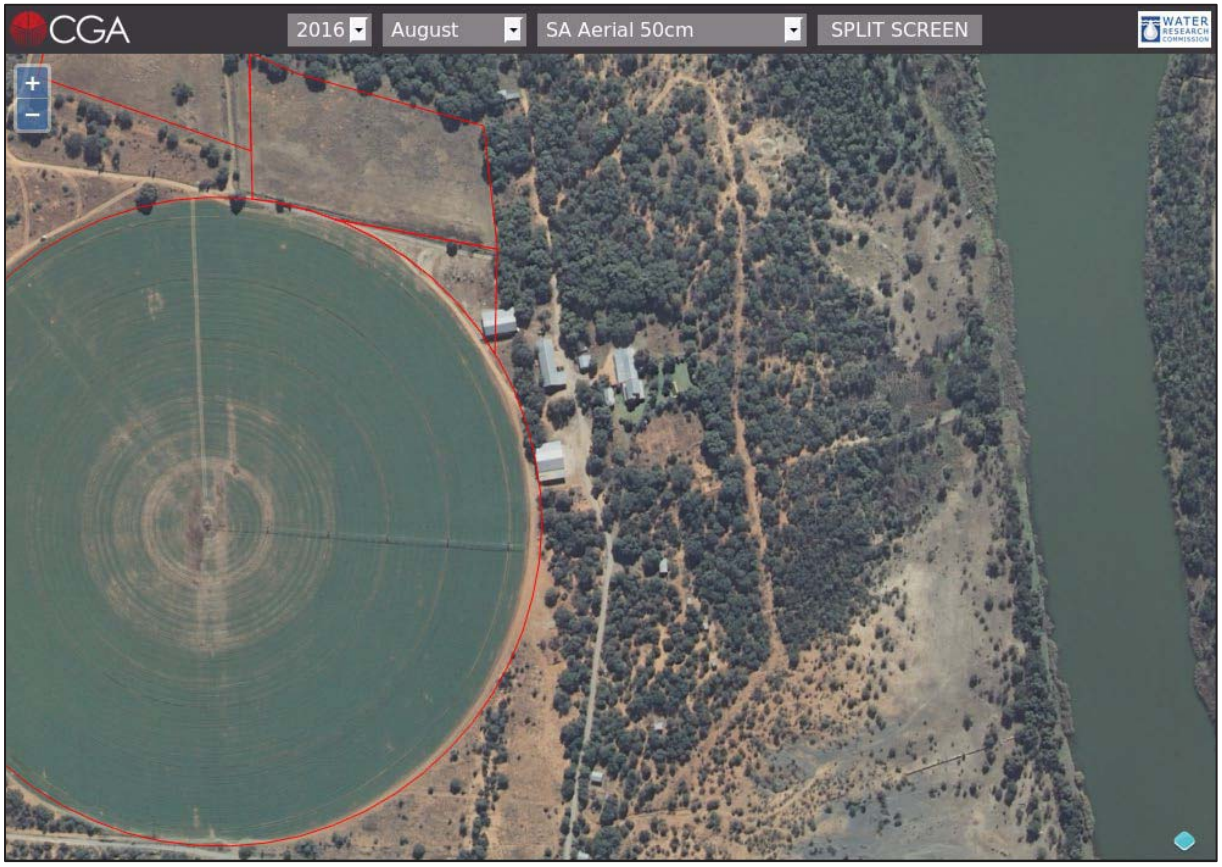

Figure 4.13: Very high resolution aerial photograph background

A mosaic of NGI's 1:50 000 topographical maps is also provided for context (Figure 4.14).

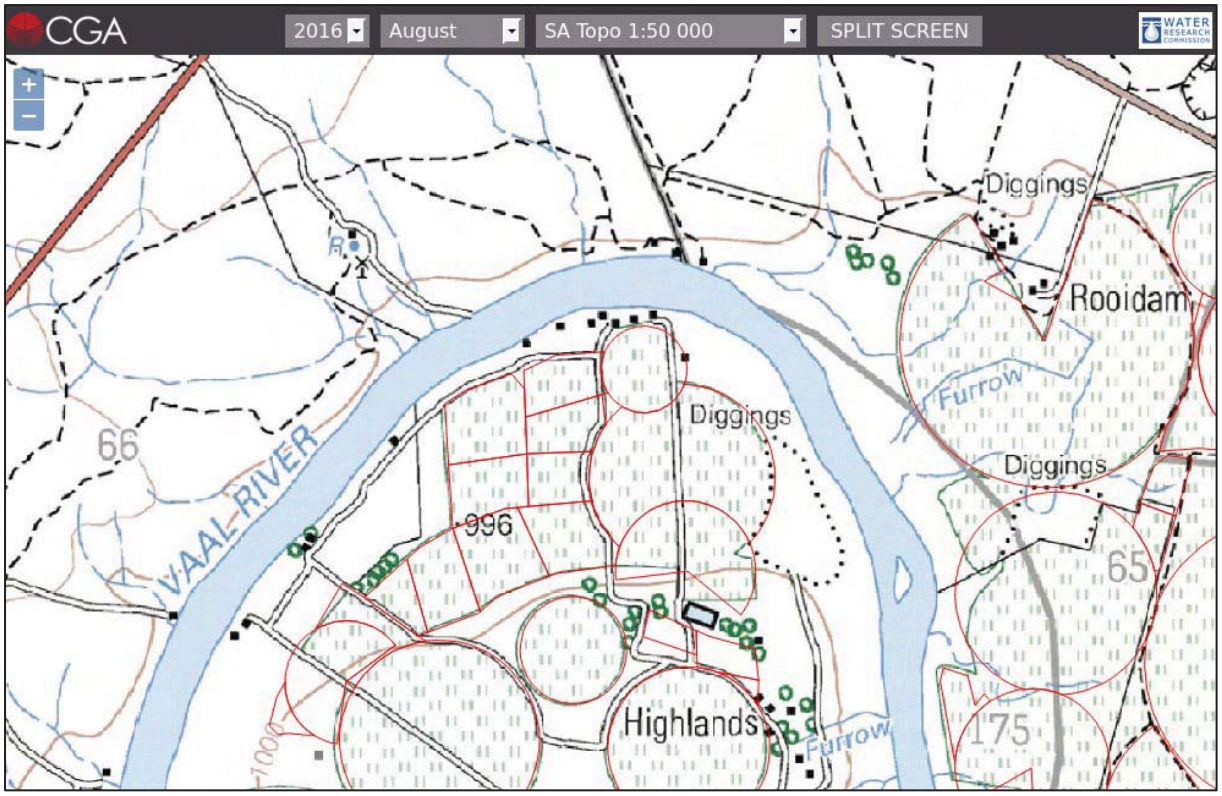

Figure 4.14: NGI topographical maps

The SAWMS web application strives to provide a simple but effective interface for viewing and interpreting the anomalies identified by the system.

5 DEMONSTRATION OF THE SAWMS IN SELECTED AREAS

To demonstrate its operational ability, the SAWMS was applied in several irrigation schemes and agricultural areas throughout SA (Figure 5.1). A brief summary of each area and comments on the implementation of the SAWMS are presented in the following subsections.

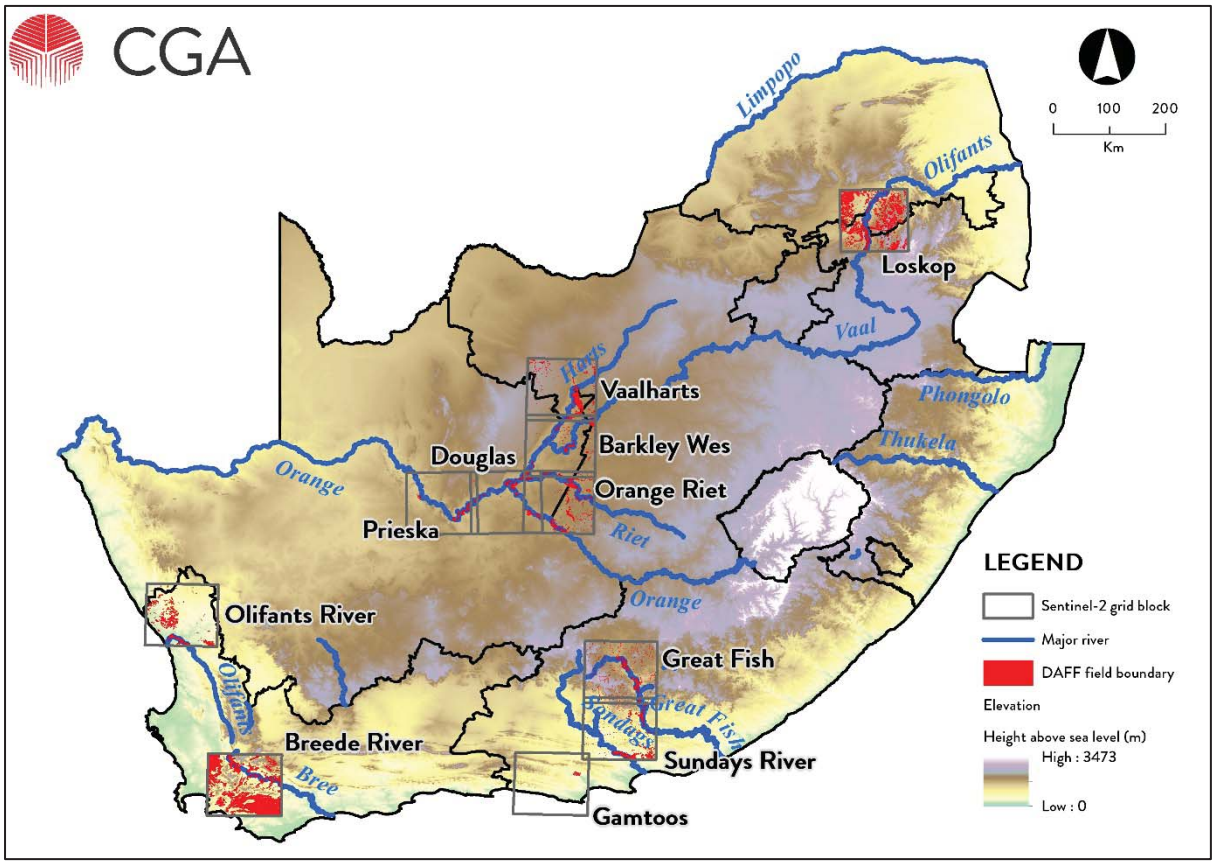

Figure 5.1: Geographical distribution of the irrigation schemes and agricultural areas where the SAWMS was applied

5.1 Orange, Riet, Vaal and Harts (ORVH) Basin

The agricultural areas adjacent to the Orange, Riet, Vaal and Harts (ORVH) Rivers formed part of the original “Douglas area” in which the SAWMS methodology was developed. The area includes the Vaalharts irrigation scheme, which intersects the towns of Hartswater and Jankempdorp in the Northern Cape, and the Orange-Riet irrigation area, which stretches between Jacobsdal and Luckhoff on the boundary separating the Free State Province from the Northern Cape. The agricultural areas surrounding Barkley Wes and Warrenton (both on the Vaal River) are situated between the Vaalharts and Orange-Riet irrigation areas. This region (labelled as Vaalharts, Barkley Wes and Orange-Riet in Figure 5.1) has a semi-arid climate with rainfall mainly occurring in the summer months in the form of thunder showers, amounting to between 300 and 400 mm a year (Schulze & Maharaj, 2006). The region has a mean annual temperature of between 17 and 19°C and the principal crops planted are maize, wheat, barley and lucerne (Schulze & Maharaj, 2006; Kruger et al., 2009).

The Douglas agricultural area (middle-to-lower Orange River) is located around the town of Douglas in

the Northern Cape, at the confluence of the Orange and Vaal rivers. The lower Orange agriculture area is located further downstream (south-west from Douglas) towards Prieska. These agricultural areas (labelled as Douglas and Prieska in Figure 5.1) are semi-arid areas with a mean annual rainfall between 200 and 300 mm and mean annual temperature ranging between 18 and 19 °C (Schulze & Maharaj 2006). The principal crops grown in these regions are similar to those grown in the Vaalharts and Orange-Riet areas, being wheat, maize, lucerne and potatoes (Armour, 2002).

The anomaly detection technique performed well in the ORVH area. Several fields were identified for inspection and most of the anomalies were confirmed to be salt-affected and/or waterlogged (Figure 5.2 and Figure 5.3). As explained in Section 3.2.5, the major limitation of the SAWMS is the use of existing field boundaries. Fields digitised from old imagery or at small mapping scales can lead to false positives. However, in the ORVH area, it constituted an insignificantly small proportion of the total number of fields and was not considered by the end-users (Appendix I) to be a major problem.

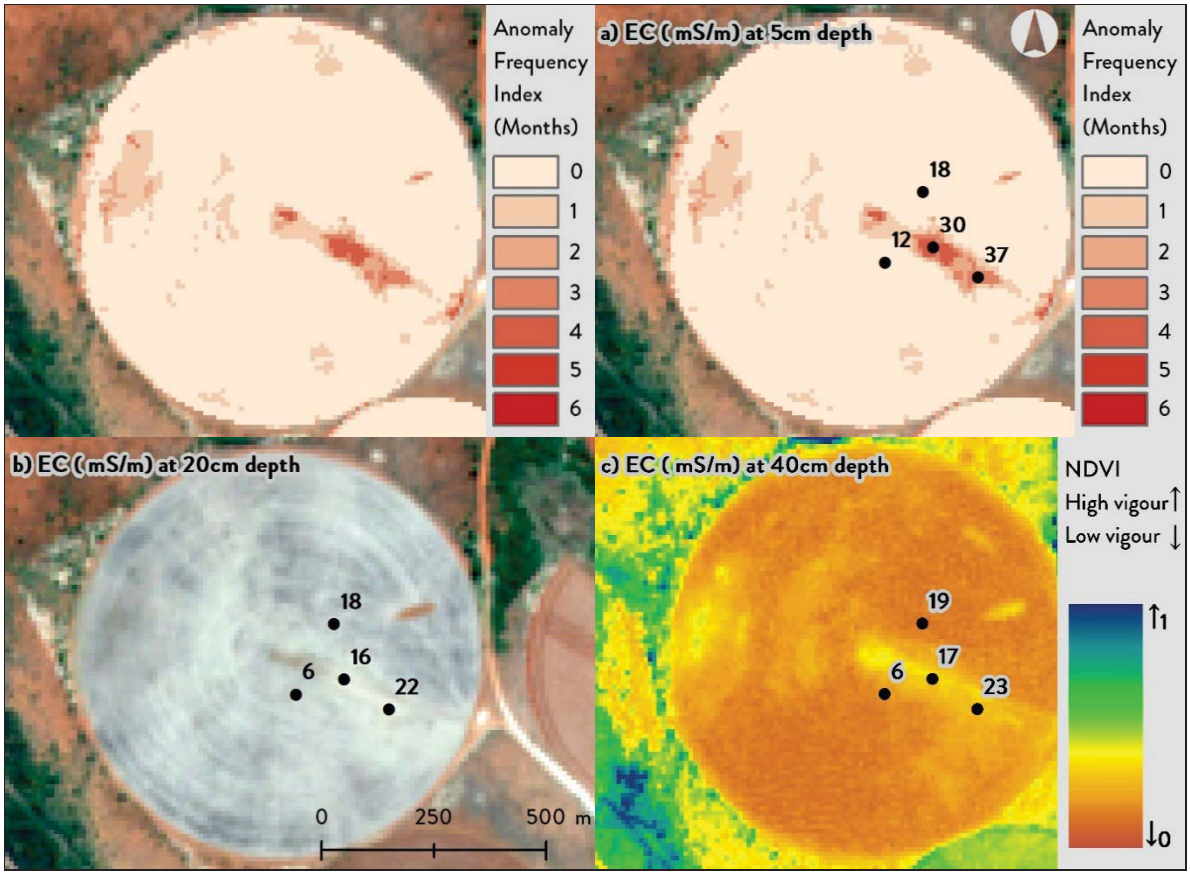

Figure 5.2: Example of the anomaly frequency index with overlaying diluted ECe[9] values at three depths with a) at 5cm depth, b) at 20cm depth and c) at 40cm depth with vegetation index background. A relative increase in salinity levels, specifically at the 5 cm depth is visible.

[9] ECe of soil samples were determined according to a saturated soil water extract method adapted by BEMLAB (bemlab.co.za) according to The Non-Affiliated Soil Analyses Work Committee (1990). A mixture of 100 g dried soil:150 ml deionised water was centrifuged and the electric conductivity of the clear solution determined.

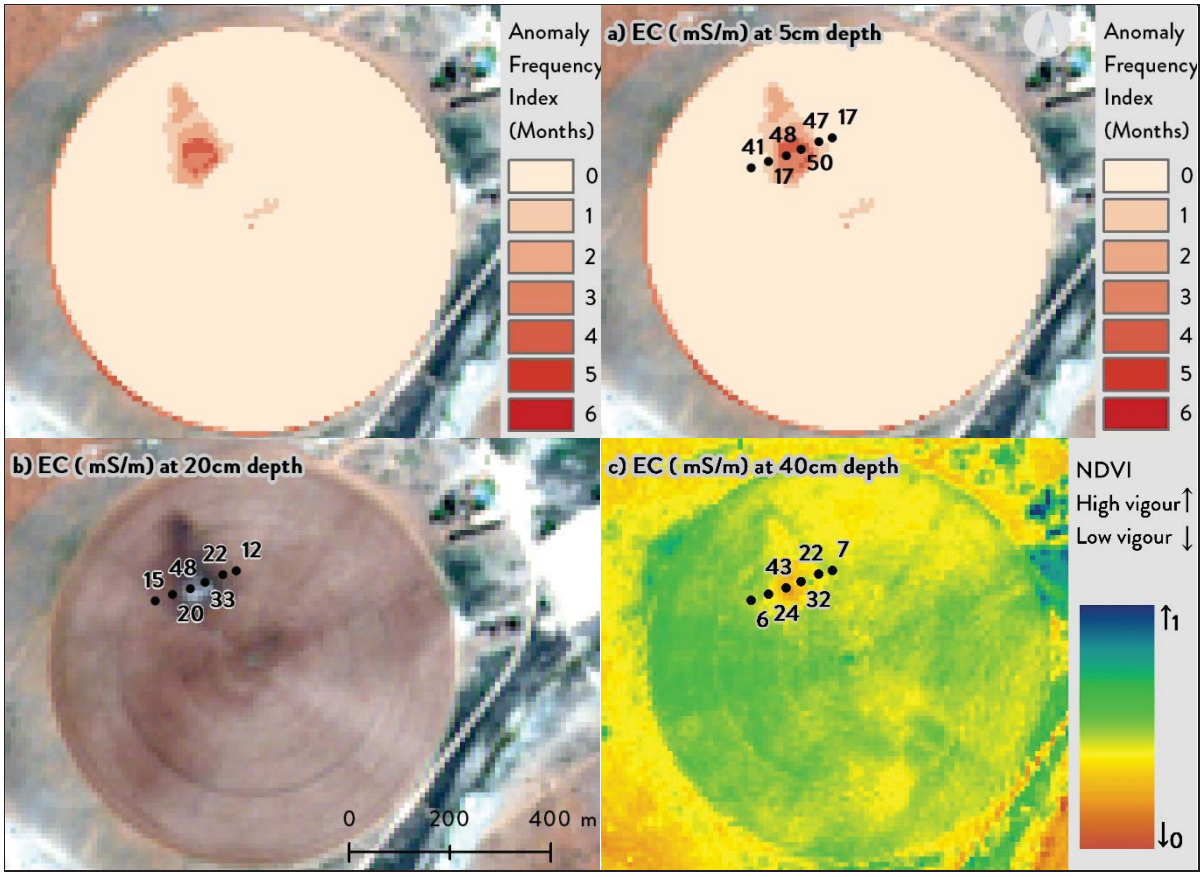

Figure 5.3: Example of the anomaly frequency index with diluted ECe[9] values at a) 5cm, b) 20cm (with colour image in background) and c) 40cm depths (with a vegetation index in background). A relative increase in salinity levels within the detected anomalies is observed at all depths.

5.2 Olifants River (Western Cape Province)

The Olifants River irrigation scheme is located in the Western Cape (WC) [10] and receives irrigation water from the Olifants River. Bordering the Atlantic Ocean, the scheme has a mean elevation of 31 m above sea level and consists mainly of the Namaqualand Riviera region (Mucina & Rutherford, 2006). The mean annual temperature of the area is between 18 and 19°C, while the mean annual rainfall is 134 mm (Schulze, 2007). Crops grown in this region are mostly grapes and citrus. Figure 5.4 shows the AFI of an 11284 ha area in the scheme. At a glance, very few anomalies are noticeable, but at closer inspection (Figure 5.5a) it is clear that many “anomalies” were generated due to generalised field boundaries. Compared to the fields in the ORVH area, the Olifants River irrigation scheme has relatively small and compact fields, which lead to false positives. However, such errors are easily differentiated from the legitimate anomalies within fields (Figure 5.5b) and can be managed by informing end-users how such false positives can be identified.

[10] Western Cape was added to the section heading to differentiate it from the Olifants River in the Limpopo Province, but is omitted in the text to improve readability.

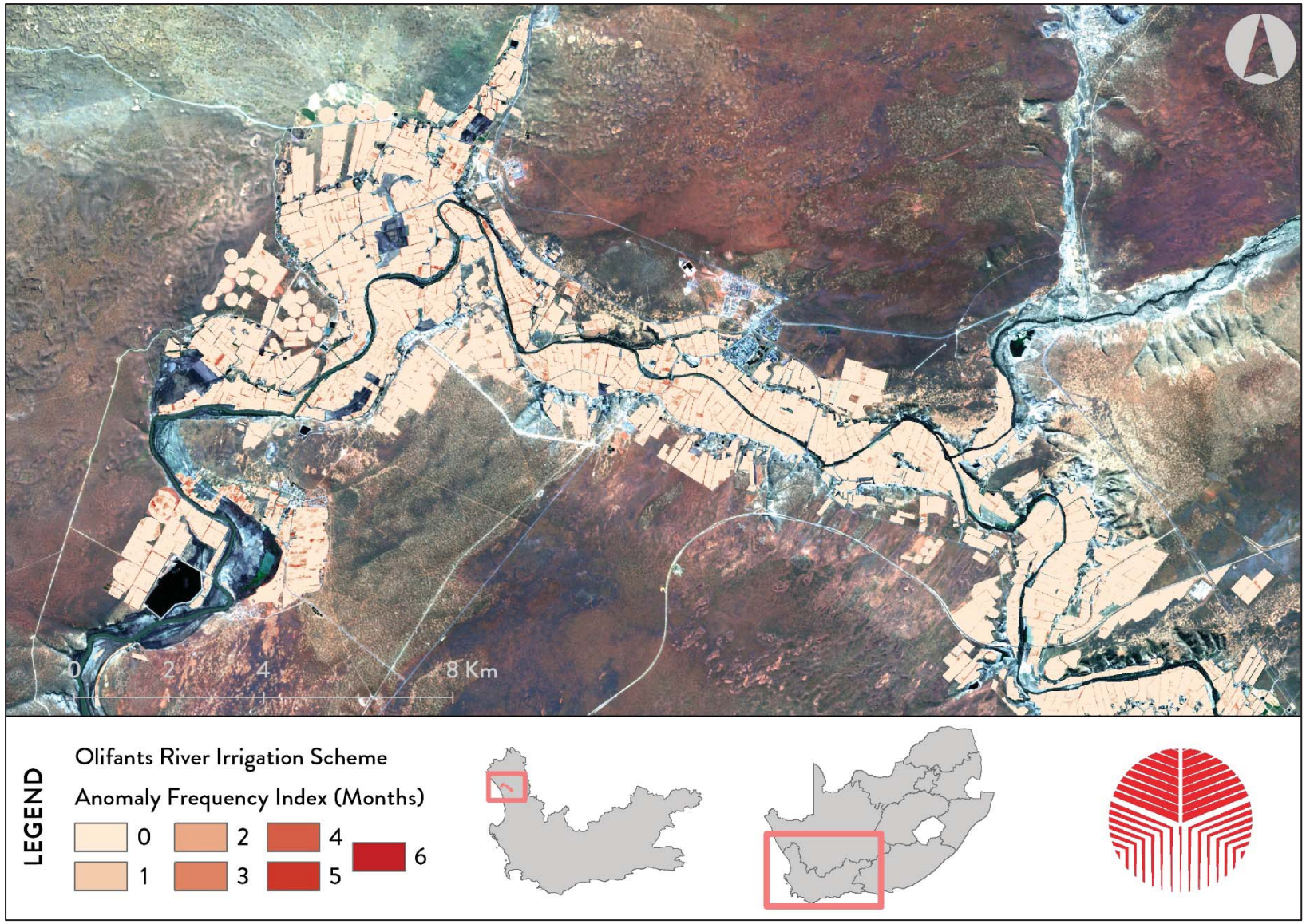

Figure 5.4: The AFI generated by SAWMS in the Olifants River irrigation scheme.

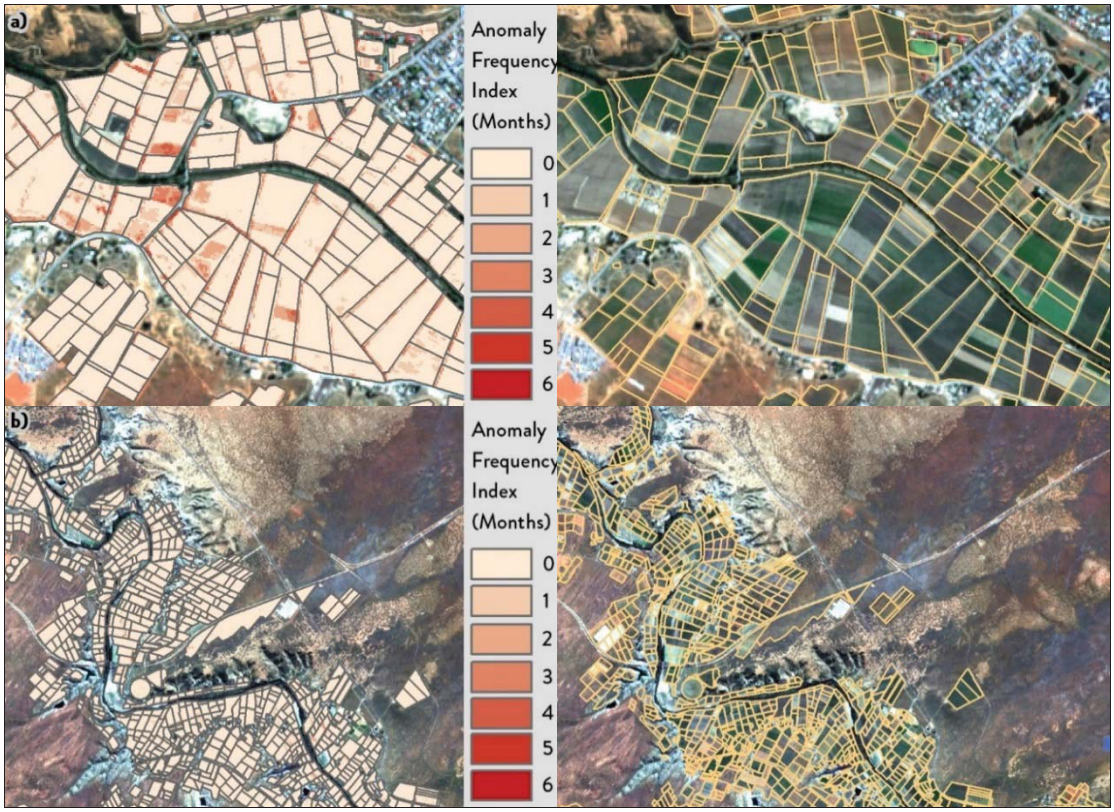

Figure 5.5: Examples of the anomaly frequency index generated by SAWMS in the Olifants River irrigation scheme for July 2018 at a (a) fine scale indicating field boundary inconsistencies, and at a (b) larger scale.

5.3 Breede River

The Breede River irrigation scheme is mainly fed with water from the Breede River, which originates in the Ceres Valley about 100 km North West of Cape Town and flows 320 km in a south-easterly direction to where it reaches the Indian Ocean at Witsand (Kirchner, 1995). Fields covering 29129 ha in the middle parts of the greater catchment between Worcester and Robertson were the focus of this evaluation (Figure 5.6). The area has a gentle hilly relief defined with high mountain ranges north (Langeberg Mountain) and south (Riviersonderend Mountain) parallel to the river. The focus area is located at a mean altitude of 233 m above sea level and has a Mediterranean climate with dry and hot summers and moderately warm wet winters (Flügel & Kienzle, 1989). It receives an annual rainfall of 290 mm mainly during the winter rainfall season (May to October) and is thus classified as semi-arid (Schulze 2006). The annual mean temperature for the area is 17°C (Schulze 2006). The crop mix in the Breede River irrigation scheme is less diverse compared to the ORVH area, with wine grape variations being the primary (65%) crop. Other crops include peaches and apricots (13%), vegetables (mainly tomatoes) (3%) and irrigated pastures (7%) (Moolman et al., 1999). The majority of the farm irrigation infrastructure comprises of drip and microjet systems (Beuster et al., 2003). Field sizes in the Breede River irrigation scheme vary and includes large pivots to smaller sized vine blocks (Figure 5.7a). Fields with windbreaks along its perimeter posed a problem for the WFAD approach in this area as it introduces linear false positive anomalies (Figure 5.7b). However, in general, it would seem that the SAWMS performed reasonably well in this area, with most fields being unaffected by salt accumulation and waterlogging (Figure 5.7c).

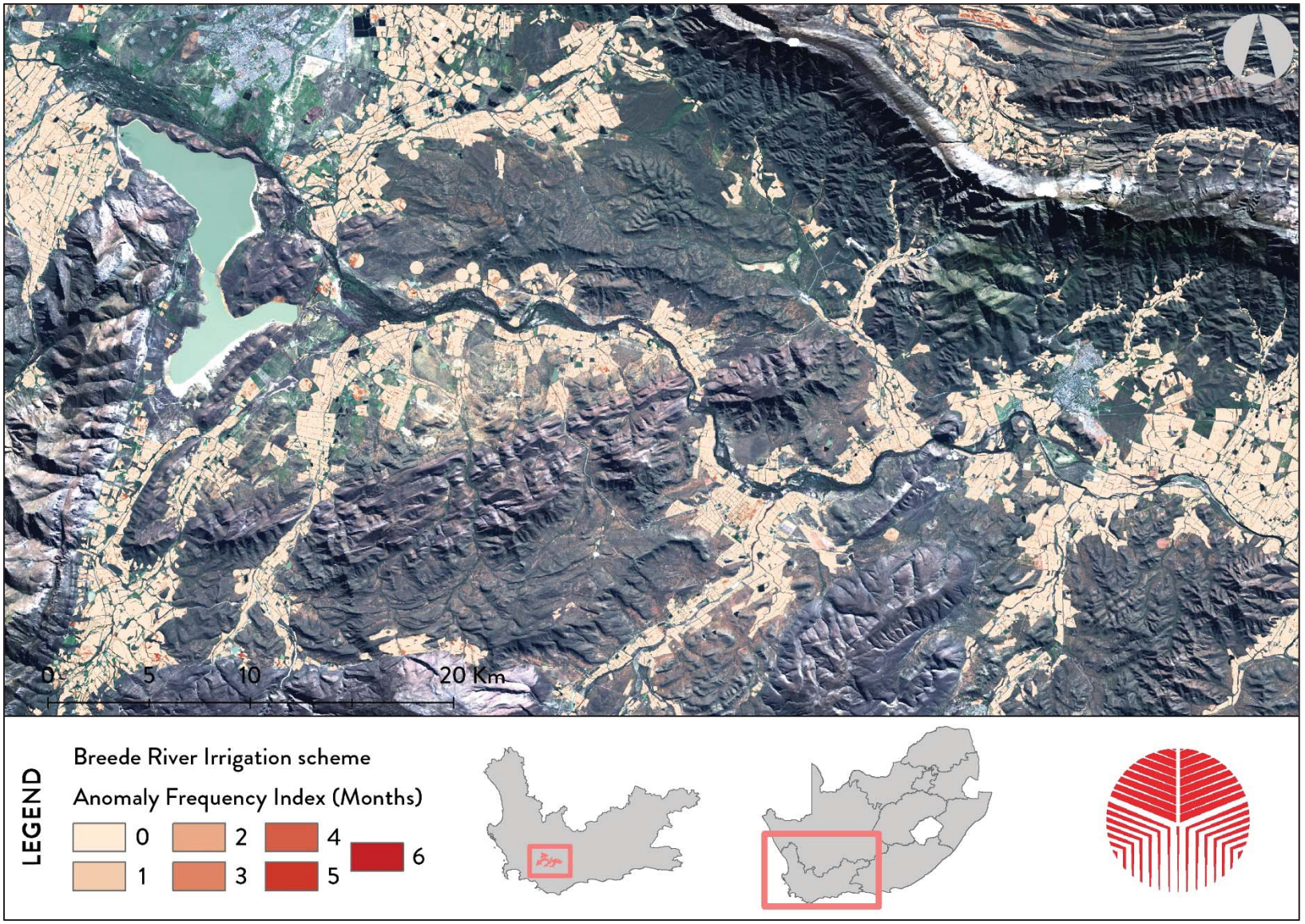

Figure 5.6: Example of the anomaly frequency index generated by SAWMS in a portion of the Breede River irrigation scheme selected for demonstration

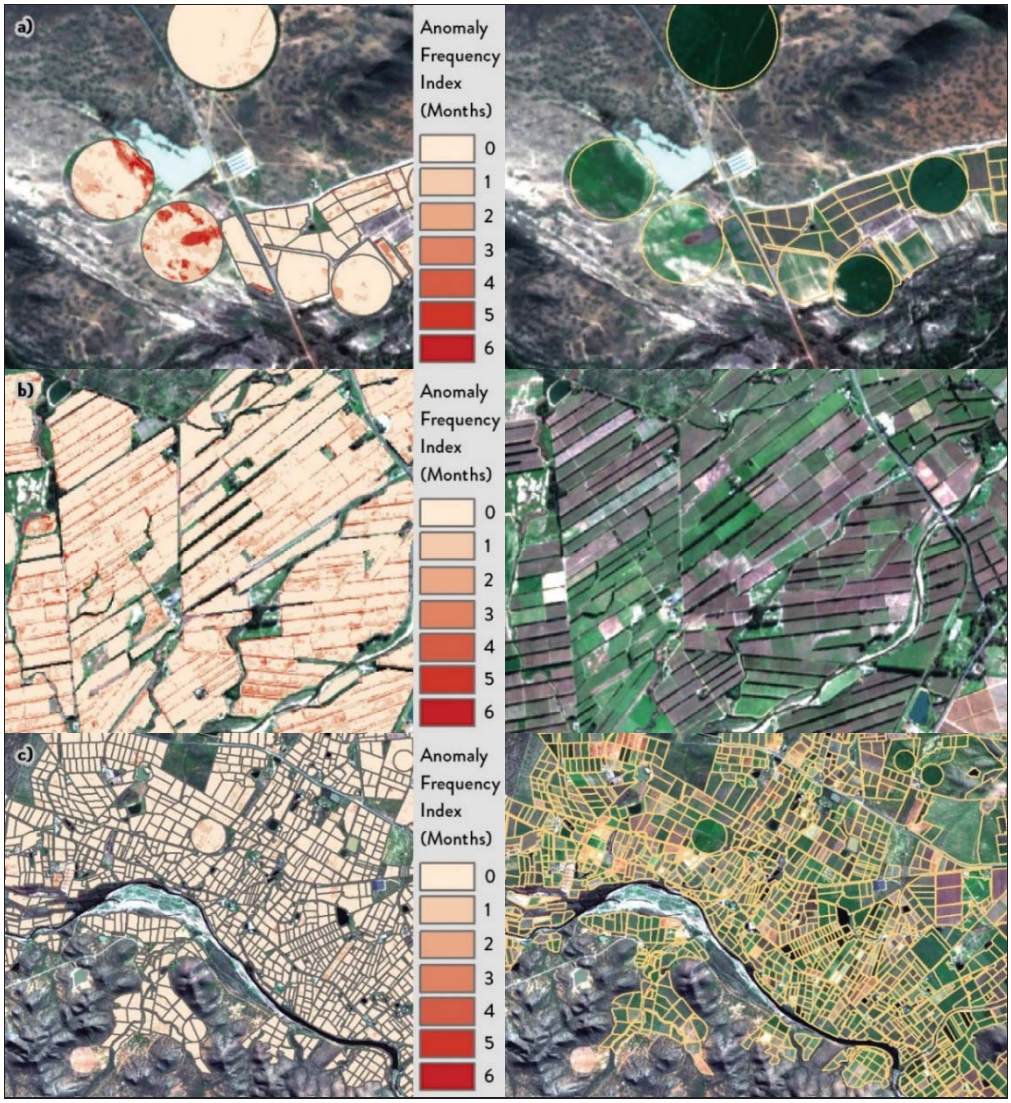

Figure 5.7: Specific examples of the anomaly frequency index generated by SAWMS in the Breede River irrigation scheme for July 2018, where a) illustrates anomalies in pivot fields, b) shows false positive anomalies due to wind breaks, and c) shows the anomaly frequency index at a larger scale.

5.4 Sundays River

The Sundays River irrigation scheme is located at 83 m above mean sea level at the foot of the Zuurberg Mountain range in Eastern Cape, 40km from the Indian Ocean. The scheme is situated predominantly between two series of alluvial terraces and, according to Mucina & Rutherford (2006), mostly forms part of the Albany alluvial vegetation region. The area has a mean annual temperature of between 18 and 19°C and mean annual rainfall of 380 mm (Schulze 2006). Citrus is the dominant crop in this irrigation scheme and comprised the majority of the 18608 ha region selected for evaluation. It is evident from Figure 5.8 and Figure 5.10 that the SAWMS performed poorly when using the standard DAFF (Crop-Estimations-Consortium 2017) field vector boundaries due to the generalised nature of the data. This prompted the project team to re-digitise the fields in this area. The result was significantly improved, as shown in Figure 5.9 and Figure 5.11. This exercise clearly indicates that where the standard DAFF field boundaries are too generalised, a manual correction of the field vector boundaries is essential for the effective functioning of the SAWMS.

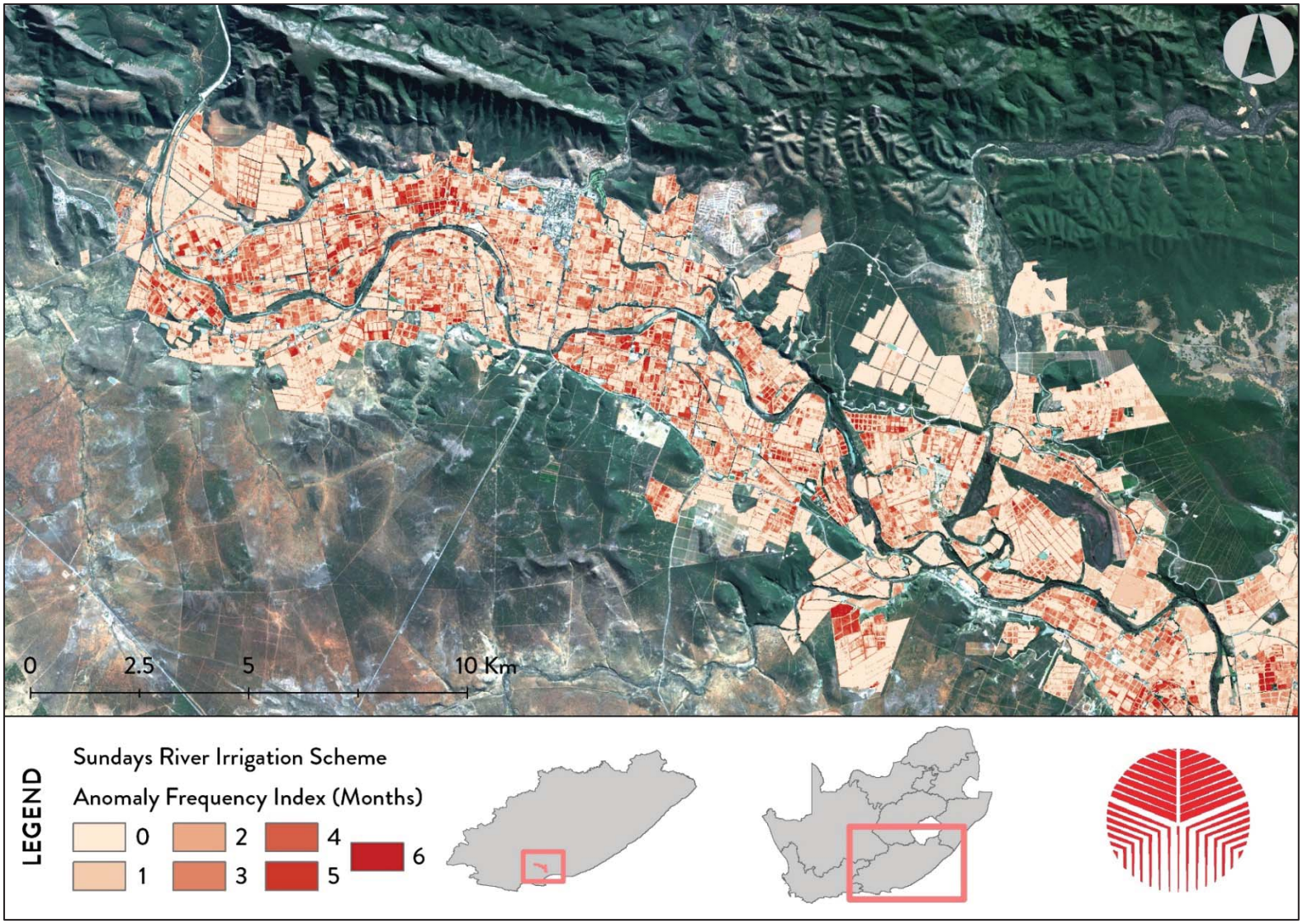

Figure 5.8: Example of the anomaly frequency index generated by SAWMS for part of the Sundays River irrigation scheme included in the evaluation using DAFF field boundaries

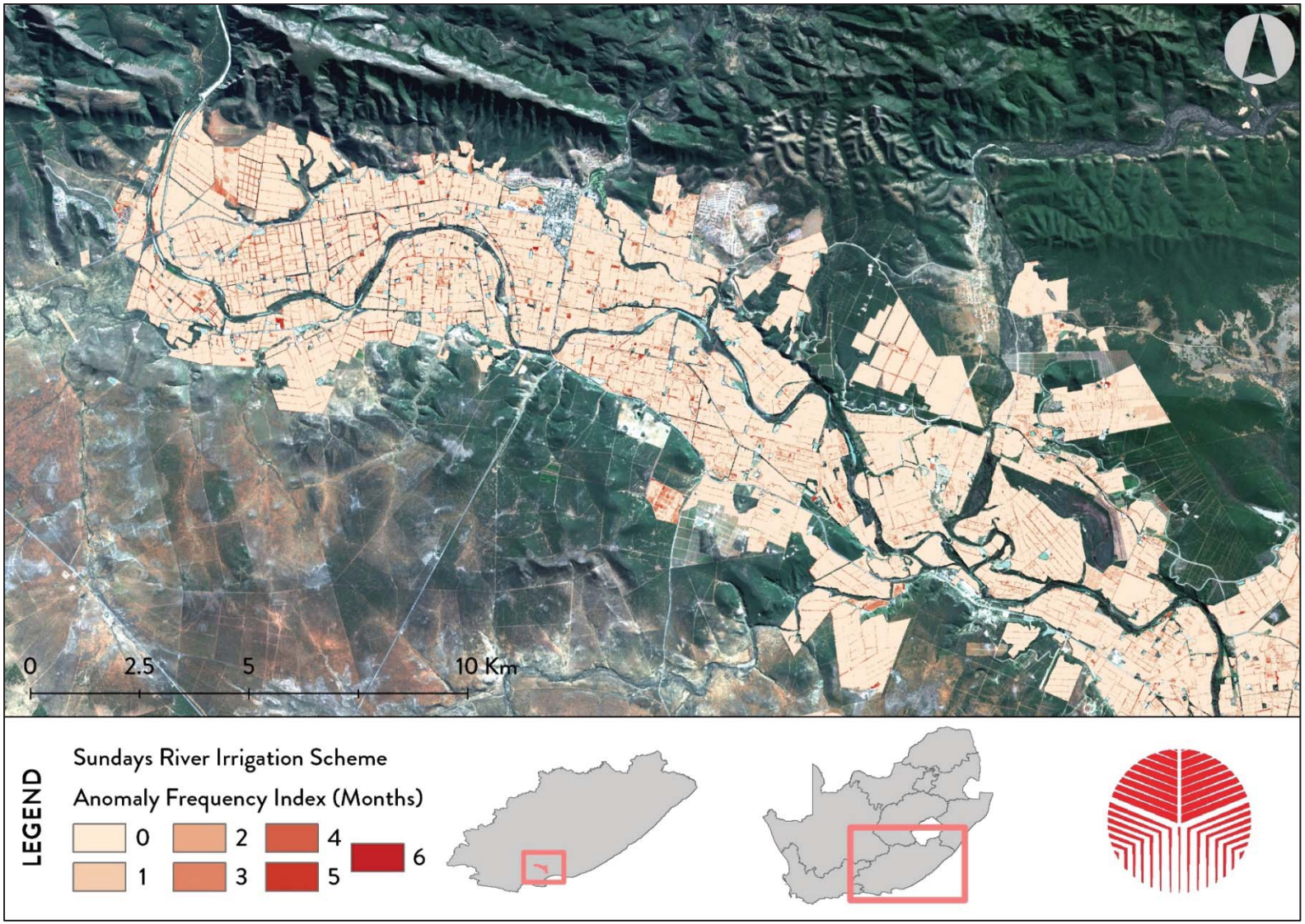

Figure 5.9: Example of the anomaly frequency index generated by SAWMS for part of the Sundays River irrigation scheme included in the evaluation, with manually re-digitised field boundaries

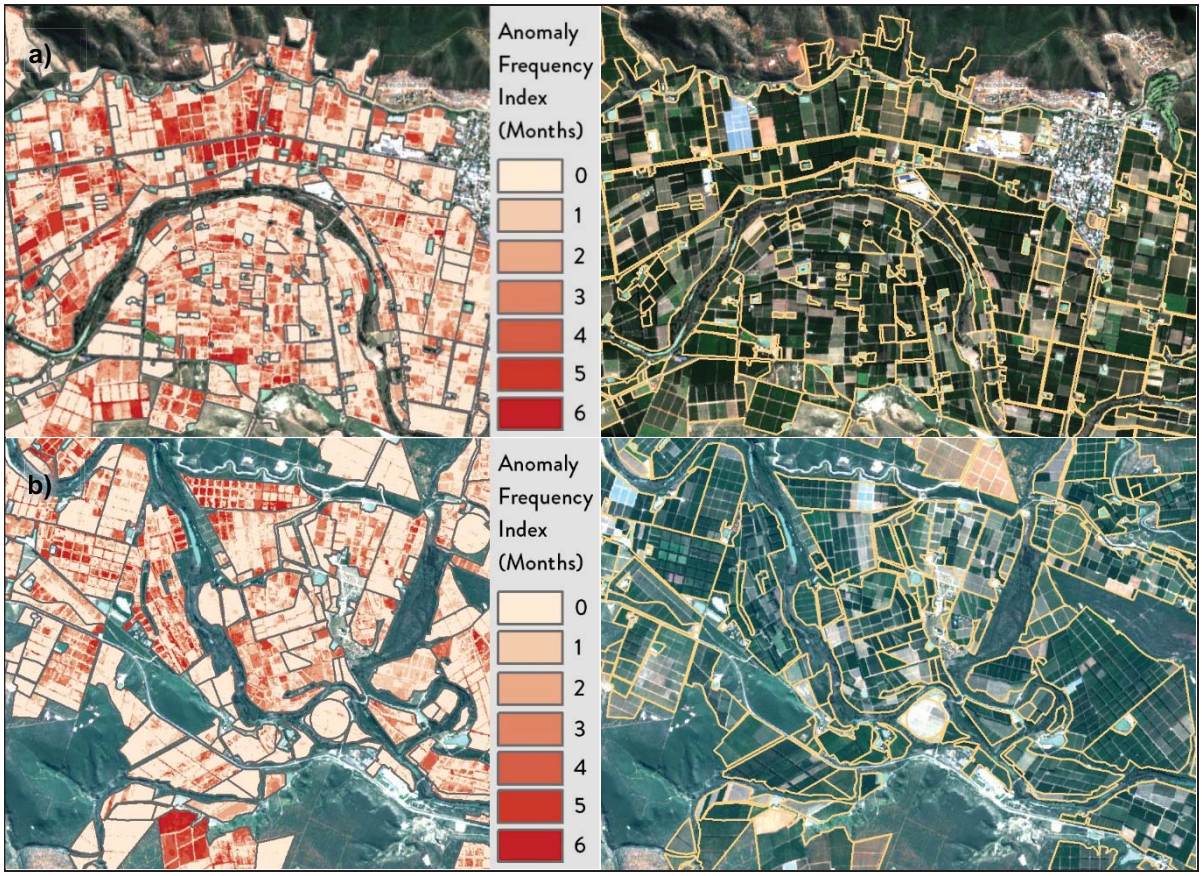

Figure 5.10: Examples of the anomaly frequency index generated by SAWMS in the Sundays River irrigation scheme for July 2018, where a) and b) give different examples where generalised field boundaries was the main cause of the anomalies identified

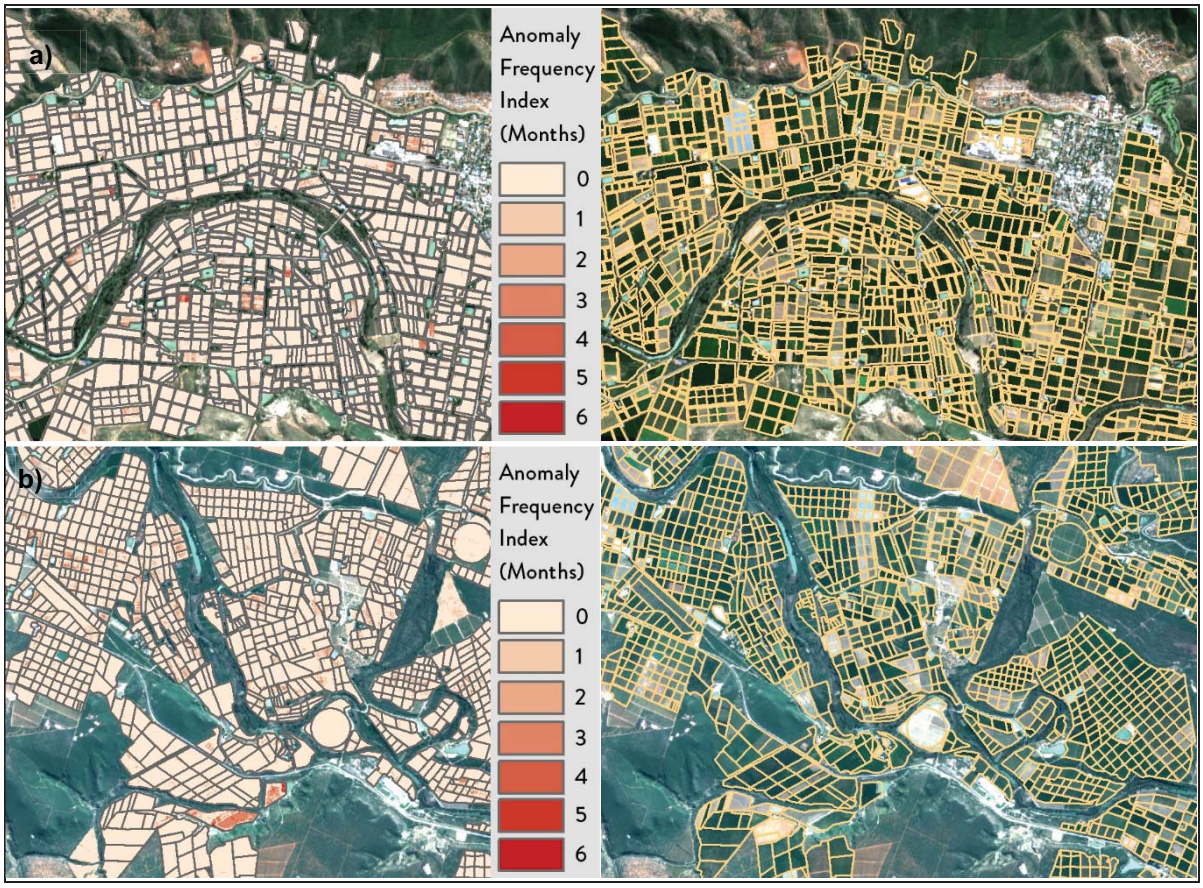

Figure 5.11: Examples of the anomaly frequency index generated by SAWMS applied in the Sundays River irrigation scheme for July 2018, where a) and b) represent the same area as Figure 5.10 with manually re-digitised field boundaries.

5.5 Olifants River (Mpumalanga Province)

The Loskop irrigation scheme is located in the Limpopo Province (Figure 5.12), with a total of 38831 ha being cultivated. The scheme forms part of the Olifants River[11] Basin, where salinisation has been identified as the main agricultural pollution problem (Aihoon et al., 1997). The area is situated at 916 m above mean sea level and the geography ranges from mountainous bushveld to undulating terrain with thorn trees (Tren & Schur, 2000). The region comprises a mixture of central sandy bushveld and the Springbokvlakte and Loskop thornveld regions (Mucina & Rutherford 2006). Loskop has a mean annual temperature of 20°C and a mean annual rainfall of 552 mm (Schulze 2006). A wide variety of crops are grown in the scheme, including citrus, table grapes, maize, wheat, soya bean, cotton, tobacco and groundnuts. The field boundaries in the Loskop irrigation scheme are of similar quality to that of Douglas and Vaalharts, which resulted in the SAWMS producing acceptable results (Figure 5.13).

[11] This river should not be confused with the Olifants River in the Western Cape that was the focus of Section 5.2.

Figure 5.12: Example of the anomaly frequency index generated by SAWMS for the Loskop Irrigation scheme

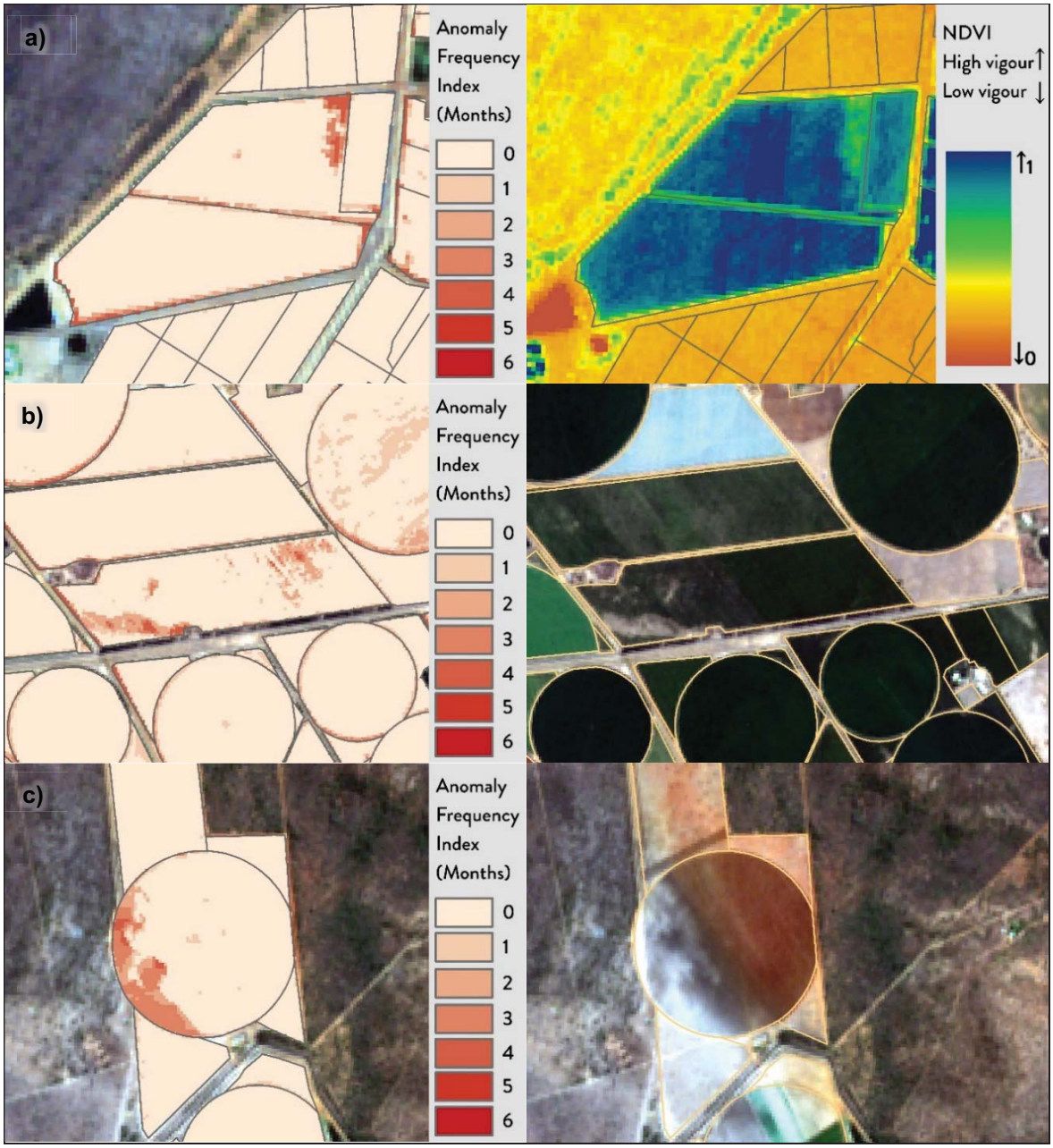

Figure 5.13: Specific examples of the anomaly frequency index generated by SAWMS in the Loskop River irrigation scheme for July 2018, where a) shows an anomaly identified with a corresponding NDVI image and b) and c) show anomalies with corresponding true colour images.

5.6 Great Fish River

Irrigated agriculture along the Great Fish River stretches from north-west of Cradock (upper Great Fish, Figure 5.14) to south-east of Somerset East (lower Great Fish, **Error! Reference source not found.**) in the Eastern Cape Province. The Great Fish Basin is classified as semi-arid and has a mean annual precipitation of between 350 and 400 mm and a mean annual temperature of between 16 and 17°C Schulze (Schulze & Lynch, 2007). SAWMS performed well in the Great Fish irrigation scheme where suitable field vector boundaries were available. Figure 5.16a shows the identification of anomalies at the centre of the pivot fields, which might be due to leaky pivots or the pivot infrastructure itself. Figure 5.16b and c show examples of anomalies detected with Sentinel-2 true colour and NDVI respectively for comparison.

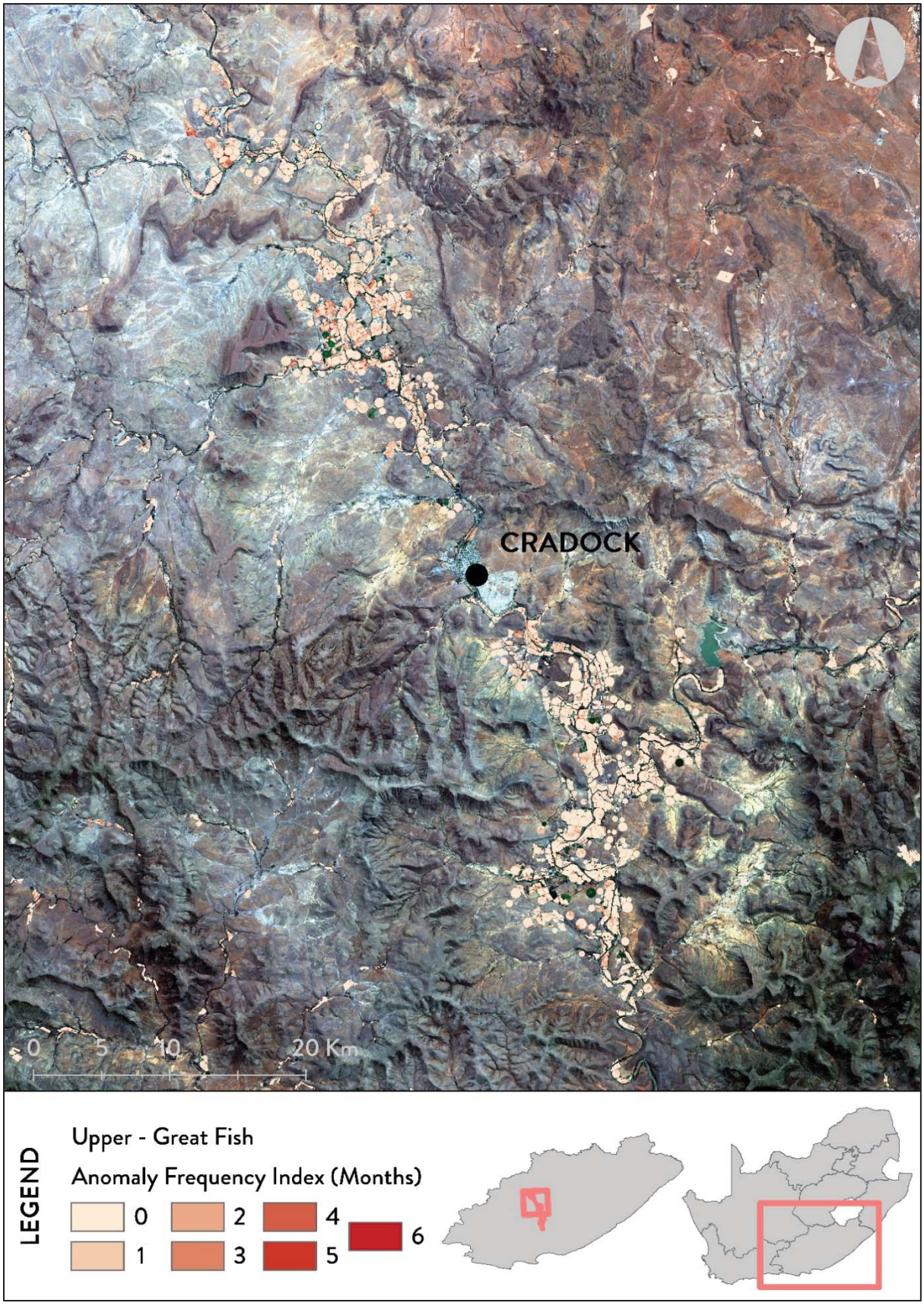

Figure 5.14: Example of the anomaly frequency index generated by SAWMS for the upper part of the Great Fish River irrigation scheme

Figure 5.15: Example of the anomaly frequency index generated by SAWMS for the lower part of the Great Fish River irrigation scheme

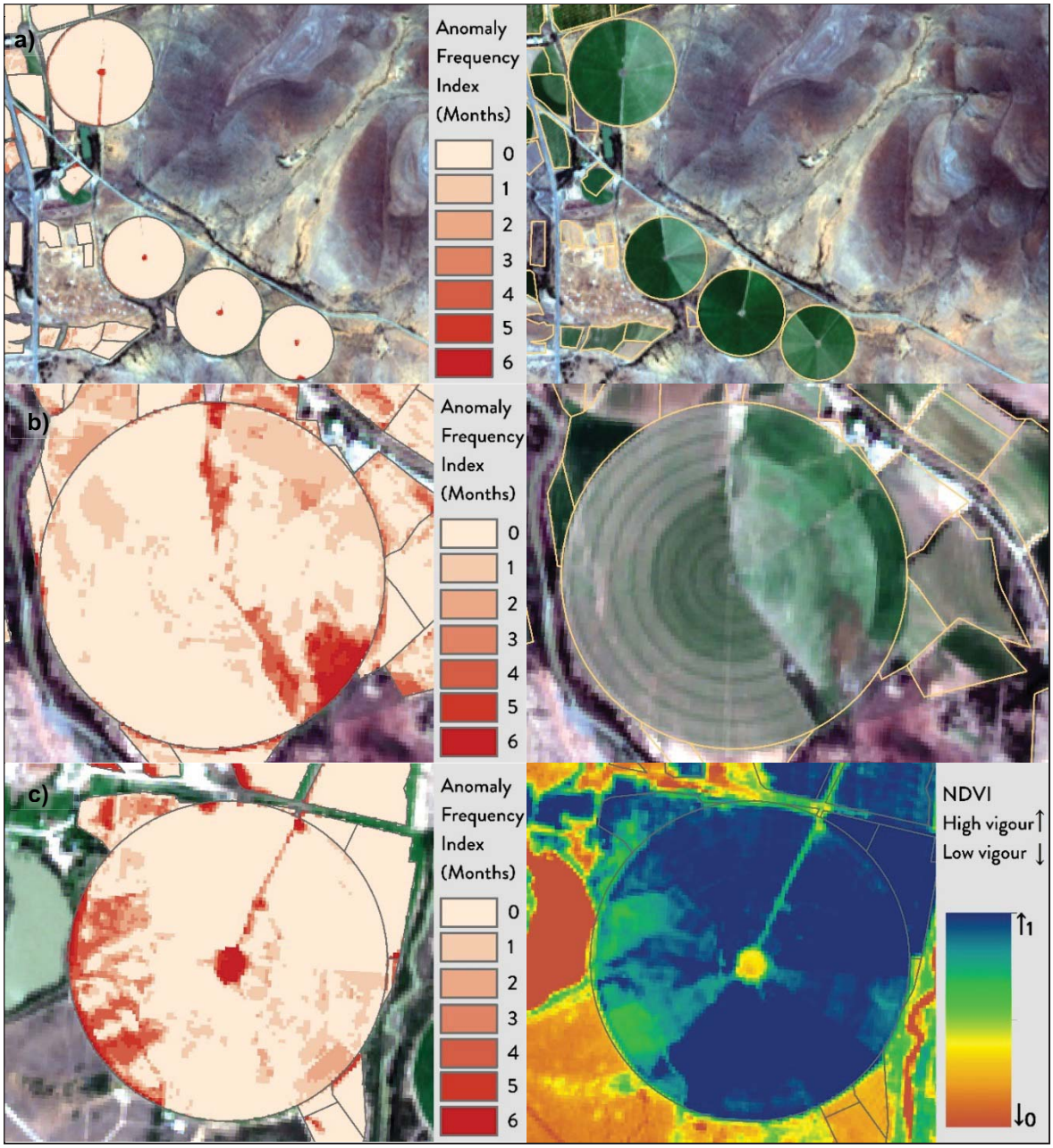

Figure 5.16: Examples of the anomaly frequency index generated by SAWMS in the Great Fish irrigation scheme, with a) anomalies at the centre of pivots, likely due to infrastructure, b) a field with severely affected areas, and c) anomalies with a corresponding NDVI image.

5.7 Gamtoos River

The Gamtoos region, in particular Patensie, was included in the demonstration on request of the targeted end-users at Humansdorp Koöperasie. The main crop in this region is citrus, although tobacco, field crops and vegetables are also grown. The region normally receives rainfall throughout the year, but has been in the grip of a drought for several seasons, leading to an increase in salinity levels in the severely constrained water supply. The DAFF field boundaries in this area were grossly generalised and are not suitable for use in the SAWMS (Figure 5.17 and Figure 5.18). In a similar fashion to the Sundays River irrigation scheme, the project team re-digitised the fields in this area. Figure 5.19 and Figure 5.20 show the significant improvements resulting from accurate field boundary data. Figure 5.21 shows a large scale view of where the SAWMS identified anomalies.

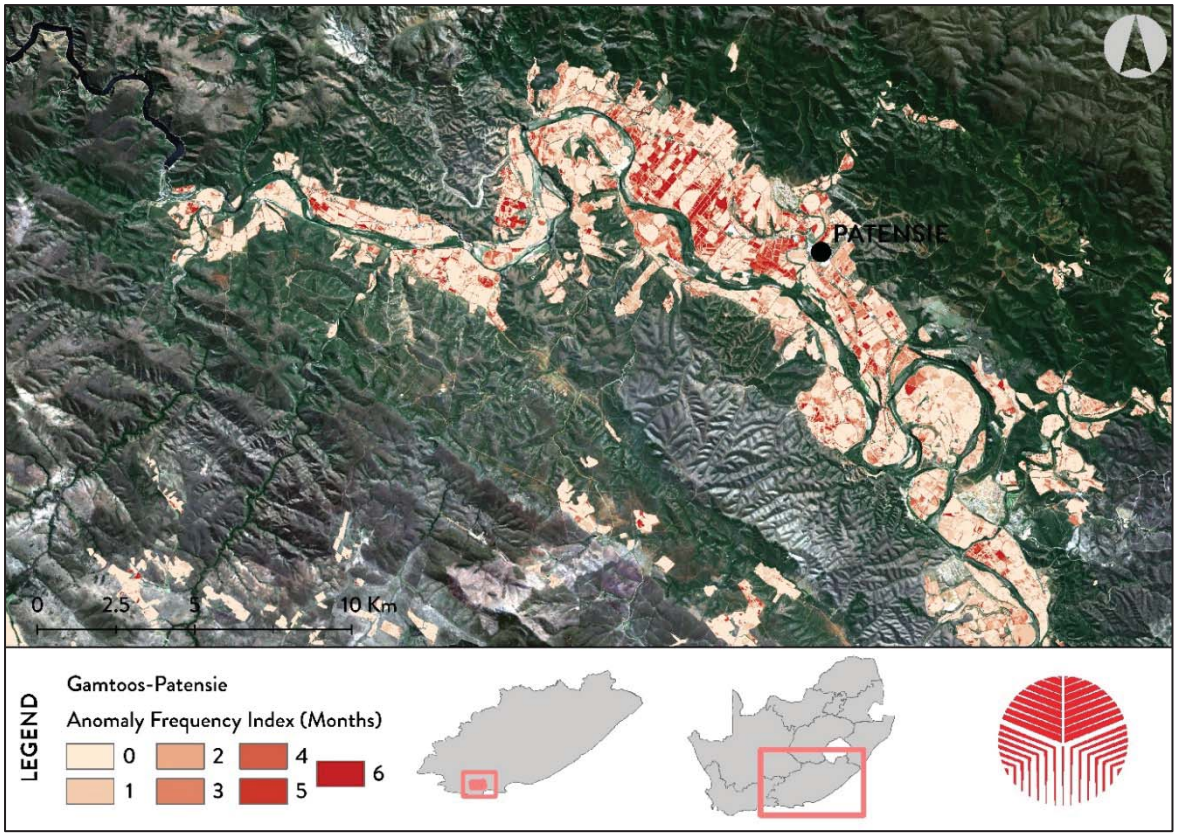

Figure 5.17: Example of the anomaly frequency index generated by SAWMS in the Gamtoos region with DAFF field boundaries

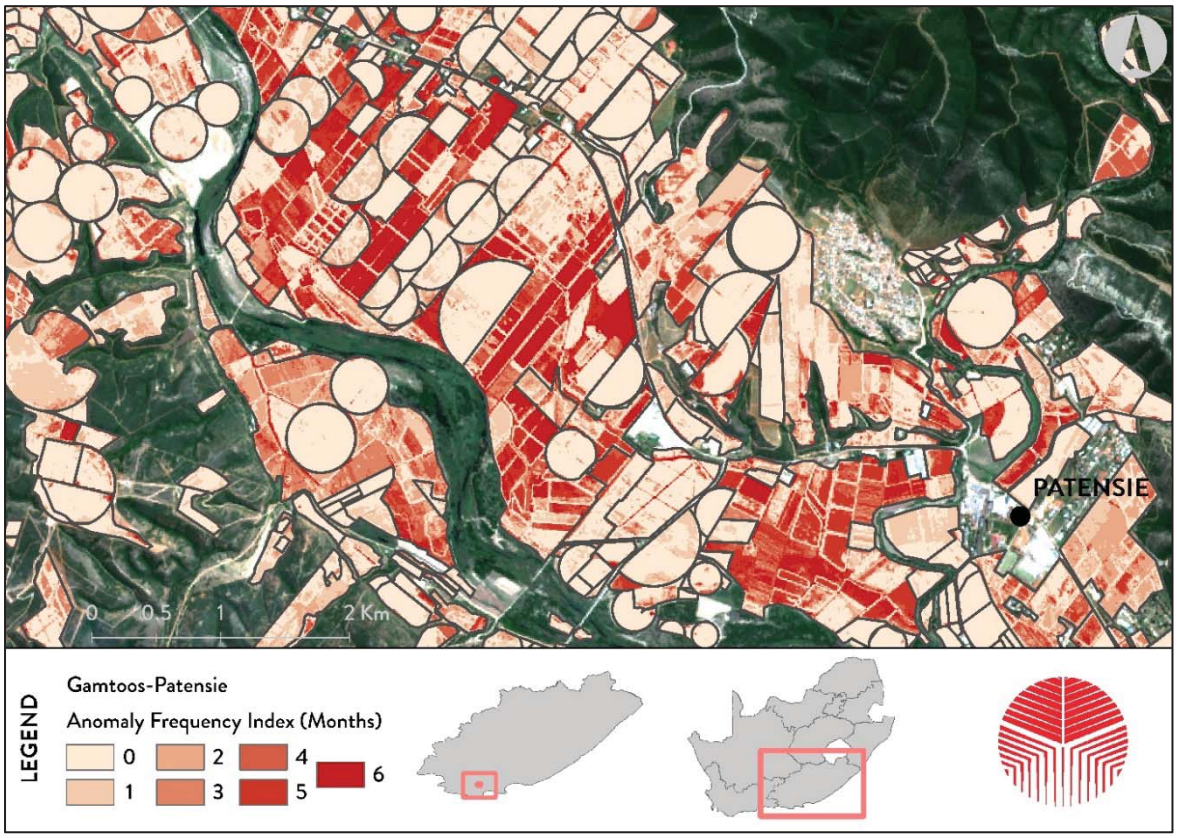

Figure 5.18: A close-up of the anomaly frequency index in the Gamtoos region with DAFF field boundaries

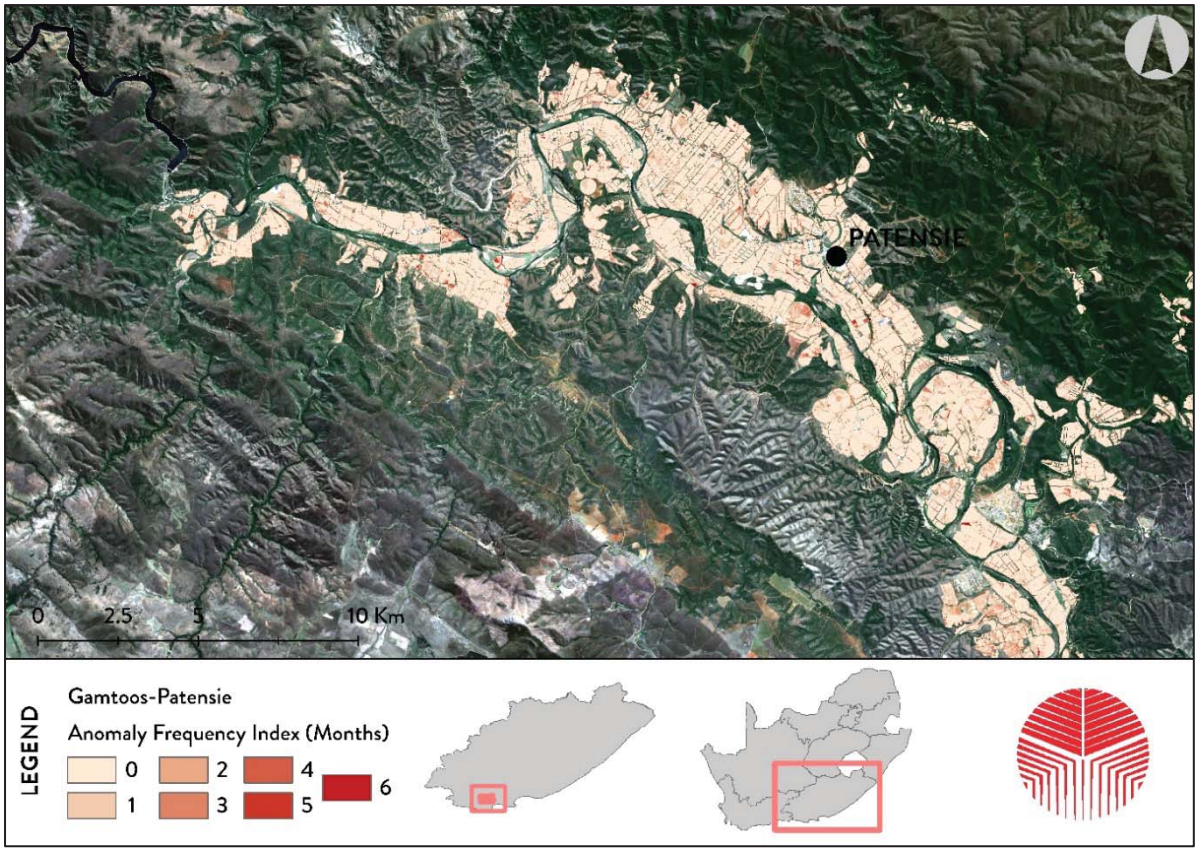

Figure 5.19: Example of the anomaly frequency index generated by SAWMS in the Gamtoos region with manually created field boundaries

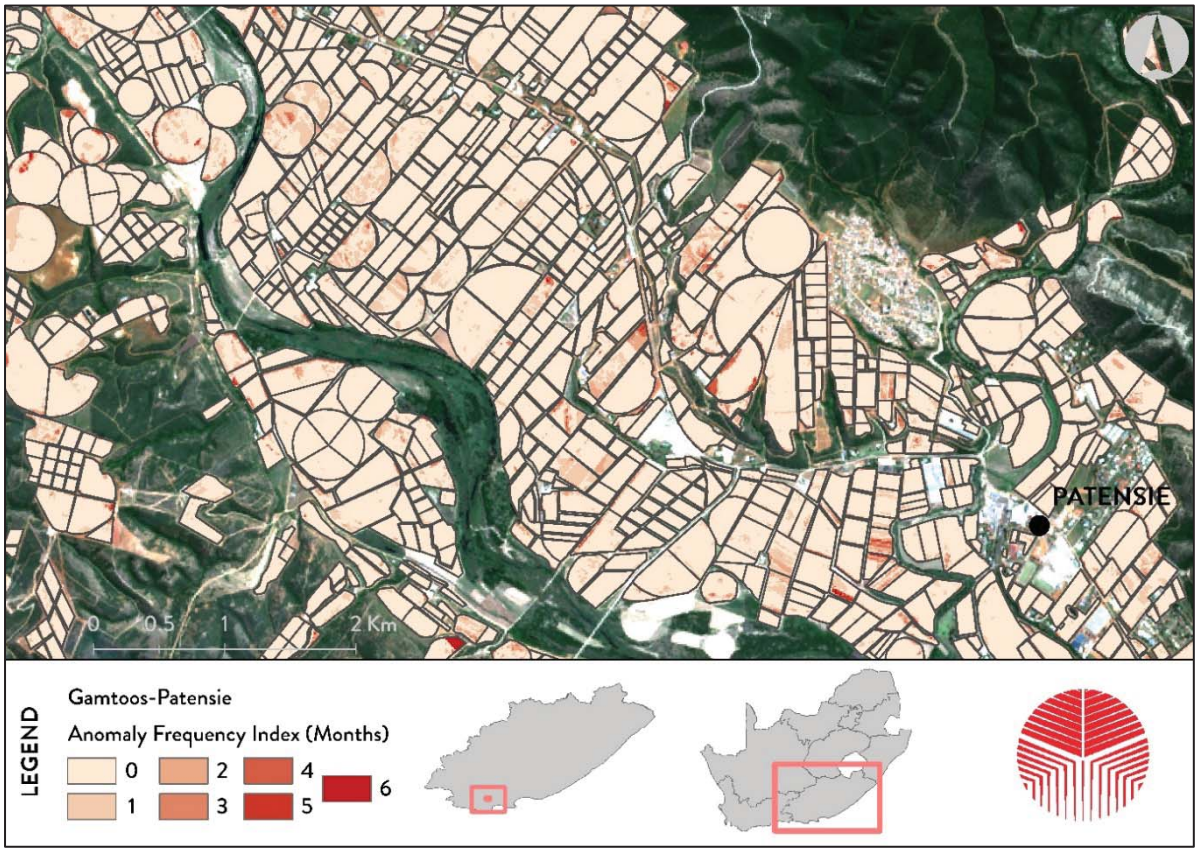

Figure 5.20: A close-up of the anomaly frequency index in the Gamtoos region with manually created field boundaries

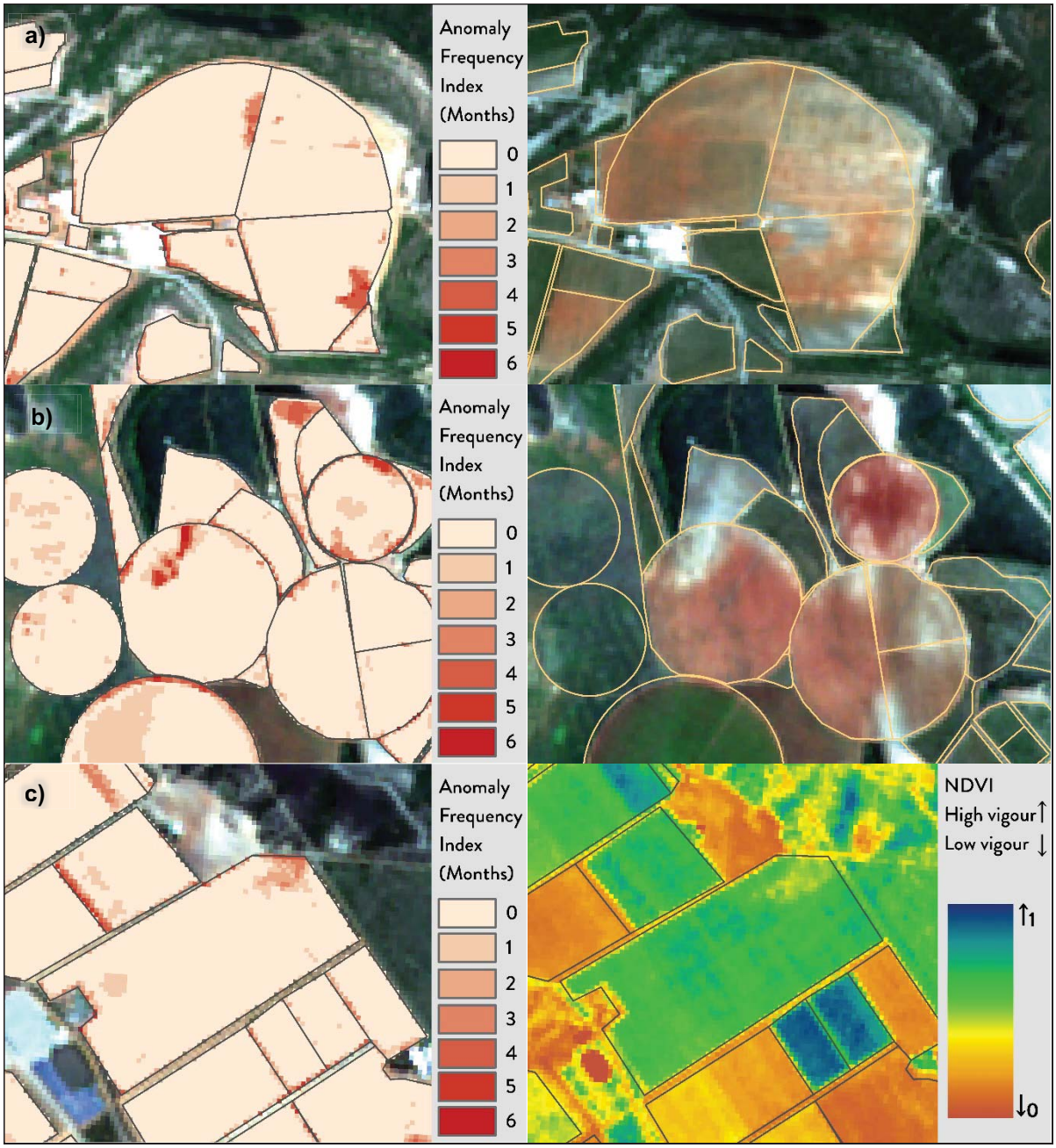

Figure 5.21: Various examples of the anomaly frequency index in the Gamtoos region where a) and b) show localized anomalies occurring with corresponding true colour images, and c) compares the result with a corresponding normalised difference vegetation index image.

A preliminary method for automated field boundary delineation, which makes use of multi-temporal imagery to identify field edges from multiple images, has been developed in this project (Watkins & Van Niekerk, 2019)(Appendix II). For purposes of evaluation, the technique was applied to the Patensie region (Figure 5.22) and the resulting field boundaries were used in the SAWMS methodology. The results are shown in Figure 5.23, where the automatically derived field boundaries outperformed those obtained from DAFF. However, the current procedure only derives actively growing fields and, as such, not all of the fields were included in the anomaly detection. Despite this limitation, the results are encouraging and suggest a cost-effective solution for obtaining accurate field boundaries in the future.

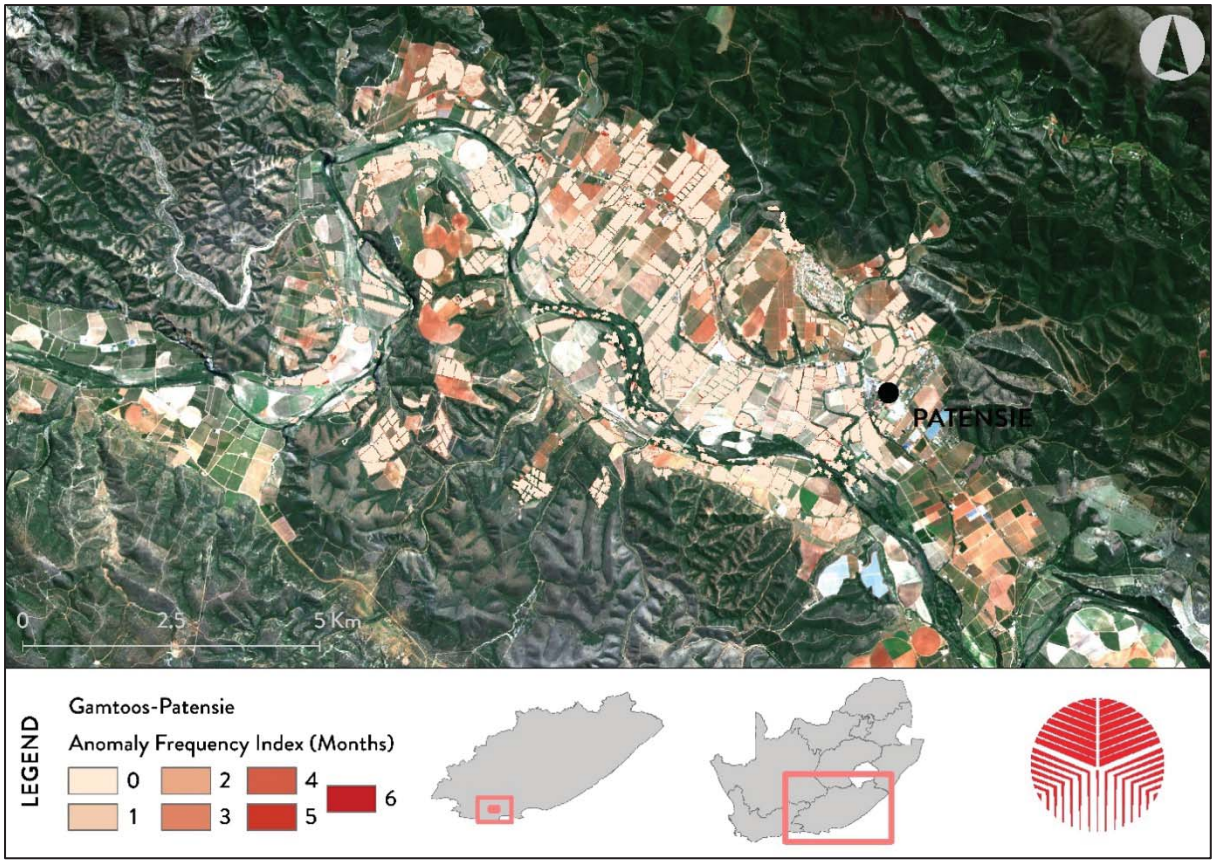

Figure 5.22: Example of the anomaly frequency index generated using automatically derived field boundaries in the Patensie agricultural area in the Gamtoos irrigation scheme

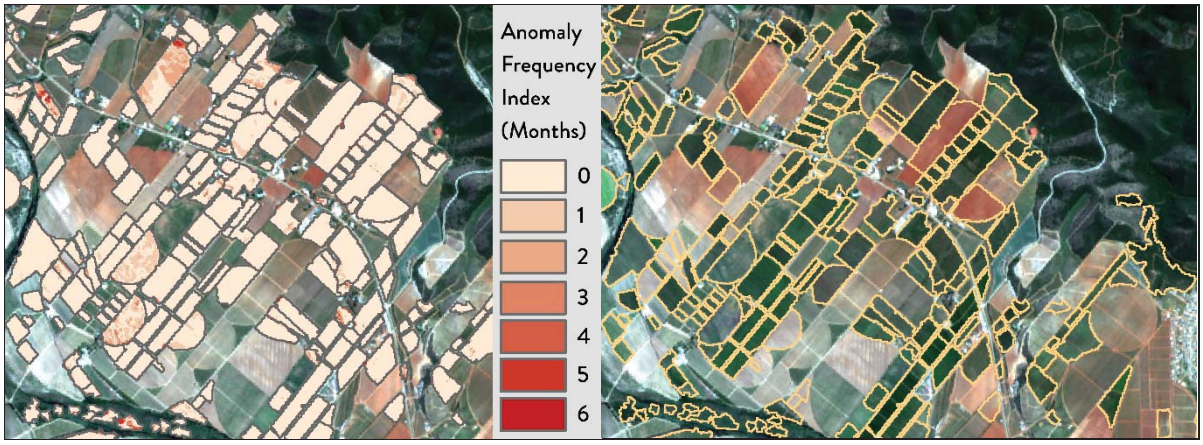

Figure 5.23: Automatically delineated field vector boundaries (right) in the Patensie agricultural area showing relatively homogenous areas (few anomalies identified by the anomaly frequency index on the left)

From the results presented above, it is evident that the most significant factor determining the effectivity of the SAWMS is the quality of the field boundary database. Field boundary inaccuracies seem to be more prominent in areas where field sizes are small. In the Olifants River irrigation scheme it introduced many false positives, and in the Sundays River irrigation scheme it resulted in almost a complete failure. For the successful implementation of the SAWMS at national scale it is therefore imperative that field boundaries are accurate. Recommendations regarding this are made in Section 6.3.

6 DISCUSSION, CONCLUSIONS AND RECOMMENDATIONS

6.1 Main findings from applying the SAWMS in various irrigated areas

The general agreement among the SAWMS end-users (and reference group members) is that salt accumulation and waterlogging is of growing concern, especially with increasing uncertainties over water supply and quality. Although producers are improving water use efficiencies, there is concern that this may lead to a gradual accumulation of salts due to the decrease in leaching. There is thus clearly a growing need for monitoring salt accumulation.

Targeted end-users (mainly agronomists, soil scientists and agricultural advisors) commented that the WFAD approach is innovative and that the principle of identifying areas (management zones) in fields/orchards that are consistently underperforming is sound. It was agreed that multi-temporal image analysis is essential for monitoring salt accumulation and waterlogging, because the direct and indirect manifestations of salt accumulation and waterlogging vary, depending on the crop type and growth stage.

The main finding of implementing and applying the SAWMS in seven very diverse irrigated areas throughout South Africa is that the system provides invaluable information in support of soil conservation. The experience gained in the implementation process exposed several technical challenges, which were not anticipated prior to this project. Solutions to most of these problems were found during the course of the project, but some still require additional research and development. The SAWMS worked very well in the ORVH Basin, mainly because most of the crops planted are annuals such as maize, wheat and barley. These crops respond dramatically to salinity and waterlogging and affected areas could thus be easily differentiated from non-affected areas. The field sizes are also large, which meant that fewer errors were caused by inaccurate (generalised) field boundaries. Similar observations were made in the Olifants River (Mpumalanga) and Great Fish River. Applying the SAWMS in the Olifants River (Western Cape) was much more challenging as the fields are more compact. Many errors in the existing field boundaries were noted and these had a detrimental effect on the WFAD method. Similar observations were made in Sundays and Gamtoos River areas – to such an extent that new field boundaries had to be manually delineated. Field boundaries that were automatically generated from multi-temporal Sentinel-2 imagery (the focus of the capacity building component of the project) were tested in the Gamtoos River area and showed potential for incorporation in future implementations of the SAWMS. However, more research is needed to improve the results and to operationalise such techniques.

Despite the remaining challenges, the project demonstrated that the WFAD method is very effective for identifying zones in fields that are likely affected by salt accumulation and/or waterlogging, as it compares pixels within each individual agricultural field to other pixels within the same field. This eliminates the variations in salinity tolerances and spectral characteristics of different crop types, as well as variations in growth stages of the same crop type planted on separate fields.

Several improvements were made to the WFAD method since its conceptualisation (Nell et al., 2015). In particular, the use of Sentinel-2 imagery improved anomaly detection accuracies by allowing for the generation of anomaly layers at five-day intervals, instead of once a season. This high frequency approach enabled the development of monthly cloud-free anomaly layers, which were used to generate an AFI over a specified period (rolling window).

It was agreed by the project team, end-users and reference group that the AFI should be used as a scoping mechanism to identify areas that need to be prioritised for field visits. This functionality was seen by the end-users as the major contribution of the system. The AFI will also be helpful in identifying areas where probes should be placed and where soil and leaf samples should be collected. It is also useful for identifying areas to be prioritised for remedial action. Currently, this is done by walking through the fields, and in large fields it can be easy to miss problematic areas. Based on the feedback from end-users, the maps are also invaluable for seasonal discussions by advisors with clients, as the SAWMS provides a historical record of areas in fields that are underperforming. Once the cause is determined (through site visits and, if needed, analyses of samples), agronomists can make recommendations about how production in such areas can be improved. It was agreed that the major value of the system is that a historical record is provided, which can be used for retrospective assessments such as investigating when a problem started. The system can also be used as a communication tool to analyse and explain problems to producers.

The targeted end-users agreed that the SAWMS will be of lesser value for in-season management decision support. The main limiting factor is that the images and maps are provided on a monthly interval, which means that it is not ideal for informing immediate actions (e.g. irrigation scheduling). However, it was understood that the system is not meant to be used to inform such actions, but is rather a tool for inter-season planning/preparations, such as identifying areas in fields that require draining systems or different/additional soil preparations. The system's frequency of use will thus be low. Typically, each user will make use of the system once every few months.

The targeted end-users agreed that the SAWMS' current functionality is sufficient and no suggestions for improvement were made. The ease of use of the web interface was widely complemented, particularly its ability to compare different dates and datasets side-by-side (through the "split screen" function).

The targeted end-users were concerned that the six-month running window currently being used for generating the AFI might not be long enough to identify salt-affected areas. Users indicated that the period should preferably be longer (i.e. it should consider more than one season) because salt accumulation and waterlogging are typically recurring phenomena and will likely only be separable from other problems over a longer period. Twelve months was considered a more appropriate period.

The biggest limitation of the SAWMS is that it relies on pre-defined field boundaries as parent object layer (see Section 3.1 for definition). The current methodology for generating such a layer is to visually interpret VHR satellite imagery or aerial photography and manually delineate (digitise) individual fields.

Mapping every field in South Africa in this manner requires substantial financial, human and computer resources. The Crop Estimates Consortium produces a national field boundary layer on a regular basis. The latest version (Crop Estimates Consortium 2017) of the agricultural field boundaries comprises the majority of agricultural field boundaries of SA, digitised from a 1.5 m SPOT 6/7 true colour mosaic. However, for the purposes of the SAWMS, it has a number of drawbacks, namely:

- The digitising was carried out at a relatively small (1:10 000) mapping scale and as such the boundaries are in some instances too generalised to be used for the WFAD method;
- The boundaries were digitised from a mixture of 2013, 2014 and 2015 imagery, resulting in some outdated boundaries; and
- The dataset does not include sugarcane fields.

These limitations led to research into automated field boundary delineation (Watkins & Van Niekerk, 2019) (Appendix II). A wide range of EO data were considered, including aerial photography, LiDAR, and satellite (Sentinel-2) imagery. The results (see Appendix II for details) are very promising. In particular, the LiDAR-based extractions were very encouraging, but the limited availability (spatially and temporally) of LiDAR data makes this approach unfeasible in the immediate term. The use of GEOBIA and multi-temporal Sentinel-2 imagery seems to be the most viable option. However, the approach has a number of limitations:

- Only actively growing fields are delineated, which means that fallow fields, or areas (zones) in fields that are have very poor growth, are excluded; and
- The 10 m resolution of the Sentinel-2 imagery is too low to accurately delineate small or irregularly-shaped fields (due to the mixed pixel effect).

Based on user feedback and visual inspections of the AFIs in several areas throughout South Africa (see Chapter 5), it seems that using Sentinel-2 imagery as input to the WFAD works very well in areas with medium (3 ha) to large (>10ha) fields. However, due to its relatively low (10 m) spatial resolution, it is less effective in areas with very small (<1ha) fields. However, the high (five-day) temporal resolution of Sentinel-2 imagery is ideal for agricultural monitoring as 73 images (observations) are used to generate the AFI (if a rolling window of 12 months is used). This effectively removes the influence of short-term fluctuations and interference (e.g. clouds, cloud shadows, heatwaves, wind, irrigation events, harvesting), allowing emphasis to be placed on the long-term status of each pixel (zone) within each field.

Based on the discussion above, it should be clear that the all four aims of the project were met. The SAWMS was successfully developed (Aim 1) and the information that was generated was effectively disseminated to end-users through a series of meetings (Aim 2). The SAWMS was implemented and demonstrated in several irrigation schemes throughout South Africa (Aim 3) and, based on feedback from end-users, the system was improved (Aim 4). The feedback from end-users was also critical for

making operational recommendations (see Section 6.3).

6.2 Proposals for future research

Several gaps in knowledge were identified during the course of this technology exchange project. For instance, it became clear from interactions with end-users that little is known about the optimal observation period (moving window during which anomalies should be aggregated to produce the AFI) for capturing anomalies caused by salt accumulation and waterlogging. The general agreement was that 12 months should be adequate, but more research is needed to investigate whether shorter periods may be beneficial.

The SAWMS currently makes use of the SAVI for assessing whether a crop is stressed. The NDVI was also tested in Nell et al. (2015), but more work is needed to investigate whether other vegetation indices (e.g. MSAVI2, moisture indices) are more effective for detecting salt accumulation and waterlogging.

The original WFAD method (Nell et al., 2015) was designed to make use of multiresolution image segmentation (MRS) to group pixels with similar spectral values into meaningful management zones (objects). These objects were then compared to the spectral characteristics of the field (parent object) in which they occur to determine whether they are anomalies. Currently, the SAWMS uses a per-pixel approach, mainly because of the lower (10 m) resolution of the Sentinel-2 imagery used (compared to the 2.5 m resolution SPOT-5 imagery used to develop the WFAD), but also because MRS is a proprietary algorithm (in eCognition software) and could thus not be incorporated into the automated workflow. Future efforts should investigate the suitability and performance of alternative, open source segmentation algorithms for grouping pixels within fields into meaningful management zones.

Another aspect that warrants investigation is the use of machine learning to differentiate between different types of anomalies. For instance, it is likely that the temporal and spectral characteristics of anomalies caused by salt accumulation and waterlogging are different from anomalies caused by other problems (e.g. water stress, pests, inappropriate application of fertilisers).

The range of automated field boundary delineation experiments carried out by the MSc students (Appendix II) suggests that the accuracy and completeness of the automated field boundary delineations can be improved by making use of more than one source of data. However, more research is needed to find a technique that can be operationalised. For instance, the efficacy of combining multiple Sentinel-2 and one VHR (e.g. WorldView/SPOT) image per season (or longer period) needs to be investigated. It is also unlikely that any single method or data fusion/combination will be effective on all types of crops and in all regions. More work is needed to investigate whether a crop-specific (e.g. perennials and annuals) approach would be more suitable.

The SAWMS end-users noted that it would take time for agronomists, technical advisors and growers to become familiar and comfortable with using satellite-based maps to support management decisions. For instance, it is not yet clear how effective the Sentinel-2 (10 m) resolution imagery is for monitoring tree crops. Drone imagery has gained much popularity in recent years, but it is unclear whether such

imagery offers the same level of radiometric and geometric quality of satellite images. However, drone imagery is more intuitive to interpret due to its relatively high resolution. Research that investigates how high (10 m) and very high (0.3–2 m) satellite imagery compares to ultra-high (<0.3 m) resolution drone imagery is needed to assist producers and advisors to acquire the imagery that is most appropriate for their purposes.

This project did not focus on verifying and validating ("ground truthing") the AFI. Once the system is operational, it is recommended the accuracy of the AFI is continuously monitored and calibrated against in situ observations (e.g. soil analyses). Comparisons between the AFI and data generated by an EM38 would also be of great interest from both a research and practical perspective.

6.3 Operational recommendations

The SAWMS was implemented in several irrigated areas throughout South Africa for demonstration purposes (see Chapter 5). To cover all irrigated areas in South Africa (as mapped Van Niekerk et al. (2018)), a total of 150 Sentinel-2 tiles will be required. At a five-day interval, this translates to 10 950 images, which equates to 8.5 terabytes (TB) of data per year. Using Stellenbosch University's fast Internet infrastructure, the download time for an image is between 10 and 30 minutes. At this rate, the downloading of all these images is achievable if the SAWMS requires updating once a month. For an operational system covering all irrigation areas, a fibre-based (200 Mb/s), uncapped account provided by an Internet service provider is recommended. The cost for such an account will be in the order of R2000 per month.

Much of the downloaded data are discarded once it has been processed. The only data that are retained are the layers ingested into the web application (e.g. the anomaly layer, AFI and the severely affected areas, vegetation indices and true-colour bands). It is estimated that about 1TB of additional storage will be required per year of operation. The cost for this storage is in the order of R1000[12] per year if a standard workstation is used to carry out the processing. The cost for the workstation will be in the order of R20 000[13] per year (assuming replacement every three years). A separate web server (R30 000[13] per year) will be required to host the web application.

Given the large volumes of satellite imagery required by the system and the unstable nature of power generation in South Africa, it is recommended that the system be operationalised as a cloud-based service. Most cloud-computing services, such as Amazon Web Services (AWS), Microsoft Azure, Google Cloud and IBM Cloud, have very fast Internet connectivity to ESA (the source of the Sentinel-2 imagery). Some of these service providers offer unlimited bandwidth in one direction (e.g. Azure offers unlimited inbound traffic), which means that all the required imagery can be downloaded much faster and at no cost.

Currently, the SAWMS mostly runs on open source software, although ESRI's ArcGIS proprietary software is used for some of the processing steps (e.g. calculating zonal statistics as illustrated in

[12] At 2019 prices.

Section 3.2.4.2). Academic licenses of ArcGIS were used for this project and commercial licenses will have to be acquired should the system be commercialised. The estimated costs will be R80 000[13] initially and R10 000[13] annually. Alternatively, the system code that makes use of proprietary libraries can be modified to make use of open source libraries, but this will require additional work and will thus also have an (initial) cost implication.

The SAWMS processes are fully automated, but (as with most complex computer systems) a system administrator is required to monitor activities and to ensure that the servers remain fully functional. Some of the software used (e.g. operating systems, database management systems and processing software) will require periodic updates, which will most likely require modifications to the system code. A system administrator familiar with the SAWMS procedures and code is consequently recommended.

Those who participated in the end-user feedback sessions (Appendix I) recommended that the operational costs of the SAWMS be funded by national government, in it was suggested that DAFF act as lead organisation, given their mandate to conserve agricultural soil and water. DWS should be a key partner, given the clear linkages between water use/quality and salt accumulation. Water user associations and agribusiness will play a critical role in the operationalisation of the SAWMS. Although producers will benefit from using the SAWMS, salt accumulation has a relatively small impact on yields compared to other factors such as cultivar selection, water availability, fertilisation and pest control. The users indicated that producers will only pay for something that has a direct and clear “value proposition”. The “FruitLook” model, where the Western Cape Provincial Government pays for the service to make it freely available to producers, was proposed as the best solution for the SAWMS, at least until the “value proposition” becomes apparent.

This project focused on detecting areas (zones) with irrigated fields affected by salt accumulation and waterlogging, but the same techniques and procedures can be used to support other types of agronomic decisions. The findings of this project directly links to another WRC project (K5/2499//4) carried out by the University of the Free State, entitled *Guidelines for technology transfer to manage irrigation-Induced salinity with precision agriculture.*

Through this project, as well as through other completed and running projects e.g. *An Earth observation approach towards mapping irrigated areas and quantifying water use by irrigated crops in South Africa* (Report number TT 745/17) and *The application of national scale remotely sensed evapotranspiration (ET) estimates to quantify water use and differences between plantations in commercial forestry regions of South Africa* (Project K5/2966//4), the WRC is taking a leading role in supporting research and technology development in EO. The increasing availability of EO data, often at no cost to the user, provides countless additional opportunities for the development and validation (“ground truthing”) of new innovative tools and technologies targeting the agricultural sector. However, more needs to be done to build capacity in remote sensing at national research and academic institutions, so that the provision of services is strengthened and diversified.

REFERENCES

Abbas A, Khan S, Hussain N, Hanjra M & Akbar S 2013. Characterizing soil salinity in irrigated agriculture using a remote sensing approach. *Physics and Chemistry of the Earth* 56-57: 43-52.

Abood S, Maclean A & Falkowski M 2011. *Soil salinity detection in the Mesopotamian agricultural plain utilizing WordView 2 imagery.* Houghton: Michigan Technological University.

Aihoon JK, Groenewald JA & Sartorius von Bach HJ 1997. Agricultural salinization in the Olifants River At Loskop Valley, Mpumalanga / Landbou-geïnduseerde versouting in die Olifantsrivier by die Loskopvallei, Mpumalanga. *Agrekon* 36: 268-283.

Aldakheel YY 2011. Assessing NDVI spatial pattern as related to irrigation and soil salinity management in Al-Hassa Oasis, Saudi Arabia. *Journal of the Indian Society of Remote Sensing* 39: 171-180.

Allbed A, Kumar L & Aldakheel YY 2014. Assessing soil salinity using soil salinity and vegetation indices derived from IKONOS high-spatial resolution imageries: Applications in a date palm dominated region. *Geoderma* 230-231: 1-8.

Armour RJ 2002. The economic effects of poor and fluctuating irrigation water salinity levels in the lower Vaal and Riet Rivers. M.Sc.Agric, Agricultural Economics. Bloemfontein: University of the Free State.

Azabdaftari A & Sunar F 2016. Soil salinity mapping using multitemporal landsat data. International Archives of the Photogrammetry, Remote Sensing and Spatial Information Sciences, Vol XLI-B7. XXIII ISPRS Congress, 12-19 July 2016, Prague, Czech Republic.

Baatz M & Schäpe A 1999. Multiresolution segmentation: an optimization approach for high quality multi-scale image segmentation. In Strobl J, Blaschke T & Griesebner G (eds) *Angewandte Geographische Informationsverarbeitung 2000*, 12-23. Salzburg: Herbert Wichmann Verlag.

Backeberg GR, Bembridge TJ, Bennie ATP, Groenwald JA, Hammes PS, Pullen RA & Thompson H 1996. Policy proposal for irrigated agriculture in South Africa. Pretoria: Water Research Commission.

Badhwar GD 1982. Profile modeling for crop discrimination. Symposium on machine processing of remote sensing ddata, Perdue University, West Lafayette.

Baraldi A, Durieux L, Simonetti D, Conchedda G, Holecz F & Blonda P 2010. Automatic spectral-rule-based preliminary classification of radiometrically calibrated SPOT-4/-5/IRS, AVHRR/MSG, AATSR, IKONOS/QuickBird/OrbView/GeoEye, and DMC/SPOT-1/-2 imagery Part I: System design and implementation. *IEEE Transactions on Geoscience and Remote Sensing* 48: 1299.

Benz UC, Hofmann P, Willhauck G, Lingenfelder I & Heynen M 2004. Multi-resolution, object-oriented fuzzy analysis of remote sensing data for GIS-ready information. *ISPRS Journal of Photogrammetry and Remote Sensing* 58: 239-258.

Beuster H, Shand MJ & Carter CA 2003. Breede River basin study. Pretoria: DWAF.

Blaschke T 2010. Object based image analysis for remote sensing. *ISPRS Journal of Photogrammetry and Remote Sensing* 65: 2-16.

Blaschke T, Lang S, Lorup E, Strobl J & Zeil P 2000. Object-oriented image processing in an integrated GIS/remote sensing environment and perspectives for environmental applications. In Cremers A & Greve K (eds) *Environmental information for planning, politics and the public*, 555-570. Marburg: Metropolis Verlag.

Bock M, Xofis P, Mitchley J, Rossner G & Wissen M 2005. Object-oriented methods for habitat mapping at multiple scales – Case studies from Northern Germany and Wye Downs, UK. *Journal for Nature Conservation* 13: 75-89.

Brooks EB, Thomas VA, Wynne RH & Coulston JW 2012. Fitting the multitemporal curve: A Fourier series approach to the missing data problem in remote sensing analysis. *IEEE Transactions on Geoscience and Remote Sensing* 50: 3340-3353.

Campbell J 2007. *Introduction to remote sensing.* 4th Edition. London: Taylor & Francis.

Campbell JB & Wynne RH 2011. *Introduction to remote sensing.* New York: Guilford Publications.

Castillejo-González IL, López-Granados F, García-Ferrer A, Pe˜na-Barragán JM, Jurado-Expósito M, De la Orden MS & González-Audicana M 2009. Object- and pixel-based analysis for mapping crops and their agro-environmental associated measures using QuickBird imagery. *Computers and Electronics in Agriculture* 68: 207-215.

Crop Estimates Consortium 2017. Field crop boundary data layer, 2017. Pretoria: Department of Agriculture, Forestry and Fisheries.

Csillag F, Pásztor L & Biehl LL 1993. Spectral band selection for the characterization of salinity status of soils. *Remote Sensing of Environment* 43: 231-242.

Dehaan RL & Taylor GR 2002. Field-derived spectra of salinized soils and vegetation as indicators of irrigation-induced soil salinization. *Remote Sensing of Environment* 80: 406-417.

Dehaan RL & Taylor GR 2003. Image-derived spectral endmembers as indicators of salinisation. *International Journal of Remote Sensing* 24: 775-794.

Dutkiewicz A, Lewis M & Ostendorf B 2009. Evaluation and comparison of hyperspectral imagery for mapping surface symptoms of dryland salinity. *International Journal of Remote Sensing* 30: 693-719.

Dwivedi R, Fyzee M, Khan Q, Rao B, Sreenivas K, Ramana K & Thammappa S 1998. An inventory of salt-affected soils and waterlogged areas in the Nagarjunsagar canal command area of Southern India, using space-borne multispectral data. *Land degradation Development* 9: 357-367.

Dwivedi R, Ramana K & Sreenivas K 1999. Inventory of salt-affected soils and waterlogged areas: A remote sensing approach. *International Journal of Remote Sensing* 20: 1589-1599.

Dwivedi RS & Sreenivas K 1998. Delineation of salt-affected soils and waterlogged areas in the Indo-Gangetic plains using IRS-1C LISS-III data. *International Journal of Remote Sensing* 19: 2739-2751.

Elnaggar AA & Noller JS 2010. Application of remote-sensing data and decision-tree analysis to mapping salt-affected soils over large areas. *Remote Sensing* 2: 151-165.

FAO 1995. Land and water integration and river basin management. Proceedings of an FAO Informal Workshop, Rome, Italy.

Fernandez-Buces NS, C; Cram, S; Palacio, JL 2006. Mapping soil salinity using a combined spectral response index for bare soil and vegetation: A case study in the former lake Texcoco, Mexico. *Journal of Arid Environments* 65: 644-667.

Flügel W-A & Kienzle S 1989. Hydrology and salinity dynamics of the Breede River, Western Cape Province, Republic of South Africa. *Balitomore Symposium, Regianla Characterization of water quality.* Baltimore.

Furby S, Caccetta P, Wallace J & Wheaton G 1995. Detecting and monitoring salt affected land. Report to LWRRDC, Project CDM1. CSIRO, Division of Mathematics & Statistics.

García Rodríguez P, Pérez González ME & Guerra Zaballos A 2007. Mapping of salt-affected soils using TM images. *International Journal of Remote Sensing* 28: 2713-2722.

Ghassemi F, Jakeman A & Nix HA 1995. *Salinisation of land and water resources: human causes, extent, management and case studies* Sydney, New South Wales: University Press.

Gilbertson JK, Kemp J & Van Niekerk A 2017. Effect of pan-sharpening multi-temporal Landsat 8 imagery for crop type differentiation using different classification techniques. *Computers and Electronics in Agriculture* 134: 151-159.

Hay GJ, Castilla G, Wulder MA & Ruiz JR 2005. An automated object-based approach for the multiscale image segmentation of forest scenes. *International Journal of Applied Earth Observation and Geoinformation* 7: 339-359.

Iqbal F 2011. Detection of salt affected soil in rice-wheat area using satellite image. *African Journal of Agriculture Research* 6: 4973-4982.

Jia K, Liang S, Wei X, Yao Y, Su Y, Jiang B & Wang X 2014. Land Cover Classification of Landsat Data with Phenological Features Extracted from Time Series MODIS NDVI Data. *Remote Sensing* 6: 11518.

Khan NM, Rastoskuev VV, Sato Y & Shiozawa S 2005. Assessment of hydrosaline land degradation by using a simple approach of remote sensing indicators. *Agricultural Water Management* 77: 96-109.

Kirchner J 1995. Investigation into the contribution of groundwater to the salt load of the breede river, using isotopes and chemical tracers. WRC Report no. 344/1/95. Pretoria: Water Research Commission.

Koshal K 2010. Indices Based Salinity Areas Detection through Remote Sensing and GIS in parts of South West Punjab *International conference and exhibition on geospatial information technology and applications.* Gurgaon, India

Kruger M, Van Rensburg JBJ & Van den Berg J 2009. Perspective on the development of stem borer resistance to Bt maize and refuge compliance at the Vaalharts irrigation scheme in South Africa. *Crop Protection* 28: 684-689.

Kyere I, Möckel T, Graß R & Wachendorf M 2018. Multi-temporal analysis of agricultural land cover in Northern Hesse using satellite data. *Mitteilungen der Gesellschaft für Pflanzenbauwissenschaften* 30: 169-170.

Lang S 2008. Object-based image analysis for remote sensing applications: Modelling reality - dealing with complexity. In Blaschke T, Lang S & Hay G (eds) *Object-based image analysis: Spatial concepts for knowledge-driven remote sensing applications*, 3-26. Berlin/Heidelberg: Springer Verlag.

Lenney MP, Woodcock CE, Collins JB & Hamdi H 1996. The status of agricultural lands in Egypt: The use of multitemporal NDVI features derived from landsat TM. *Remote Sensing of Environment* 56: 8-20.

Leverington DW 2009. Mapping surface cover using EO-1 Hyperion data: Ongoing studies in arid environments. 17th International Conference on Geoinformatics, Fairfax, Virginia.

Lobell DB, Lesch SM, Corwin DL, Ulmer MG, Anderson KA, Potts DJ, Doolittle JA, Matos MR & Baltes MJ 2010. Regional-scale assessment of soil salinity in the Red River Valley using multi-year MODIS EVI and NDVI. *Journal of environmental quality* 39: 35-41.

Lucas R, Rowlands A, Brown A, Keyworth S & Bunting P 2007. Rule-based classification of multi-temporal satellite imagery for habitat and agricultural land cover mapping. *ISPRS Journal of Photogrammetry and Remote Sensing* 62: 165-185.

Mather PM 2004. *Computer Processing of Remotely-Sensed Images.* 3rd. Chicester, West Sussex: Wiley.

Meddens AJH, Hicke JA, Vierling LA & Hudak AT 2013. Evaluating methods to detect bark beetle-caused tree mortality using single-date and multi-date Landsat imagery. *Remote Sensing of Environment* 132: 49-58.

Metternicht GI 2003. Categorical fuzziness: a comparison between crisp and fuzzy class boundary modelling for mapping salt-affected soils using Landsat TM data and a classification based on anion ratios. *Ecological Modelling* 168: 371-389.

Metternicht GI & Zinck JA 2003. Remote sensing of soil salinity: potentials and constraints. *Remote Sensing of Environment* 85: 1-20.

Mitri GH & Gitas I 2002. The development of an object-oriented classification model for operational burned area mapping on the Mediterranean island of Thasos using LANDSAT TM images. In Viegas X (ed) *Forest Fire Research & Wildland Fire Safety*, Rotterdam: Millpress.

Moolman J, Clercq WD, Wessels W, Meiring A & Molman C 1999. The use of saline water for irrigation of grapevines and the development of crop salt tolerance indices. WRC Report no. 303/1/1999. Pretoria.

Mougenot B, Pouget M & Epema G 1993. Remote Sensing of Salt affected soils. *Remote Sensing Reviews* 7: 241-259.

Mucina L & Rutherford M 2006. The vegetation of South Africa, Lesotho and Swaziland. Pretoria: South African National Biodiversity Institute.

Muller SJ 2017. Indirect soil salinity detection in irregated areas using earth observation methods. MSc Thesis. Stellenbosch: Geography & Environmental Studies, Stellenbosch University.

Muller SJ & Van Niekerk A 2016a. An evaluation of supervised classifiers for indirectly detecting salt-affected areas at irrigation scheme level. *International Journal of Applied Earth Observation and Geoinformation* 49: 138-150.

Muller SJ & Van Niekerk A 2016b. Identification of WorldView-2 spectral and spatial factors in detecting salt accumulation in cultivated fields. *Geoderma* 273: 1-11.

Nell JP, Van Niekerk A, Muller SJ, Vermeulen D, Pauw T, Stephenson GR & Kemp J 2015. Methodology for monitoring waterlogging and salt accumulation on selected irrigation schemes in South Africa. WRC Report No. TT 648/15. Pretoria: Water Research Commission.

Pax-Lenney M & Woodcock CE 1997a. The effect of spatial resolution on the ability to monitor the status of agricultural lands. *Remote Sensing of Environment* 61: 210-220.

Pax-Lenney M & Woodcock CE 1997b. Monitoring agricultural lands in Egypt with multitemporal Landsat TM imagery: How many images are needed? *Remote Sensing of Environment* 59: 522-529.

Peña-Barragán JM, Ngugi MK, Plant RE & Six J 2011. Object-based crop identification using multiple vegetation indices, textural features and crop phenology. *Remote Sensing of Environment* 115: 1301-1316.

Penuelas J, Isla R & Aruas J 1997. Visible and near-infrared reflectance assessment of salinity effects on barley. *Crop Science* 37: 198-202.

Platonov A, Noble A & Kuziev R 2013. Soil salinity mapping using multi-temporal satellite images in agricultural fields of Syrdarya province of Uzbekistan. In Shahid SA, Abdelfattah MA & Taha FK (eds.) *Developments in soil salinity assessment and reclamation: Innovative thinking and use of marginal soil and water resources in irrigated agriculture.* Dordrecht: Springer.

Rao BRM, Sankar TR, Dwivedi RS, Thammappa SS & Venkataratnam L 1995. Spectral behaviour of salt-affected soils. *International Journal of Remote Sensing* 16: 2125-2136.

Sanhouse-Garcia AJ, Bustos-Terrones Y, Rangel-Peraza JG, Quevedo-Castro A & Pacheco C 2017. Multi-temporal analysis for land use and land cover changes in an agricultural region using open source tools. *Remote Sensing Applications: Society and Environment* 8: 278-290.

Schulze RE 2007. *South African atlas of climatology and agrohydrology. WRC Report No. 1489/1/06.* Pretoria: Water Research Commission.

Schulze RE & Lynch SD 2007. Annual Precipitation. In E SR (ed) *South African Atlas of Climatology and Agrohydrology, WRC Report No. 1489/1/06*, Pretoria: Water Research Commission.

Schulze RE & Maharaj M 2006. Temperature Database. In Schulze RE (ed) *South African Atlas of Climatology and Agrohydrology, WRC Report No. 1489/1/06*, Pretoria: Water Research Commission.

SEOS 2016. Supplement 1.2 Remote sensing instruments used in marine pollution [online]. Available from http://www.seos-project.eu/modules/marinepollution/marinepollution-c01-s02-p01.html [Accessed 14 March 2018].

Setia R, Lewis M, Marschner P, Raja Segaran R, Summers D & Chittleborough D 2013. Severity of salinity accurately detected and classified on a paddock scale with high resolution multispectral satellite imagery. *Land Degradation and Development* 24: 375-384.

Shiba M & Itaya A 2006. Using eCognition for improved forest management and monitoring systems in precision forestry. Proceedings of the International Precision Forestry Symposium, Stellenbosch, South Africa.

Sidike A, Zhao S & Wen Y 2014. Estimating soil salinity in Pingluo County of China using QuickBird data and soil reflectance spectra. *International Journal of Applied Earth Observation and Geoinformation* 26: 156-175.

Smith RB 2012. Remote sensing of environment (RSE) [online]. Available from https://www.microimages.com/documentation/Tutorials/introrse.pdf [Accessed 19/03/2019].

Steiner D & Maurer H 1969. The use of stereo height as a discriminating variable for crop classification on aerial photographs. *Photogrammetria* 24: 223-241.

The Non-Affiliated Soil Analyses Work Committee 1990. Handbook of standard soil testing methods for advisory purposes. Pretoria: Soil Science Society of South Africa.

Tren R & Schur M 2000. Olifants River Irrigation Schemes, Reports 1 & 2. Colombo, Sri Lanka: IWMI.

Van Niekerk A, Jarmain C, Goudriaan R, Muller J, Ferreira F, Munch Z, Pauw T, Stephenson GR & Gibson LA 2018. An earth observation approach towards mapping irrigated areas and quantifying water use by irrigated crops in South Africa. WRC Report TT 745/17. Pretoria: Water Research Commission.

Verhulst N & Govaerts B 2010. *The normalized difference vegetation index (NDVI) GreenSeekerTM handheld sensor: Toward the integrated evaluation of crop management. Part A: Concepts and case studies.* Mexico, DF: CIMMYT.

Vermeulen D & Van Niekerk A 2016. Evaluation of a WorldView-2 image for soil salinity monitoring in a moderately affected irrigated area. *Journal of Applied Remote Sensing* 10: 026025.

Vermeulen D & Van Niekerk A 2017. Machine learning performance for predicting soil salinity using different combinations of geomorphometric covariates. *Geoderma* 299: 1-12.

Watkins B & Van Niekerk A 2019. A comparison of object-based image analysis approaches for field boundary delineation using multi-temporal Sentinel-2 imagery. *Computers and Electronics in Agriculture* 158: 294-302.

Wiegand CL, Rhoades JD, Escobar DE & Everitt JH 1994. Photographic and videographic observations for determining and mapping the response of cotton to soil salinity. *Remote Sensing of Environment* 49: 212-223.

Zhang TT, Zeng SL, Gao Y, Ouyang ZT, Li B, Fang CM & Zhao B 2011. Using hyperspectral vegetation indices as a proxy to monitor soil salinity. *Ecological Indicators* 11: 1552-1562.

APPENDIX I: USER FEEDBACK SESSIONS

The project team – in consultation with the reference group – identified agribusiness, agronomists, technical advisors and extension officers as the main end-users of the SAWMS. Two agribusinesses, namely GWK in the Northern Cape and the Humansdorp Koöperasie (Humkoop) in the Eastern Cape, were targeted to gain insights into the:

- need for monitoring salt accumulation and waterlogging from the agricultural industry's perspective;
- conceptual validity of EO and the WFAD approach;
- value of an online system to monitor salt accumulation and waterlogging;
- usefulness of the SAWMS in particular;
- functional and technical limitations of the SAWMS (and suggestions for improvement);
- likelihood of adoption of the SAWMS for supporting agricultural decisions; and
- operational strategy (business case) that will most likely ensure the SAWMS' sustainability.

Feedback was obtained during two workshops. The first workshop was held on 24 October 2018 at the GWK offices in Kimberley, while the second was held on 14 November 2018 at Humkoop head office in Humansdorp. Both meetings were well attended (see list of participants below). The workshops followed the following agenda:

1. PowerPoint presentation (project team)
    a. Background to the project
    b. Conceptual overview of the WFAD method
2. Demonstration of the SAWMS (project team)
3. Discussion among participants
4. Closure and way forward

The format of the workshops was informal and participants were encouraged to ask questions during the presentations and demonstrations. The feedback was incorporated into the conclusions and recommendations of this report (Chapter 6).

Table AI.1: Feedback session participants

Name	Organisation
Badenhorst, Bennie	GWK
Bekker, Abraham	HUMKOOP
Bergh, Evert	GWK
De Jager, Mossie	HUMKOOP
Du Plessis, Casper	GWK
Du Raan, Reinier	GWK
Gumede, Thabani	GWK
Haarhoff, Dup	GWK
Hattingh, Hannes	GWK
Jacobs, Bertus	HUMKOOP
Janse van Vuuren, Gerhard	HUMKOOP
Le Roux, Eugene	GWK
Myburgh, Ivan	GWK
Prins, Andre	GWK
Reid, Christopher	GWK
Slabbert, Danie	HUMKOOP
Sounes, Johan	GWK
Van Eck, Armand	GWK
Veldsman, MC	HUMKOOP

APPENDIX II: CAPACITY BUILDING

As reported in Nell et al. (2015) and as discussed in Section 6.1, the quality of the vector field boundaries used in the SAWMS workflow is critical for accurate anomaly detection. The Crop Estimates Consortium, in collaboration with the DAFF, regularly releases a national database of field boundaries. The latest release (April 2017) of this database is used in the SAWMS (Crop Estimates Consortium, 2017). This dataset was produced from imagery dated 2013–2015. Given that the field boundary dataset is produced by visual interpretation and on-screen digitising (at 1:10 000 scale) of VHR satellite images (e.g. 2.5 m SPOT-5 and 1.5 m SPOT 6/7) – acquired over several seasons/years – it is not possible (and cost-effective) to update the field boundaries on a regular (annual or seasonal) basis. Clearly, a different approach is needed. The advent of high resolution, highly temporal, freely available satellite imagery has opened up a multitude of new possibilities and research into the use of such imagery for automated generation of frequently updated (seasonal, even monthly), actively growing crop extent maps (i.e. field boundaries) is urgently needed. However, very little progress towards developing operational solutions for automated field boundary delineation has been made.

Geographic object-based image analysis (GEOBIA) has been shown to be effective for crop type mapping and a call for MSc research proposals relating to GEOBIA and automated field boundary delineation was made at the beginning of this project. The recruitment process was detailed in Deliverable 4 of this project. To summarise, two students, namely Messrs Prins and Watkins, responded with innovative ideas and sensible proposals, which were subsequently accepted. Messrs Prins and Watkins were both registered on this project and experimented with different methods for automated field boundary delineation. Mr Prins' work focusses on the use of VHR imagery and LiDAR data, whereas Mr Watkins is seeking solutions that make use of multi-temporal Sentinel-2 imagery. Given that LiDAR data is still relatively scarce in South Africa (owing to its high costs), Mr Prins' expected solutions will likely only be applicable in very intensive agricultural areas (e.g. Vaalharts), while Mr Watkins' work will likely have more universal application.

Both students opted to report their findings as research articles, which will form part (chapters) of their theses. The theses will consist of an introductory chapter (Chapter 1), a literature review (Chapter 2), two articles (Chapters 2 and 3), and a concluding chapter (Chapter 5). At the time of writing this report, both students were progressing well and have submitted to their supervisor (Prof Van Niekerk) a draft of all these chapters. Some of the chapters have gone through several refinements and have been accepted for examination. However, some of the chapters (in particular the research articles) still require some work, although they are nearing completion. The working titles and status of the four research articles that will emanate from this research are given in Appendix III.

In addition to the students working on this project, capacity was also built through the feedback sessions with users (Appendix I). Participants to these sessions were not only exposed to the SAWMS, but gained insights into the principles of remote sensing and how EO data can be used to support agricultural decisions. The sessions also created awareness of the use of remotely sensed imagery for salt accumulation and waterlogging monitoring. Most of the participants regularly advise farmers and producers and it is thus likely that these sessions will have a much wider, indirect impact on those in the agricultural community.

APPENDIX III: PUBLICATIONS

To date, two publications have emanated from this project, namely

Van Niekerk A, Stephenson GR, Muller SJ & Pauw T 2019. Earth observation for monitoring salt accumulation and waterlogging. *PositionIT*, February 2019. Available at: https://www.ee.co.za/article/earth-observation-for-monitoring-salt-accumulation-and-waterlogging.html

Watkins B & Van Niekerk A (2019). A comparison of object-based image analysis approaches for field boundary delineation using multi-temporal Sentinel-2 imagery. *Computers and Electronics in Agriculture*, 158: 294-302. Available at: https://www.sciencedirect.com/science/article/pii/S0168169918317733

Several publications are in press, review or in preparation.

Muller SJ & Van Niekerk A (in press). Within-field monitoring of secondary salinity in irrigated areas of South Africa, in Rattan L & Stewart BA (eds) *Advances in Soil Science: Soil Degradation and Restoration in Africa*. Boca Raton, CRC Press.

Prins A & Van Niekerk A (in review). Regional mapping of vineyards using LiDAR data and machine learning. Target journal: *Computers and Electronics in Agriculture.*

Prins A & Van Niekerk A (in preparation). Mapping crop types by applying machine learning to combinations of aerial photography, Sentinel-2 imagery and LiDAR data. Target journal: *International Journal of Applied Earth Observation and Geoinformation.*

Watkins B & Van Niekerk A (in preparation). Inter-regional agricultural field boundary delineation using multi-temporal Sentinel-2 imagery. Target journal: *European Journal of Remote Sensing*.

APPENDIX IV: GUIDELINE TO USERS ABOUT THE IMPACT OF FIELD BOUNDARY QUALITY ON ANOMALY DETECTION

The following guideline was incorporated into the SAWMS to inform users of the impact of poor (generalised and outdated) field boundary data on the identified anomalies.

Welcome to the Salt Accumulation and Waterlogging Monitoring System (SAWMS). Before using the online tool, please read the following guidelines.

The main purpose of the SAWMS is for it to be used as a scoping mechanism to identify areas within irrigated fields where salt accumulation and waterlogging are most likely to occur. Because satellite imagery and earth observation techniques are used, there is no assurance that a detected anomaly is directly or indirectly related to salt accumulation and/or waterlogging. It is thus recommended that the detected anomalies are prioritised for field inspections and that soil samples are taken to determine whether the cause of the anomaly can be attributed to salinity and/or waterlogging.

The SAWMS uses existing field boundary data to identify salt-affected and waterlogged areas within irrigated fields. The latest (2017) national database of field boundaries, developed by the Crop Estimates Consortium in collaboration with the Department of Agriculture, Forestry and Fisheries (DAFF), is currently the main source of field boundary data. The dataset was created by visually interpreting and manually capturing (digitising) imagery dated 2013–2015. Field boundaries are indicated as **red** lines in the SAWMS (Figure A3.1).

Figure A3.1: Example of field boundaries (in red) delineating individual fields

The SAWMS makes use of very recent (usually not older than a few weeks) Sentinel-2 imagery for the identification of anomalies. Inaccuracies (mismatches) between the field boundary layer and the Sentinel-2 imagery are thus unavoidable.

There are mainly two types of mismatches between the field boundaries and the Sentinel-2 imagery. The first is a misalignment between the current field extent and the digitised field boundary (red line).

This is because fields may have changed since the creation of the boundary layer. Figure A3.2 provides an example of this misalignment and the anomalies created (see the yellow boxes) due to this misalignment. When such misalignments exist, it is good practice to ignore all anomalies within the field.

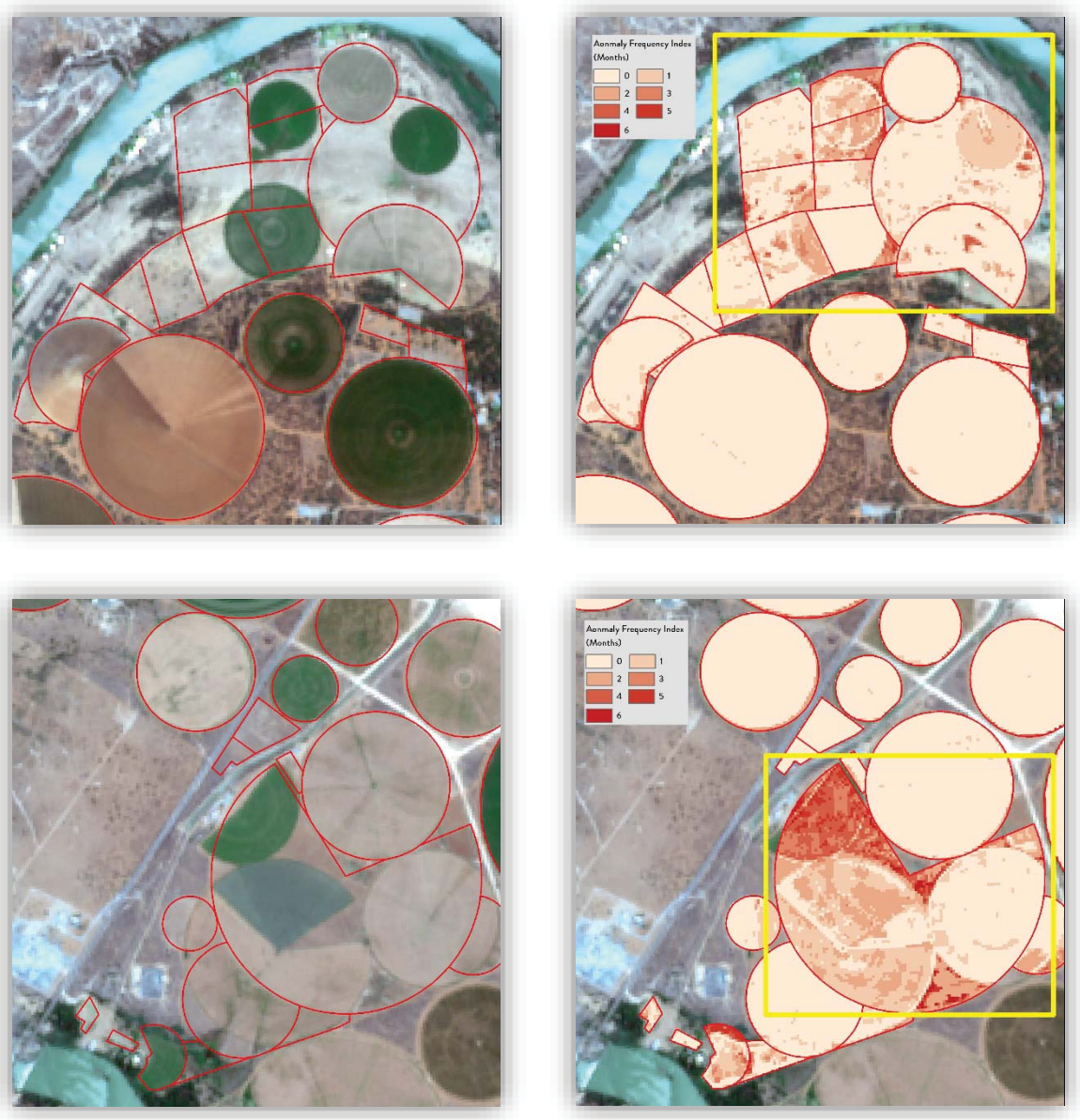

Figure A3.2: Examples of misaligned field boundaries compared to up-to-date Sentinel-2 imagery

The second source of error occurs when more than one crop is grown in a single production unit. Different crop types in a single field are usually spectrally different (brighter or darker) and therefore lead to confusion (Figure A3.3). When the shape of the anomaly in a field corresponds to that of a different crop type (as indicated in the yellow boxes in Figure A3.3) it should be disregarded.

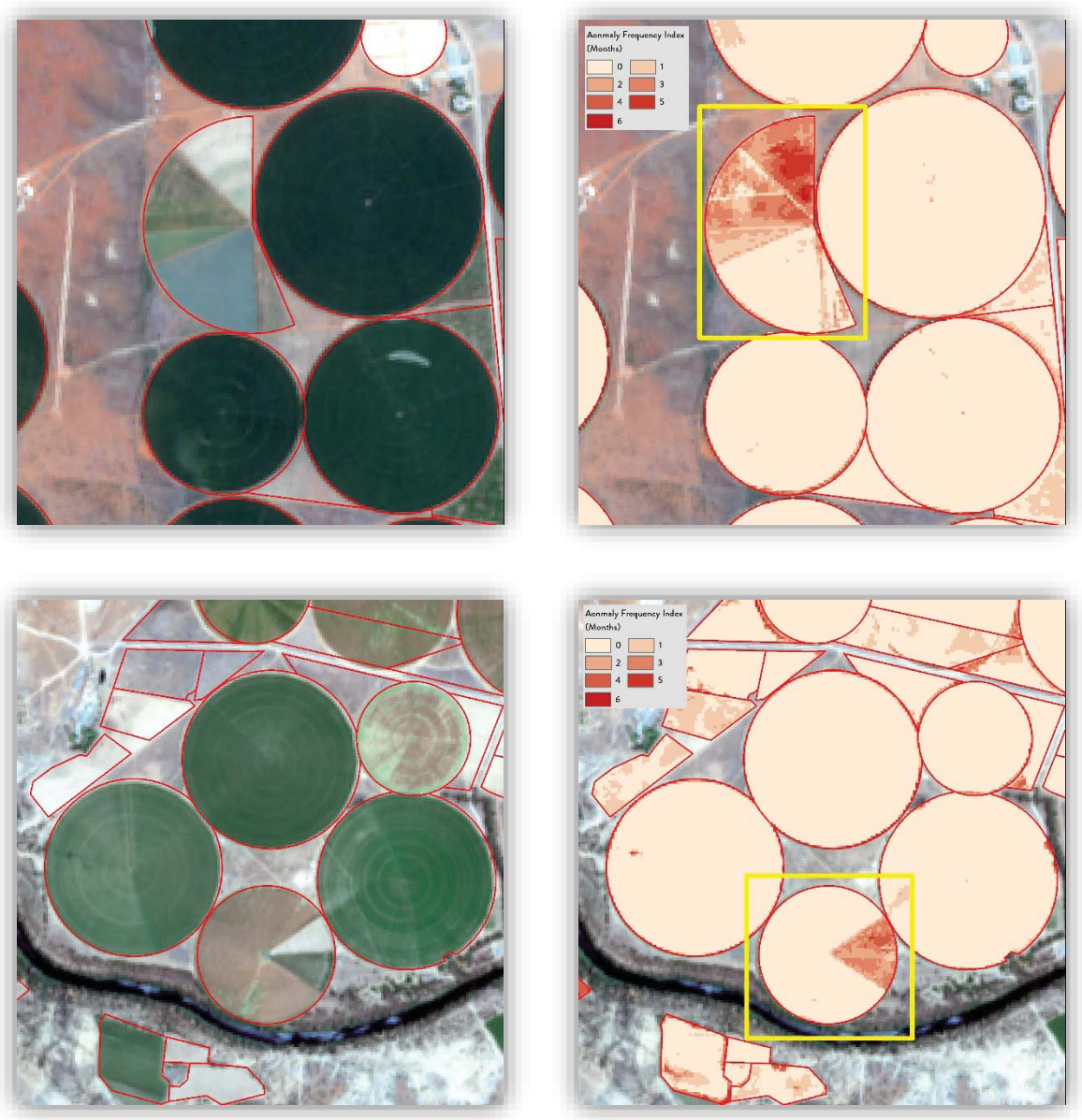

Figure A3.3: Examples of misaligned field boundaries compared to up-to-date Sentinel-2 imagery

Stellenbosch University is carrying out research to automatically delineate field boundaries from the same imagery used in the SAWMS, which has the potential to substantially reduce mismatches caused by dated field boundary datasets. However, an operational solution is not yet available and it is recommended that users pay close attention to the current set of field boundaries when interpreting the anomaly layers.

APPENDIX V: ACCESS TO DATA GENERATED THROUGH THIS PROJECT

All the data that was collected as part of this project are archived electronically and is accessible from the Centre for Geographical Analysis at Stellenbosch University. Kindly contact Prof Adriaan van Niekerk at avn@sun.ac.za to gain access to the data. Alternatively Mr Garth Stephenson (garth@sun.ac.za) can be contacted.